C.P. No. 107
(13,539)
A.R.C. Technical Report

MINISTRY OF SUPPLY

AERONAUTICAL RESEARCH COUNCIL

CURRENT PAPERS

Some Investigations into the Design of Wind Tunnels with Gas Turbine Jet Engine Drives

By

H. J. Higgs, B.Sc., B.E.

LONDON: HER MAJESTY'S STATIONERY OFFICE

1953

Price 16s. 0d. net

C.P. No. 107

Report No. Aero.2369

May 1950

ROYAL AIRCRAFT ESTABLISHMENT

Some investigations into the design of wind tunnels with gas turbine jet engine drives

by

H.J. Higgs, B.Sc., B.E.

SUMMARY

The basic design of wind tunnels suitable for jet engine drives has been investigated by matching the predicted mass flows and total pressure losses of typical tunnel configurations with the estimated mass flow and total pressure rise characteristics of possible pumping systems.

There are three possibilities of jet engine pumping (i) induction pumping (ii) suction pumping and (iii) parallel suction and induction pumping, of which induction pumping is shown to be the most favourable. Using this system a typical 5,000 lb thrust jet engine (such as a R.R. Nene II) can drive

(i) A high speed subsonic tunnel of 4 ft^2 working section up to M = 1.0.

(ii) A supersonic tunnel of 2 ft^2 working section up to M = 1.2.

(iii) A supersonic tunnel of 1 ft^2 working section up to M = 1.8.

For these three cases it has been assumed that humidity effects can be controlled by partial recirculation of the hot engine exhaust gases to raise the working section temperature to 60°C. In the supersonic case 60°C might not be sufficient and other methods of humidity control have been discussed in relation to jet engine drives. Induction pumping readily allows multiple engine drive, i.e. the above working section areas can be increased in proportion to the number of engines used.

LIST OF CONTENTS

LIST OF APPENDICES

LIST OF ILLUSTRATIONS

LIST OF ILLUSTRATIONS (Contd.)

1 Introduction

It has been usual to regard the jet engine purely as a thrust producing power plant but it also forms in itself a pump as the intake air is raised (i.e. pumped) to greater total temperatures and pressures. However the air at outlet from the pump is not near stagnation conditions but has high kinetic energy which would need to be diffused to give a true total head pump. Alternatively this kinetic energy could be used directly as the drive in a secondary induction pump.

These possibilities for wind tunnel drives were first realized at the end of World War II when more conventional drives for high speed wind tunnels were not available.

Since then a number of tunnels with jet engine drives have been built by the Aircraft industry and further tunnels are projected.

This type of tunnel has proved attractive for the routine development of high speed aircraft in that a readily accessible tunnel with a working section of reasonable size can be obtained by a relatively cheap and quick construction.

When jet engines are surplus or in mass production the capital cost will be quite low The drive uses maintenance and operating staffs and also a fuel system which are well known to aircraft firms and may already be available. Though running costs are high they are in part offset by the poor "load factor" characteristics of wind tunnels.

A considerable amount of work has been done on these tunnels but the literature is not very extensive, referring in general to particular tunnels. The present aim is to collate some of this information and to examine the various theories to form a basis for future designs and to examine the possibilities of extended use of the system to give a supersonic tunnel.

1.1 Methods of wind tunnel drive by turbo-jet engines

A turbo-jet engine may be used to drive a wind tunnel in three ways,

(a) by using the jet as the driving jet in an induction pump,

(b) by coupling the tunnel directly to the engine air intake and using the engine itself as a pump,

(c) by combining (a) and (b) so that the two pumping systems are in parallel, i.e. so that the engine is contained in the tunnel with flow around it as well as through it.

The main considerations in selecting the method of drive is not in the pump characteristics alone but also in the operational features as related to engine location. It must be emphasised that ease of engine maintenance and repair is of prime importance in wind tunnel availability with drives such as these where the engine has a relatively short life.

The first method (see Figure 1) allows any number of engines to be used (hence a wide range of tunnel sizes) all of which are easily accessible for maintenance and repair as they need not be cowled but housed in a separate room. Also in multiple engine installations a limited operation of the tunnel would be possible with an engine removed for replacement.

The second method is most simply applied to drives by a single engine (see Figure 2), an engine with a high compression ratio (about 10 : 1) being most suitable. This arrangement still allows ready accessibility for maintenance and repairs. By dividing the tunnel flow at the end of the diffuser down stream from the working section it might be possible to use a number of engines in parallel but the engines would have to be closely matched to give an even flow distribution. In general the total pressure in the diffuser may be taken as the engine inlet total pressure.

For the third method the tunnel flow must pass both through and around the engines (see Figure 3) i.e. the engine is contained within the tunnel. Consequently this configuration is most suited to a single engine, the axial flow type being best as they give small flow deflections hence minimizing the losses. The engine is fairly inaccessible and maintenance will be difficult as it will involve the removal of both the engine cowling and tunnel walls.

1.2 Possible configurations of wind tunnels

In any method of wind tunnel drive by a jet engine, provision must be made for the continuous entry of atmospheric air so that sufficient oxygen will be available to support combustion in the engine, i.e. a closed system is not possible.

Also each of the three methods of drive will be downstream of the working section so that the air passing through the working section would normally be from atmospheric sources. This means that the main configuration problem, apart from the working section and balance arrangements, will be the methods employed to control the effects of atmospheric humidity and dust.

Some form of humidity control is essential even for subsonic tunnels because of

(a) the difficulties and uncertainties of any humidity corrections,

(b) the possibilities of condensation shocks in local supersonic regions[16].

Of course in supersonic tunnels humidity control becomes a prime consideration and can vitally affect the whole design.

Three main methods of controlling humidity effects are possible,

(i) by increasing the stagnation temperature in the working section.

(ii) by pre-drying the air.

(iii) by pre-expansion of the air in an auxiliary nozzle.

The first method of control can be achieved by a heat exchanger at the inlet or more elegantly with the present method of drive by a partial recirculation of the hot exhaust gases from the jet engine. Possible configurations of tunnels employing these various methods of humidity control are illustrated in Figures 4 to 7 and their relative merits are discussed in Appendix A.

For most of the following discussion humidity control by partial recirculation of the hot gases has been assumed as this is the most economical and simply achieved method of control but the consequent

increase in working section stagnation temperature does have a marked effect on the overall tunnel performance. However any general tunnel configuration can be obtained by combining at station 2 any one of the pumping systems of Figures 1-3 with any one of the working section configurations of Figures 4-7.

1.3 Basic design considerations

For any method of drive the design basis is either to establish the range of working section areas and Mach numbers that can be attained for a given engine array, or conversely to determine the minimum number of engines necessary to give a desired range of working section areas and Mach numbers. In practice operation over a range of Mach numbers is usually required for a fixed working section area.

These relations can only be obtained by matching the pressure recovery and mass flow characteristics of the pumping system with the pressure loss and mass flow characteristics of that portion of the tunnel upstream of the pump.

The wind tunnel characteristics and also the pump characteristics of a jet engine used as a suction pump (as in the second method of drive) can be determined independently as is indicated in the following sections. The matching process simply involves the selection, from the pump characteristics, of the engine operating speed (if it is within the allowable engine temperature range) at which the mass flow and pressure difference are the same as those given by the tunnel characteristic.

However when induction pumping is used (as is the case in the first and third methods of drive) the pump characteristics cannot be determined independently of the tunnel. These characteristics depend on the configuration of the induction system, i.e. the area ratio α

where $$\alpha = \frac{A_J}{A_a} = \frac{\text{area of Driving Jet Nozzle}}{\text{area of induced air annulus}}$$

and the mass flow ratio β

where $$\beta = \frac{m_J}{m_a} = \frac{\text{mass flow rate of driving Jet}}{\text{mass flow rate of induced air}}$$

In any matching of the pump system to the tunnel the number of engines and operating conditions will be known, i.e. m_j is known. Also for the tunnel the working section area and Mach number will be given, i.e. m_a is known, thus β can be readily determined. The value of α will depend on the configuration of the induction pump which is not initially known consequently only arbitrary values of α can be assumed

However for basic design purposes it would be very desirable to have an indication of the best value of α and consequently a set of charts was developed (see section 3.12) for likely values of the other induction chamber parameters showing the variation of the pressure recovery to the mass flow ratio (β) for a series of values of α. From these charts (Figure 11-13) it can be seen that, in general, for a given pressure rise the ratio β is least for the smallest value of α that will give the required pressure rise. Hence for a given jet mass flow (i.e. a given

jet engine maximum performance) the tunnel mass flow will be maximum when α has this minimum value. This condition for α then corresponds with the general basic design considerations outlined at the beginning of this section.

An estimate of this value of α for any given tunnel characteristics can be made from these charts as, also, can be the pump characteristics by interpolation. The methods of determining the tunnel characteristics and the pump characteristics of the three methods of drive are discussed in detail in the following sections, as are the appropriate matching methods

2 Determination of wind tunnel flow characteristics

2.1 High speed subsonic tunnel

For an initial design study only a generalized total pressure loss characteristic is needed. Usually such pressure loss curves are presented on the basis of the working section Mach number. However each Mach number will correspond to a particular mass flow/unit area of working section which can be determined thus giving the required total pressure loss to mass flow characteristic for the tunnel.

In determining the mass flow/unit area of working section corresponding to a particular Mach number it is convenient to assume that the flow through the settling length and inlet contraction is isentropic, i.e. that total head conditions in the tunnel working section correspond to atmospheric conditions. This assumption will give slightly greater mass flow than will be obtained ir practice and hence for matching purposes will be conservative.

Hence from continuity

$$m_1 = m_a = A_1 \rho_1 v_1 = A \rho_o \frac{\rho_1}{\rho_o} a_o \frac{v_1}{a_o}$$

where station 1 refers to the working section (see Figures 4-7) and $\frac{\rho_1}{\rho_o}$ and $\frac{v_1}{a_o}$ are obtained for M_1 from standard tables and ρ_o and a_o refer to atmospheric conditions. This mass flow must be corrected by the factor $\sqrt{\frac{288}{T_{T_1}}}$ if T_{T_1}, the total temperature in the working section, differs from the standard atmospheric temperature 288°K.

To obtain sonic speeds with a small model in position the pressure ratio must, in general, be the same as that required to choke the tunnel when empty. It may need to be somewhat larger still to allow for the probable reduction in diffuser efficiency due to interference from the model supports.

The likely drop in total pressure up to the downstream end of the diffuser following the working section under these conditions would be 1.6 to 1.8 lb/in^2, i.e. a total pressure ratio of 1.12 to 1.14 would be required to drive the tunnel. Curve 5 of Figure 8 illustrates a typical total pressure loss characteristic for this type of tunnel.

2.2 Supersonic tunnel

As with high speed subsonic tunnels the generalized total pressure loss curve is given in terms of working section Mach number; the corresponding mass flow/unit area of working section must be determined as before.

The total pressure loss curve here used (Curve 1 Figure 8) obtained from that of Crocco quoted in reference 1, being based on a diffuser with a normal shock followed by subsonic diffusion with a polytropic efficiency of 75% (i.e. an adiabatic efficiency of 78%). However the theoretical values of total pressure loss have been increased at Mach numbers near to unity so that the curve corresponds more closely with experimental results. It is faired into the subsonic curve in an arbitrary manner.

3 Jet induction pump drive

3.1 Determination of induction pump characteristic

3.11 Engine performance

For basic tunnel design purposes only the injector characteristics under maximum engine performance conditions need be considered. If the pressure difference developed by the injector system is equal to or slightly greater than, the pressure difference required to maintain flow at each working section velocity of interest, then the engine and injector configuration will be satisfactory.

If at some part of the range of working section velocities the pressure difference is much greater than that required to maintain flow, then the engine R.P.M. can be reduced to give more economical working at the required lower pressure difference, but it is the maximum output conditions that will determine the basic design.

At maximum R.P.M. it is usual for the final nozzle of a jet engine to be choked, hence the induction jet is assumed to have a Mach number = 1 in all cases. Though better pressure recoveries in the induction system may be possible with supersonic jet velocities they were not investigated as the pressure difference across the final nozzle is never likely to exceed the critical value so far as to warrant the fitting of a divergent portion after the nozzle throat.

3.12 Flow in the mixing section

The analysis of air induction systems has been made by a number of investigators[5,6,7,8] but in general their treatment is based for simplicity on one dimensional flow using the four steady flow equations of

(a) Continuity

(b) Momentum

(c) Energy

(d) State

Any comparison of the different analyses is, however, complicated by the variation in the further assumptions namely whether

(a) Flow is assumed compressible or not,

(b) Mixing is assumed complete or not,

(c) The ratio of specific heats is assumed the same for both gas streams or not,

(d) The flow in the mixing chamber is assumed frictionless or not,

(e) The static pressures of the induction jet and the induced air are assumed to be the same or not.

Naturally the final justification for any of these assumptions depends on whether the resulting analysis gives a sufficiently accurate correspondence to actual test results.

However at the present stage no systematic experimental investigation has been made to check the various analyses available. Consequently a theoretical analysis must be used as the basis for any design study and the choice between the various theoretical analyses must be a compromise between excessive complication and unrealistic simplification.

The analysis, which is given in Appendix B is similar to that given in reference 7 but has been modified to suit available flow tables and all values of the jet to air annulus total temperature ratio. The assumptions of the analysis are

(a) Flow is compressible,

(b) Mixing is complete by station 4 (see Figure 1),

(c) Flow is not frictionless,

(d) Ratio of specific heats is the same for both gases ($\gamma = 1.4$),

(e) The static pressure of the induced air and the jet need not necessarily be equal.

The analysis gives five independent variables

$$M_j, \quad M_a, \quad \frac{P_{T_j}}{P_{T_a}}, \quad \frac{T_{T_j}}{T_{T_a}} \quad \text{and} \quad \alpha$$

from which two dependent variables $\frac{\Delta P_T}{P_o} \times 14.7$ and β may be calculated.

Hence fixing four of the independent variables M_j, $\frac{P_{T_j}}{P_{T_a}}$, $\frac{T_{T_j}}{T_{T_a}}$ and α

(of which M_j always equals one from the previous section) curves of $\frac{\Delta P_T}{P_o} \times 14.7$ to β can be obtained by varying M_a. These curves are the mixing section characteristics which form the basis of the injector characteristics.

Investigations were also made into the analyses due to Hawthorne and Cohen[5] and Rolls Royce Ltd.[8] but these were both based on the assumption of equal static pressures in the induced air and jet section of the mixing chamber. As the Hawthorne and Cohen[5] analysis is based on compressible flow it becomes a particular solution of the foregoing analysis, for the assumption of equal static pressures at the inlet to the mixing chamber eliminates the parameter $\frac{P_{T_j}}{P_{T_a}}$.

The Rolls Royce analysis[8] is based on incompressible flow and is presented in the form of a generalized mixing chamber and exit diffuser characteristic based on a flow parameter and a pressure parameter that are ideally equal. When compared with experimental results any inequality is taken as a measure of the efficiency of mixing though other assumptions of the analysis such as the equality of jet and induced air static pressures, may also be invalid and may also contribute to any discrepancy between experimental and theoretical results.

Figure 9 gives a comparison between the injector characteristics based on each system for $\alpha = 0.10$ and $\frac{T_{T_j}}{T_{T_a}} = 3.0$. It shows assuming equal static pressures in the induced air and jet inlet that the assumption of compressible flow (Hawthorne and Cohen analysis) gives a lesser pressure recovery than does the assumption of incompressible flow (Rolls Royce analysis) whereas if the jet static pressure is assumed to be higher than the induced air static pressure (i.e. the jet is not completely expanded) considerably higher pressure rises can be obtained than when the inlet static pressures are assumed the same. Consequently as in practice the inlet static pressures need not be the same this inlet pressure parameter $\frac{P_{T_j}}{P_{T_a}}$ is important and should be considered.

3.13 <u>End diffuser and generalized induction pump characteristics</u>

The end diffuser will in general exhaust to atmosphere hence the exit static pressure will be P_o. From continuity the exit Mach number can be found for either 100% or lesser efficiencies and hence the static pressure rise characteristics against inlet Mach number (see Appendix B).

Figure 10 illustrates such diffuser characteristics for isentropic efficiencies of 100% and 80%. The case for 100% is the same as the reciprocal of Figure 16 of reference 9.

For the three area ratios chosen it can be seen that an area ratio of 4 gives good pressure recoveries without an excessively large diffuser structure.

These characteristics have been combined with the mixing section characteristics to give the combined injector characteristics of Figures 11, 12 and 13.

The values of the parameters used in developing these characteristics have been chosen so that they will correspond as far as possible to the maximum output of an engine such as a R.R. Nene II and a working section total temperature of about 50°C. These considerations give

values of $\frac{T_{T_j}}{T_{T_a}} = 3.0$ and $\frac{P_{T_j}}{P_{T_a}} = 2.0, 2.5$ and 3.0. A series of values of $\alpha = 0.05, 0.10, 0.15, 0.20$ and 0.50 have been taken which covers all likely values of α. It has been necessary to assume that $\Delta P_f = 0$ (i.e. flow frictionless) to obtain any generalization, as the estimation of ΔP_f depends on the specific mixing chamber configuration Methods of allowing for friction in the mixing chamber are discussed in the following section.

The resulting characteristic curves for induction pumping are suitable for initial design study purposes and also give an indication of the relative importance of the various parameters so that optimum mixing chamber configurations can be aimed at.

3.14 Friction loss in mixing chamber

In the development of the foregoing generalized injector characteristics it was necessary to assume that the flow in the mixing chamber was frictionless as the term for pressure loss due to friction can only be estimated for a particular configuration when the flow conditions are known.

In a specific case the dimensions of the mixing chamber would be known and a first estimate of the flow conditions could be made assuming frictionless flow and thus an approximate value of the term for pressure loss due to friction could be deduced and the analysis repeated.

For frictional compressible flow in a pipe Young and Winterbottom[11] found for a simplified theory such as Hawthorne's (which assumed the local friction coefficient was constant along the pipe) that the friction coefficient must be estimated with close accuracy to give a satisfactory estimate of the choking distance and other flow parameters.

Consequently, as the present mixing theory gives no indication of the flow changes along the length of the pipe (i.e. chamber) but only the end conditions, the friction coefficient was estimated from the wall Reynolds numbers at the two end planes and these coefficients were used in conjunction with the assumed flow conditions for the respective planes. (For analysis see Appendix B).

As the assumed flow conditions were estimated for frictionless flow a more refined estimate of the pressure loss due to friction (and hence the mixing process) could be made by repeating the analysis using the flow conditions found from the second analysis allowing for friction. However for the cases examined the difference was negligible and in fact as shown by the following table of a typical engine-tunnel condition, the pressure recovery was estimated with sufficient accuracy if the estimate of pressure loss due to friction was subtracted directly from the value of the pressure recovery assuming frictionless flow without repeating the mixing analysis.

TABLE

Tunnel Conditions $P_{T_a} = 13.1$ lb/in^2 $T_{T_a} = 333^\circ$K $\alpha = 0.15$

Engine Conditions R.P.M. 12000

	Assumption	Pressure Recovery
1	Chamber assumed frictionless.	1.70 lb/in^2
2	Friction loss (ΔP_f) estimated from flow conditions as in 1. Mixing analysis repeated using this value of ΔP_f.	1.61
3	Friction loss (ΔP_f) estimated from flow conditions found in 2. Mixing analysis repeated using this value of ΔP_f.	1.60
4	Value of ΔP_f as estimated in 2, subtracted directly from 1.	1.61

For initial design estimates it is only possible to assume frictionless flow hence some arbitrary allowance should be made for the pressure loss due to the neglected friction. On the basis of the above table the required pressure recovery would need to be about 0.1 to 0.2 lb/in^2 greater than the estimated tunnel loss. For mixing chambers for supersonic tunnel drives the outlet velocities are higher hence the allowance for friction loss would need to be somewhat higher than the above value.

3.2 Matching of tunnel and injector characteristics

For the jet, data curves for the engine will give T_{T_j} m_j A_j and fuel consumption for the maximum R.P.M. but not P_{T_j}. However P_{T_j} can be determined if the final nozzle is choked from Figure 28.

Hence for each working section Mach number of interest $\frac{P_{T_j}}{P_{T_a}}$, $\frac{T_{T_j}}{T_{T_a}}$ and $\beta \left(= \frac{m_j}{m_a} \right)$ are determined from the tunnel and engine characteristics. From the injector characteristics values of $\frac{\Delta P_T}{P_o} \times 14.7$ can be obtained by interpolation for the values of α of interest. These pressure rises (less an allowance for pressure loss in the mixing chamber) can be compared with the pressure drop required to give the particular working section Mach number, hence a satisfactory value of α can be determined.

4 Jet engine suction pump drive

4.1 Determination of suction pump characteristics

4.11 Engine performance

The determination of the characteristics of the jet engine when used as a suction pump is only a particular case of the general problem of determining the performance of the engine under different flight conditions. The cycle is modified so that the exhaust gases are made to discharge into air at higher pressures than the intake, that is the cycle operates as though the ram pressure ratio was less than one.

Nominally, as with the induction pump drive, only the suction pump characteristics at maximum engine performance need be considered for basic design purposes. As shown in the following section, under these

conditions, with some further assumptions, it is possible to predict the pump characteristics for any compression ratio and inlet conditions thus giving an indication of the likely performance of any engine of similar component efficiencies.

For detail design and general operation it is desirable to have an indication of the suction pump characteristics of the engine when it is running at part load. In such cases the performance of a particular engine must be considered. If the component characteristics are known, this is a straightforward matter but, in general, these are not given by the Manufacturers Performance Data Sheets. However it was possible to make an estimate of the compressor, turbine, and jet pipe characteristics from the data sheets by the methods described in Appendix C.

4.12 Suction pump characteristics at normal maximum R.P.M.

(a) Engine with normal jet pipe

In reference 12 it is shown that if

(a) The final nozzle and turbine inlet guide vanes are assumed choked

(b) Turbine efficiency assumed constant

(c) The compressor work input is assumed a function of R.P.M. alone

then the turbine pressure ratio $P_{T_{III}}/P_{T_{IV}}$, the maximum temperature $T_{T_{III}}$ and the jet pipe temperature $T_{j_{IV}}$ are all constant for a given engine at a given R.P.M.

Hence it is possible to predict what the mass flow to pump pressure rise characteristics will be for various compressor ratios and inlet temperatures as is indicated in Appendix C.

Figure 14 shows some typical curves for compressor ratios of 5 : 1 and 10 : 1 under two different inlet temperatures and maximum temperatures.

As might be expected the use of a higher temperature in the combustion chamber increases the mass flow at a given pressure rise, the increase being more marked in the case of the compressor ratio of 10 : 1, i.e. with the greatest temperature rise..

At standard test bed inlet conditions the pressure rise obtainable at any given mass flow is greater for the engine with the compressor ratio 10 : 1 but for high inlet temperatures as may be obtained when coupled to a recirculation tunnel (for humidity control) the pressure rise will be about the same as for the engine with a compressor ratio of 5 : 1, or even less with low values of combustion chamber temperature. With either compressor ratio the effect on performance of the inlet temperature changes is much more marked than combustion chamber temperature changes. In all cases above the choking conditions the variation of mass flow to pressure rise is linear as the ratio $P_{T_{IV}}/P_o$ is changed linearly and the flow parameter $\frac{m_{IV}\sqrt{T_{T_{IV}}}}{A_{IV}\ P_{T_{IV}}}$ is constant.

The conditions when the final nozzle is not choked $\left(\frac{P_{T_{IV}}}{P_o} < 1.85\right)$ are considered in the following section but the present curves are those of main design interest as the pump characteristics below the choking line are not very suitable.

(b) Engine with end diffuser replacing normal jet pipe

The advantage of using an end diffuser instead of the normal jet pipe is that the guide vanes and inlet to the diffuser will remain choked for lower values of $\frac{P_{T_{IV}}}{P_o}$. From Figure 17 it may be seen that the choking value of $\frac{P_{T_{IV}}}{P_o}$ has been theoretically estimated at 1.2 (for an adiabatic efficiency = 80% and an area ratio 4 : 1) and consequently a higher pressure rise should be obtained with the engine still in the choked condition, i.e. the favourable section of the pump characteristics can be extended into regions of higher pressure recovery.

Tests on diffusers with a 4 : 1 area ratio by Young and Green[9] have shown that for rectangular diffusers with diffusion semi-angles of 5.3° that the choking value of $\frac{P_{T_{IV}}}{P_o}$ corresponds to 1.2 or 1.25. These tests showed a very serious fall in diffuser efficiency at Mach numbers of about 0.75 but Rolls Royce[8] have found that good efficiency can be maintained up to inlet Mach numbers approaching unity by putting a faired transition from the inlet to the beginning of the diffuser. It should be possible to meet these conditions in the present arrangement.

4.13 Suction pump characteristics at engine part load

To determine these characteristics the engine component characteristics must be known, i.e.

(a) Compressor characteristics showing compressor temperature rise θ_c against R.P.M. (N) on the assumption that θ_c is a function of N alone. See Figure 15.

(b) Turbine temperature ratio characteristic showing the ratio of the temperature drop through the turbine to the total temperature at the turbine inlet $\left(\frac{\theta_t}{T_{T_{III}}}\right)$ plotted against

(i) the ratio of the total pressure at the turbine inlet to the total pressure at the turbine outlet $\left(\frac{P_{T_{III}}}{P_{T_{IV}}}\right)$ and

(ii) the ratio of the total pressure at the turbine inlet to the atmospheric pressure $\left(\frac{P_{T_{III}}}{P_o}\right)$. See Figure 16.

(c) Jet pipe characteristics showing the dimensionless mass flow parameter $\frac{m_{IV}\sqrt{T_{T_{IV}}}}{A_{IV}\ P_{T_{IV}}}$ against $\frac{P_{T_{IV}}}{P_o}$. See Figure 17.

From these characteristics it may be seen that at any given R.P.M. and value of $\frac{P_{T_{III}}}{P_o}$ greater than the choking value then $\frac{\theta_{t_{III}}}{T_{T_{III}}}$ is constant and hence, as θ_t (and therefore θ_c) is constant for a given R.P.M., $T_{T_{III}}$ will be constant. However at values of $\frac{P_{T_{III}}}{P_o}$ below the choking value the corresponding value of $\frac{\theta_t}{T_{T_{III}}}$ will not be constant but will decrease, that is, for the given R.P.M. values of $T_{T_{III}}$ (and $T_{T_{IV}}$) must increase as the value of $\frac{P_{T_{III}}}{P_o}$ drops below the choking value. As $T_{T_{III}}$ depends on θ_t it will also be seen that the obsolute value of $T_{T_{III}}$ will be greater at higher R.P.M. for from Figure 15 θ_c (i.e. θ_t) increases with R.P.M. increasing.

The effect on the cycle, of using the engine as a suction pump is to have ram pressure ratios less than one, i.e. if the R.P.M. is constant to decrease $\frac{P_{T_{III}}}{P_o}$ and if this value falls below the choking value to decrease $\frac{\theta_t}{T_{T_{III}}}$. Consequently as an engine is normally designed at static conditions so that $T_{T_{III}}$ has its maximum allowable value when the R.P.M. is greatest and $\frac{P_{T_{III}}}{P_o}$ is above the choking value, i.e. $\frac{\theta_t}{T_{T_{III}}}$ is maximum, use of the engine as a suction pump at maximum R.P.M. will mean that the combustion chamber temperature $T_{T_{III}}$ must rise above the maximum allowable once the suction pressure difference is great enough for $\frac{P_{T_{III}}}{P_o}$ to fall below the choking value for the engine.

At lower R P M's, due to the decrease in θ_t it is possible to operate the engine at values of $\frac{P_{T_{III}}}{P_o}$ less than the choking value without the maximum temperature being exceeded. Greater suction pressure differences will not be obtained as the ratio $\frac{P_{T_{II}}}{P_{T_I}}$ is decreased,

(as is the mass flow through the engine), corresponding to the R.P.M. This is illustrated in Figures 18 and 19.

It can be seen that the use of the jet engine directly coupled as a suction pump involves the further restriction of minimum flow rates as well as the existing maximum flow rates through the engine. This is due to the rapid increase in total temperature at the turbine inlet both at low mass flow at low R.P.M. and at high suction pressure difference at maximum R.P.M. This low limitation can be met by having bleed valves from atmosphere at the inlet to the engine allowing additional air to pass through the engine, as described in reference 13.

The advantages of fitting an end diffuser are in the main, the same as already shown in section 4.12 in that the choking value of $\frac{P_{T_{III}}}{P_o}$ is reduced thus increasing the suction that may be obtained at maximum R.P.M. without exceeding the maximum allowable temperature for $T_{T_{III}}$ (see Figures 18 and 19).

In calculating the effect of an end diffuser, the annulus area was not known, it was more convenient to assume that the diffuser started from the final nozzle of the jet pipe. In practice it would start immediately from the annulus thus obviating the jet pipe losses, consequently the present assumption should be conservative for conditions below choking at the diffuser inlet. Once the diffuser has choked flow downstream of the inlet will be supersonic being followed by a normal shock and subsonic flow, the position of the shock being determined by the pressure difference across the diffuser[9]. As the present purpose is to utilise any excess of pressure that may exist at the inlet to the diffuser above the choking pressure ratio for pumping purposes flow in this regime need not be considered in detail. Details of the calculation of the characteristics are given in Appendix C.

4.2 Matching of pump characteristics to tunnel characteristics

No difficulties are involved in the matching process for this case as both the tunnel and pump characteristics can be determined independent of one another and consequently the selection of possible working section Mach numbers and areas can be readily made.

One method of matching the mass flow, that has been used experimentally[13] is to provide air bleed valves immediately in front of the pump.

5 Jet engine drive by suction and induction pumping in parallel

5.1 Determination of combined pump characteristics

In this arrangement (see Figure 3) the engine is contained within the tunnel, part of the tunnel air flows through the engine (acting as a suction pump) whilst the remainder flows around the engine[1], the flow being maintained by the induction effect of the jet issuing from the engine.

Hence the two methods of pumping may be considered to act in parallel as the total tunnel flow is divided between them.

For tunnel design purposes it is only the combined pump characteristic that is of interest but this cannot be directly obtained as the characteristics of the two component systems are dissimilar; they must necessarily operate between different pressures (due to further

pressure loss between station 2 and 3 (Figure 3) in the flow around the engine section), and initially the division of flow between the two cannot be predicted.

Due to these and other complexities it is not possible to generalize the pump characteristics, and they must be referred to a particular configuration.

5.11 Flow around engine

To determine the combined pump characteristic for a given configuration the loss in total pressure of the flow around the engine must first be determined as the induction pump must compensate for this loss as well as the normal depression at the inlet to the pump (i.e. at station 2).

To simplify the calculation of the pressure loss an approximate method has been used based on the drag coefficients of the nacelle and struts in a uniform stream.

An estimate of the flow conditions at the two end planes can be made using these drag coefficients if they are assumed independent of pressure and Mach number. The method of analysis is given in Appendix D and Figure 20 shows the relationship between the Mach number (M_2) at the beginning of the flow around the engine section and the end Mach number (M_a) and also the total pressure ratio for different values of the "drag factor" K (where K is a function of the various drag coefficients) such that

$$K = \frac{C_{D(nacelle)}}{\pi}\left(\frac{d}{D}\right)^2 + \frac{C_{D(struts)}}{4}\,\frac{A_f}{A_3} + C_f\,\frac{L}{D}$$

where
- d = maximum diameter of engine housing
- D = diameter of tunnel at engine section
- A_f = frontal area of struts
- A_3 = area of tunnel section at station 3
- L = length of engine section
- C_f = friction drag coefficient of tunnel walls

5.12 Suction pump characteristics

From the analysis of the preceeding section the total pressure and Mach number at station 3 can be determined for any given mass flow (m_a) around the engine section, if the conditions of total pressure and temperature at station 2 are assumed corresponding to a desired tunnel working section Mach number. The total temperature of the air flowing around the engine section will be the same at station 3 as at station 2 if the heat addition due to cooling of the engine is assumed negligible.

As the Mach number of the air approaching the engine will be small the intake ram compression can be assumed isentropic, i.e. the nacelle total pressure (P_{T_I}) is assumed the same as the total pressure at station 2 (P_{T_2}). The jet will discharge into the mixing chamber at a static pressure P_a (determined as above) so the engine operates as though it had a ficticious ram pressure ratio $\frac{P_{T_2}}{P_a}$, which is greater than one.

The jet flow relations cannot be determined by assuming the final nozzle is choked at maximum R.P.M., even if this ram pressure ratio is

appreciable, if the tunnel air total temperature has been increased by partial recirculation. The jet velocity and total pressure must be determined from the thrust and flow data. However if the tunnel is running at atmospheric temperature the final nozzle will generally be choked at maximum R.P.M. Hence assuming the total mass flow at station 2 can be varied to suit the suction pump requirements, the engine mass flow (m_J) can be determined for a given mass flow (m_a) around the engine, i.e. the mass flow ratio β is determined for a given total mass flow (m_2) at station 2 where $m_2 = m_J + m_a$. This determination is, of course, made on the assumption that the induction pump characteristics are exactly those required to maintain the flow m_a in all cases.

These induction pump characteristics however will be correct for only one value of m_a, i.e. the value of β so that there will be a single value of m_2 for the assumed pressure and temperature conditions at 2 and the engine R.P.M.

5.13 Induction pump characteristics

For a given value of m_a the corresponding value of β has been determined in section 5.12 and the value of P_{T_a} and T_{T_a} in section 5.11.

Hence $\frac{P_{T_J}}{P_{T_a}}$, $\frac{T_{T_J}}{T_{T_a}}$, β and α are known so that $\frac{\Delta P_T}{P_o} \times 14.7$ can be found either by interpolation from Figures 11 to 13 or directly as in Appendix B.

Hence P_{T_a}' is determined where $P_{T_a}' = P_o - \Delta P_T$ and P_{T_a}' is compared to P_{T_a} as determined in section 5.11. The value of m_a at which $P_{T_a}' \equiv P_{T_a}$ is the flow that can be maintained by the induction pump.

From the appropriate value of β the total pump flow m_2 can then be obtained corresponding to the conditions P_{T_2}, T_{T_2}, the pump configuration and the engine R.P.M.

Two such cases showing the variation of mass flow to pressure rise are shown in Figure 21 for tunnel total temperatures. $T_{T/S} = 288^{\circ}K$ and $333^{\circ}K$ at engine maximum R.P.M. and a configuration such that the "friction factor" $K = 0.04$.

Figure 22 taken from reference 14 shows the change in engine performance for a Jumo 004 engine run both as a parallel suction and induction pump and also with portions of the centre duct removed, i.e. under test bed conditions. The difference between the two thrust curves (measured by a precimeter) gives a rough figure for the drag of the engine and support in the tunnel; it is to be noted however that the thrust has not been corrected for the exhaust depression. When running as a pump the air velocity about 10 inches in front of station 2 Figure 3 was about 230 feet per second at an engine speed of 8400 R.P.M. and 180 feet per second at an engine speed of 7600 R.P.M. It will be observed that the exhaust total heads in both sets of results are the same but that the specific fuel consumption is higher when the engine is running in the complete tunnel.

6 Discussion

6.1 The characteristics of wind tunnels with three different methods of jet engine drive have been discussed in the light of present theoretical and experimental data. Methods of determining basic designs have also been indicated for each method of drive.

The main factors to be considered in making the basic selection between each method of drive for a particular type of tunnel are,

(a) The mass flow to pressure rise characteristics of each method of pumping,

(b) The form of humidity control to be employed,

(c) The engine accessibility for maintenance.

6.2 For subsonic tunnels curves illustrating the pressure rise to mass flow characteristics are shown in Figure 21 for humidity control by recirculation, i.e. working section total temperatures raised to 60°C.

For these conditions induction pumping gives a greater mass flow at maximum performance of a R.R. Nene II than either the parallel or suction pumping systems. However if humidity is controlled by pre-drying the parallel pumping system gives a higher mass flow. Of course this comparison depends on the accuracy of the estimation of pressure losses around the engine nacelle in the parallel pumping case.

For humidity control by partial recirculation and induction pumping it is shown in Appendix E that a 5000 lb thrust engine can drive a tunnel of 4 ft^2 square working section up to $M = 1$.

Part load characteristics of such a drive are shown in Figure 29 as also is the effect of friction in the mixing chamber.

6.3 For small supersonic tunnels the pumping characteristics required are opposite to those for a subsonic tunnel, i.e. a high pressure rise with a small mass flow is wanted.

Pressure rises sufficient for working section Mach numbers up to about 1.8 to 2.0 can be achieved with induction pumping by using large area ratios ($\alpha > 0.5$) or by suction pumping if an end diffuser is used in place of the normal jet pipe. For the examples considered with humidity control by recirculation the mass flow by either method is about the same. A working section 1 ft square could probably be obtained over a Mach number range of 1.2 to 1.8 by a single 5000 lb thrust engine used as either an induction or a suction drive (see Appendix E).

A higher Mach number range could be achieved by using a second throat that has a smaller pressure loss characteristic than conventional tunnel configurations.

6.4 Satisfactory operation should also be possible with a somewhat larger working section operating at lower supersonic Mach numbers.

For example in Appendix E it is shown that with humidity control by partial recirculation and induction pumping a 5000 lb thrust engine can drive a supersonic tunnel up to $M = 1.2$ of 2 ft^2 square working section.

6.5 Induction pumping is the only system that readily lends itself to multi-engine drive, i.e. permits larger working sections to be used.

Theoretically the pressure rise to mass flow ratio characteristics would be unaltered with the present analysis if the area ratio α was maintained the same. Experimentally Rolls Royce[8] have found no real difference between the effects of a single or double jet drive with the same overall mass flow.

6.6 It has been shown by Nicholson[15] that the engine cost is the main criterion in any economic comparison of the capital cost of this type of tunnel with any other type of tunnel. If the engines are available the additional capital cost will be small, in the region of £3500 - 4000 but operating cost will be fairly high.

6.7 Tunnels with jet engine drive can be quickly developed and are very suitable for interim needs during the necessarily long design and construction times of more permanent and elaborate tunnels. Useful data could be obtained and staff trained.

SYMBOLS

A = area of cross section

A_f = frontal area of struts

a = velocity of sound

a_T = total or stagnation velocity of sound

$B = \frac{1}{1+\alpha}\left(1 + \beta \frac{v_j}{v_a}\right)$

$C = \frac{1}{1+\alpha}\sqrt{(1+\beta)\left(1+\beta\frac{T_{T_j}}{T_{T_a}}\right)} = \frac{Y}{1+\alpha}$

C_D = drag coefficient

C_F = friction coefficient

C_p = specific heat at constant pressure

D = duct diameter

d = engine diameter

F_G = gross thrust

f = fuel flow

$G = \frac{\sqrt{\frac{gY}{R}}}{\left[1+\frac{Y-1}{2}\right]^{\frac{Y+1}{2(Y-1)}}}$

$K = \left[\frac{C_{D(\text{nacelle})}}{\pi} \left(\frac{d}{D}\right)^2 + \frac{C_{D(\text{strut})}}{4} \left(\frac{A_f}{A_3}\right) + C_f \left(\frac{L}{D}\right) \right]$

L = length of mixing chamber or engine section

M = Mach number

m = mass flow

P = static pressure

P_T = total pressure

ΔP_f = pressure loss due to friction in mixing chamber

R = gas constant

S.F.C. = specific fuel consumption

T = static temperature

T_T = total temperature

v = velocity

$X = \left[\frac{P_{T_j}}{P_{T_a}} \alpha(1 + \gamma M_j^2) \frac{P_j}{P_{T_j}} + (1 + \gamma M_a^2) \frac{P_a}{P_{T_a}} - (1 + \alpha) \frac{\Delta P_f}{P_{T_a}} \right]$

$Y = \sqrt{\left(1 + \beta \frac{T_{T_j}}{T_{T_a}}\right)(1 + \beta)}$

α = ratio jet inlet area to air inlet area at beginning of mixing section

β = ratio of jet gas mass flow to induced air mass flow

γ = ratio of specific heats

η = adiabatic efficiency

$\xi = \gamma \pm (1 + \alpha) K$

$\phi_1(M) = (1 + \gamma M^2) \frac{P}{P_T}$

$\phi_2(M) = \frac{A}{A^*} (1 + \gamma M^2) \frac{P}{P_T}$

θ = temperature rise or fall

ρ = density

SUFFIXES

0,1,2,3,4,5 refer to Stations on appropriate diagram

a Station at air inlet to mixing chamber

j Station at jet inlet to mixing chamber

t refers to turbine

c refers to compressor

I II III and IV refer to stations in jet engine (see Figure 4)

REFERENCES

Ref. No.	Author	Title, etc.
1	H.W. Liepmann and A.E. Puckett	Aerodynamics of a Compressible fluid P.85.
2	H. Eggink	The improvement in pressure Recovery in Supersonic Wind Tunnels R & M.2703, May 1949.
3	J. Lukasiewicz	Supersonic Diffusers R & M.2501, June 1946.
5	W.R. Hawthorne and H. Cohen	Pressure losses and velocity changes due to heat release and mixing in frictionless compressible flow A.R.C.7623, January 1944.
6	Wagner, Koscin and Kellermann	On the Developing of Jet Pumps Volkenrode Report and Translation No.437 A.R.C.11,274, July 1944.
7	Propulsion Branch	A theoretical and experimental investigation of flow induction systems applicable to wind tunnels C.A.L. Report No. AD-526-A-1 February 1948.
8	Experimental Department Report, Rolls Royce Ltd.	Handley Page Injector Wind Tunnel - Preliminary tests of a one tenth scale model Ref. Chr/WJA1/BH 22-4-49.
9	Young and Green	Tests of High Speed flow in Diffusers of Rectangular Cross Sections R & M.2201, July 1944.
10	W. R. Hawthorne	Simplified Analysis of Frictional and Compressible flow in pipes A.R.C.5847, March 1942.
11	Young and Winterbottom	High Speed flow in Smooth Cylindrical Pipes of Circular Section R & M.2068, November 1942.
12	A.B.P. Beeton	Calculations on effects of high forward speeds on performance of Jet Propulsion engines A.R.C.12,192, December 1948.
13	P.R. Owen	Tests on the 25 cm tunnel with a gas turbine drive R.A.E. C.W. Internal Memo No.15
14	K. Hunter	An Experimental Jet Engine Ejector Tunnel N.R.C.C. Report No. ME.167

REFERENCES (Contd.)

Ref. No.	Author	Title, etc.
15	L.F. Nicholson	A Brief Comparison of Some Alternative Types of High Speed Wind Tunnel A.R.C.11,425, April 1948.
16	J. Lukasiewicz	Humidity effects in Supersonic Flow of air R & M.2563, June 1948.
17	J.K. Royle	Control of Condensation in Supersonic Tunnels by Pre-Expansion R & M.2563, June 1948.
18	A.B.P. Beeton	Characteristics for Choking Jet Engine Nozzles Including Reheat and Water Injection A.R.C.11,569, April 1948.
19	D.F. Collins	An estimation of thrust minus drag of a ducted Fan Engine A.R.C.11,823, August 1948.

APPENDIX A

Methods of Humidity Control Applicable To Wind Tunnels with Jet Engine Drives

Three main methods of controlling humidity effects are possible

(a) Increasing the stagnation temperature in the working section

(b) Pre-drying the air

(c) Pre-expansion of the air in an auxiliary nozzle.

1.0 Humidity control by increase of stagnation temperature

With tunnels with jet engine drives the working section stagnation temperature would normally be atmospheric temperature but Lukasiewig[16] has shown that if this temperature is increased an effective humidity control can be achieved. Figure 23 (from Ref.16) shows the effect of increasing the stagnation temperature on the Mach number at which condensation will first occur for typical conditions in the British Isles.

From this figure it can be seen that a total temperature of 50°C in the working section will eliminate all humidity effects at Mach numbers up to 1.5. This temperature should not be excessive for most model and strain gauge techniques.

1.1 Increase of stagnation temperature by recirculation

Partial recirculation of the hot gases from the tunnel exhaust (see Fig.4) is one of the most convenient methods of raising the working section stagnation temperature.

The main considerations in the use of this method are

(i) The water content of the gases due to combustion

(ii) The mixing of the recirculating gases and intake air.

1.11 Humidity due to fuel combustion

Using the basic tunnel design of example 1 of Appendix E the water content of the exhaust gases from the tunnel has been estimated at from 0.013 to 0.015 lb of H_2O per lb of exhaust gas assuming the engine to be operating at Maximum R.P.M. air at summer temperature but dry, and that the fuel may be approximated to dodecane ($C_{12}H_{26}$).

The corresponding total temperatures of the exhaust gases would be 7-800°K.

Recirculation of this gas gives an absolute humidity of approximately 0.0010 to 0.0011 at a working section total temperature of 50°C (assuming intake air perfectly dry).

If the absolute humidity of the air is assumed to be 0.006 the corresponding humidity in the working section would be 0.0069 to 0.0071. The critical Mach number corresponding to the latter value of the absolute humidity will be 1.46 as compared with 1.5 given in Figure 23 for the air heated by a heat exchanger or some other method by which the water content is not changed.

To eliminate humidity effects at working section Mach numbers about 2.0 the working section stagnation temperature must approach 100°C and consequently more exhaust gases would need to be recirculated, i.e. the water content in the working section would be increased. Under similar conditions to the foregoing case the absolute humidity in the working section would be 0.011, however the relative humidity would be decreased to about 0.018. Without recirculation values would be 0.006 and 0.010 respectively.

Lukasiewig[16] states that to a first approximation the relative humidity defines the Mach number at which condensation shocks first appears where as its intensity is mainly a function of the absolute humidity. The difference in relative humidity will decrease the critical Mach number in this case by about 0.1 and as long as the shock is supressed the high absolute humidity will not be significant.

Hence, in general, the humidity due to fuel combustion will not add greatly to the effect of atmospheric humidity and the selection of fuels with low hydrogen content does not appear to be specially necessary.

1.12 Inlet mixing arrangements

The arrangements at the inlet for distributing and mixing the recirculated air must be carefully considered. The distributor must have as small as pressure loss as possible relative to both the intake air and the exhaust gas.

As the total pressure and velocity of the return gases will not be very different from the intake air there will be little 'momentum' mixing action in excess of normal turbulent mixing.

Consequently the arrangements of the distributor at the inlet should be such that the return gas flow is introduced as uniformly as possible over the whole area of the inlet thus giving a good initial mixing of the two flows. Further a long 'settling' chamber should follow so that flow mixing can be completed and turbulence reduced. A large contraction ratio of 14:1 to 20:1 should follow to minimize turbulence in the working section.

1.2 Increase of stagnation temperature by a heat exchanger

A heat exchanger with a honey comb layout can be used at the inlet to the tunnel to raise the air temperature. The heating fluid can be either from some form of combustion chamber (or steam plant) or from the actual tunnel exhaust. (See Figure 5).

The former arrangement allows a heat exchanger to be designed with the main emphasis on the aerodynamic features of the cold air side as the heating side is independent of the tunnel and its internal efficiency will not affect the tunnel working provided it functions correctly. The main features to be considered on the intake side are that the tunnel intake air should have a reasonable temperature and flow distribution and that the pressure loss through the exchanger should be as small as possible.

As the exchanger must be a cross flow type to obtain uniform heating it would be advisable to divide the exchanger into two banks in which the heating flow direction is reversed. To maintain a good flow distribution the intake flow should be through the tubes which should be of as large a diameter as possible to reduce the pressure loss.

If the tunnel exhaust gas is used for the heating fluid as much care must be given to the design of the hot side as it will also affect the tunnel performance.

The exhaust gas mass flow will usually contain much more available heat than is required by the incoming air so on the hot side the pressure loss through the exchanger will be the main consideration.

If the pressure difference required to maintain flow through the hot side of the heat exchanger is small hot air ducting similar to that used with the recirculating system may be used; the effect on the tunnel performance being small. If the pressure loss through the heat exchanger is appreciable the hot air collector must be taken off from near the end of the pump mixing chamber thus by passing a large percentage of the flow through the pump end diffuser and thus reducing the pressure recovery of the pump system.

2 Humidity control by pre drying

For continuous drying of the air by silica gel, or other chemical dryers, large quantities will be required. Also provision must be made for reactivation of the silica gel after a limited running time. With the gel arranged on horizontal beds 10 inches deep and a maximum flow velocity through the bed of 10 feet/sec the total pressure loss should not exceed 0.2 lb/in^2. For a high speed subsonic tunnel with as mass flow about 550 lb/sec (working section about 12 ft^2) the area of silica gel beds required would be about 750 sq.ft. i.e. about 23 tons of gel would be required.

The cost of this large amount of gel would probably be more than the cost of the rest of the tunnel.

3 Humidity control by pre expansion

It has been shown[17] that humidity can be controlled in supersonic tunnels by preliminary condensation by expansion in an auxiliary nozzle preceeding the test section nozzle.

Figure 24, taken from reference 17, shows the total pressure loss and flow conditions for different throat area ratios of the two nozzles of a 4" x 4" open circuit supersonic tunnel. In these tests the velocities before the main nozzle, were high and there was appreciable adiabatic cooling so that re-evaporation of the condensed water was suppressed. The reduction in total pressure before the main nozzle was about 17% of the atmospheric total pressure for complete control of humidity effects. That is an additional pumping pressure rise of about 2.5 lb/in^2 would be needed to operate this form of humidity control.

This pressure loss would be additional to the normal tunnel pressure losses and for present types of pumping the mass flow would be quite small i.e. the method of humidity control does not permit satisfactory tunnel designs of this type.

APPENDIX B

Theoretical Determination of Induction Pump Characteristics

1 General Analysis

(See paragraph 3 of discussion and reference 7).

1.1 Mixing chamber characteristics

Assumptions

(a) Flow is compressible.

(b) Mixing is complete by station 4 (see Fig. 1).

(c) Ratio of specific heats is the same for both gases.

(d) Flow is not frictionless in mixing chamber.

(e) Static pressure of the induced air and jet air need not necessarily be equal.

From Conservation of Mass

With the configuration illustrated in Fig.1

$$m_a + m_j = m_4 \tag{1}$$

$$\therefore \quad m_a (1 + \beta) = m_4$$

$$\rho_a v_a A_a (1 + \beta) = \rho_4 v_4 A_4$$

Assuming γ and R the same at all sections

$$\frac{P_a M_a A_a \sqrt{1 + \frac{\gamma - 1}{2} M_a^2}}{\sqrt{T_{T_a}}} (1 + \beta) = \frac{P_4 M_4 A_4 \sqrt{1 + \frac{\gamma - 1}{2} M_4^2}}{\sqrt{T_{T_4}}} \tag{2}$$

From Conservation of Energy

$$m_a C_{P_a} T_{T_a} + m_j C_{P_j} T_{T_j} = m_4 C_{P_4} T_{T_4}$$

Assuming C_p the same at all sections

$$T_{T_a} + \beta T_{T_j} = (1 + \beta) T_{T_4} \tag{3}$$

substituting in (2)

$$P_4 M_4 A_4 \sqrt{1 + \frac{\gamma-1}{2} M_4^2} = \sqrt{1+\beta}\, P_a M_a A_a \sqrt{1+\frac{\gamma-1}{2} M_a^2} \sqrt{1+\beta \frac{T_{T_j}}{T_{T_a}}}$$

whence

$$\frac{P_{T_4}}{P_{T_a}} = \frac{1}{1+\alpha} \frac{\dfrac{M_a}{\left(1 + \frac{\gamma-1}{2} M_a^2\right)^{\frac{\gamma+1}{2(\gamma-1)}}}}{\dfrac{M_4}{\left(1 + \frac{\gamma-1}{2} M_4^2\right)^{\frac{\gamma+1}{2(\gamma-1)}}}} \sqrt{1 + \beta \left(\frac{T_{T_j}}{T_{T_a}}\right)} \sqrt{1+\beta}$$

i.e.

$$\frac{P_{T_4}}{P_{T_a}} = \frac{1}{1+\alpha} \frac{\dfrac{M_a}{\left[\dfrac{1 + \frac{\gamma-1}{2} M_a^2}{1 + \frac{\gamma-1}{2}}\right]^{\frac{\gamma+1}{2(\gamma-1)}}}}{\dfrac{M_4}{\left[\dfrac{1 + \frac{\gamma-1}{2} M_4^2}{1 + \frac{\gamma-1}{2}}\right]^{\frac{\gamma+1}{2(\gamma-1)}}}} \sqrt{\left(1 + \beta \frac{T_{T_j}}{T_{T_a}}\right)(1+\beta)}$$

$$= \frac{1}{1+\alpha} \frac{\dfrac{A_4}{A_4^*}}{\dfrac{A_a}{A_a^*}} \sqrt{\left(1 + \beta \frac{T_{T_j}}{T_{T_a}}\right)(1+\beta)}$$

$$= \frac{Y}{1+\alpha} \frac{\dfrac{A_4}{A_4^*}}{\dfrac{A_a}{A_a^*}} \qquad (4)$$

where $Y = \sqrt{\left(1 + \beta \dfrac{T_{T_j}}{T_{T_a}}\right)(1+\beta)}$

From Conservation of Momentum

$$P_4 A_4 (1 + \gamma M_4^2) = P_j A_j (1 + \gamma M_j^2) + P_a A_a (1 + \gamma M_a^2) - A_4 \Delta P_f$$

$$P_{T_4} A_4 (1+\gamma M_4^2) \frac{P_4}{P_{T_4}} = P_{T_j} A_j (1+\gamma M_j^2) \frac{P_j}{P_{T_j}} + R_{T_a} A_a (1+\gamma M_a^2) \frac{P_a}{P_{T_a}} - A_4 \Delta P_f$$

$$\therefore \frac{P_{T_4}}{P_{T_a}} = \frac{1}{(1+\alpha)(1+\gamma M_4^2)\frac{P_4}{P_{T_4}}} \left[\frac{P_{T_j}}{P_{T_a}} \alpha (1+\gamma M_j^2) \frac{P_j}{P_{T_j}} + (1+\gamma M_a^2) \frac{P_a}{P_{T_a}} - (1+\alpha) \frac{\Delta P_f}{P_{T_a}} \right]$$

i.e.

$$\frac{P_{T_4}}{P_{T_a}} = \frac{X}{(1+\alpha)(1+\gamma M_4^2)\frac{P_4}{P_{T_4}}} \qquad (5)$$

where $X = \left[\frac{P_{T_j}}{P_{T_a}} \alpha (1+\gamma M_j^2) \frac{P_j}{P_{T_j}} + (1+\gamma M_a^2) \frac{P_a}{P_{T_a}} - (1+\alpha) \frac{\Delta P_f}{P_{T_a}} \right]$

$$= \left[\frac{P_{T_j}}{P_{T_a}} \alpha \phi_1 (M_j) + \phi_1 (M_a) - (1+\alpha) \frac{\Delta P_f}{P_{T_a}} \right]$$

where $\phi_1 (M) = (1+\gamma M^2) \frac{P}{P_T}$

hence from equations (4) and (5)

$$\frac{\gamma}{(1+\alpha)} \frac{\frac{A_4}{A_4^*}}{\frac{A_a}{A_a^*}} = \frac{X}{(1+\alpha)} \cdot \frac{1}{(1+\gamma M_4^2)\frac{P_4}{P_{T_4}}}$$

$$\therefore \frac{A_4}{A_4^*} (1+\gamma M_4^2) \frac{P_4}{P_{T_4}} = \frac{X}{\gamma} \frac{A_a}{A_a^*}$$

$$\therefore \phi_2 (M_4) = \frac{X}{\gamma} \frac{A_a}{A_a^*} \qquad (6)$$

where $\phi_2 (M_4) = \frac{A_4}{A_4^*} (1 + \gamma M_4^2) \frac{P_4}{P_{T_4}}$. As $\frac{A_4}{A_4^*}$ and $\frac{P_4}{P_{T_4}}$ are functions of M_4 and γ alone.

$\therefore \phi_2 (M_4)$ is a function of M_4 and γ alone and consequently from flow tables a curve of $\phi_2 (M_4)$ to M_4 may be plotted (see Fig.25)

X , Y and $\frac{A_a}{A_a^*}$ are determined from the inlet conditions. Hence for given intake conditions eqn.(6) determines M_4 and knowing M_4 gives $\frac{A_4}{A_4^*}$ and equation (4) gives

$\frac{P_{T_4}}{P_{T_a}}$ the required pressure ratio

It must be noted that

$$\mu = \frac{m_J}{m_a} = \frac{\rho_j v_J A_J}{\rho_a v_a A_a}$$

$$\doteq \alpha \frac{P_{T_J}}{P_{T_a}} \left[\frac{\frac{A_a}{A_a^*}}{\frac{A_J}{A_j^*}} \right] \sqrt{\frac{T_{T_a}}{T_{T_j}}} \qquad (7)$$

Hence knowing the jet and induced air Mach numbers the area ratio α and the total pressure and total temperature ratios of the jet and induced air, the exit conditions at section (4) and the pressure ratio $\frac{P_{T_4}}{P_{T_a}}$ can be determined.

1.2 Friction loss in mixing chamber

For turbulent flows the shearing stress f_s in the boundary layer can be put equal to $C_f \times \frac{1}{2}\rho v^2$ where C_f is the skin friction coefficient.

Hence considering an elementary length dL of the mixing chamber wall the friction force $\delta f = f_s \cdot S$ where S is wetted surface

$= \frac{1}{2}\rho v^2 C_f \pi D \, dL$ where D is diameter of mixing chamber

$= \frac{1}{2} \gamma P M^2 \frac{\lambda A}{D} dL$ where A is the cross sectional area of the mixing chamber and $\lambda = 4 C_f$.

Hence Total frictional force

$$F_f = \int_0^L \tfrac{1}{2} \gamma P M^2 \frac{\lambda A}{D} \, dL \qquad (8)$$

But $F_f = A \, \Delta P_f$ where ΔP_f is the total pressure loss due to friction

$$\therefore \Delta P_f = \tfrac{1}{2} \frac{\gamma}{D} \int_0^L P M^2 \lambda \, dL$$

If the driving jet is located coaxially with the mixing chamber the flow conditions at the wall at inlet will correspond to those of the induced air and at outlet will be those of station "4".

Hence to a first approximation

$$\Delta P_f = \tfrac{1}{2} \frac{\gamma L}{D} \left[\frac{\lambda_a P_a M_a^2 + \lambda_4 P_4 M_4^2}{2} \right]$$

$$= \frac{\gamma L}{4D} \left[\lambda_a P_a M_a^2 + \lambda_4 P_4 M_4^2 \right]$$

from practice it has been found that $L \approx 4D$

$$\therefore \Delta P_f = \gamma \left[\lambda_a P_a M_a^2 + \lambda_4 P_4 M_4^2 \right] \qquad (9)$$

$$\therefore (1 + \alpha) \frac{\Delta P_f}{P_{T_a}} = (1 + \alpha) \gamma \left[\lambda_a \frac{P_a}{P_{T_a}} M_a^2 + \lambda_4 \frac{P_4}{P_{T_4}} \cdot \frac{P_{T_4}}{P_{T_a}} M_4^2 \right]$$

The values of the friction coefficients λ have been given by Prandtl as

$$\frac{1}{\sqrt{\lambda}} = 2.0 \log_{10} (R_N \cdot \sqrt{\lambda}) - 0.8 \qquad (10)$$

where R_N is the Reynolds number

$$R_{N_a} = \frac{P_a M_a D}{\mu_a} \sqrt{\frac{\gamma g}{R T_a}} \qquad (11)$$

where $\mu_a = 11.51 \times 10^{-6} \left[\frac{408}{T_a + 120} \left(\frac{T_a}{288} \right)^{3/2} \right]$ lb ft^{-1} sec^{-1} T_a in $^\circ$K

and same for R_{N_4}.

Values of P_a M_a T_a and P_4 M_4 T_4 may be determined approximately by completing a mixing analysis in which

$$(1 + \alpha)\frac{\Delta P_f}{P_{T_a}} = 0 \quad \text{when determining} \quad X$$

i.e. flow is assumed frictionless.

1.3 End diffuser characteristics

From continuity

$$A_4 \rho_4 v_4 = A_5 \rho_5 v_5$$

$$\therefore \frac{A_4}{A_5} = \frac{P_5}{P_4} \frac{M_5}{M_4}\sqrt{\frac{T_4}{T_5}}$$

$$= \frac{P_5}{P_4} \frac{M_5}{M_4}\sqrt{\frac{1 + \frac{\gamma-1}{2} M_5^2}{1 + \frac{\gamma-1}{2} M_4^2}} \qquad (12)$$

as $T_{T_4} = T_{T_5}$ for no heat addition or loss

hence

$$\frac{A_4}{A_5} = \frac{P_{T_5}}{P_{T_4}} \frac{\left(1 + \frac{\gamma-1}{2} M_5^2\right)^{\frac{\gamma+1}{2(\gamma-1)}}}{\frac{M_5}{M_4}\left(1 + \frac{\gamma-1}{2} M_4^2\right)^{\frac{\gamma+1}{2(\gamma-1)}}}$$

$$= \frac{P_{T_5}}{P_{T_4}} \left[\frac{\frac{A_4}{A_4^*}}{\frac{A_5}{A_5^*}}\right] \qquad (13)$$

For given values of $\frac{A_4}{A_5}$ and $\frac{P_{T_5}}{P_{T_4}}$ and $\frac{A_4}{A_4^*}$ corresponding to M_4 it is possible to obtain $\frac{A_5}{A_5^*}$ i.e. M_5, once M_5 is determined $\frac{P_5}{P_{T_5}}$ can be obtained.

Thus

$$\frac{P_{T_4}}{P_0} = \frac{P_{T_4}}{P_5} = \frac{P_{T_4}}{P_{T_5}} \Big/ \frac{P_5}{P_{T_5}}$$ is obtained for M_4 as $P_5 = P_0$ atmospheric pressure.

Hence the diffuser characteristic of inlet total head to atmospheric pressure ratio is obtained for the inlet Mach number.

It is also convenient to be able to express the diffuser characteristic in terms of the "dimensionless" mass flow parameter

$$\frac{m_4 \sqrt{T_{T_4}}}{A_4 P_{T_4}}$$

at the inlet rather than the Mach number. This parameter is obtained as follows.

From continuity

$$m_4 = \rho_4 v_4 A_4$$

$$= \frac{A_4 P_4 M_4}{\sqrt{T_4}} \sqrt{\frac{g\gamma}{R}}$$

$$= \frac{A_4 P_{T_4}}{\sqrt{T_{T_4}}} \frac{M \left(1 + \frac{\gamma-1}{2} M_4^2\right)^{\frac{\gamma}{1-\gamma}}}{\left(1 + \frac{\gamma-1}{2} M_4^2\right)^{-\frac{1}{2}}} \sqrt{\frac{g\gamma}{R}}$$

i.e.

$$\frac{m_4 \sqrt{T_{T_4}}}{A_4 P_{T_4}} = \sqrt{\frac{g\gamma}{R}} \frac{M_4}{\left[\frac{1 + \frac{\gamma-1}{2} M_4^2}{1 + \frac{\gamma-1}{2}}\right]^{\frac{\gamma+1}{2(\gamma-1)}}} \times \frac{1}{\left[1 + \frac{\gamma-1}{2}\right]^{\frac{\gamma+1}{2(\gamma-1)}}}$$

$$= \frac{\sqrt{\frac{g\gamma}{R}}}{\left[1 + \frac{\gamma-1}{2}\right]^{\frac{\gamma+1}{2(\gamma-1)}}} \cdot \frac{1}{\left(\frac{A_4}{A_4^*}\right)}$$

$$= \frac{G}{\left(\frac{A_4}{A_4^*}\right)} \quad \text{where} \quad G = \frac{\sqrt{\frac{g\gamma}{R}}}{\left[1 + \frac{\gamma-1}{2}\right]^{\frac{\gamma+1}{2(\gamma-1)}}} \qquad (14)$$

as G is a constant and $\frac{A_4}{A_4^*}$ a function of M_4 alone then values of $\frac{m_4 \sqrt{T_{T_4}}}{A_4 P_{T_4}}$ can be obtained corresponding to M_4 and hence $\frac{P_{T_4}}{P_o}$ to $\frac{m_4 \sqrt{T_{T_4}}}{A_4 P_{T_4}}$ may be plotted.

N.B.

$\gamma = 1.33$ $\quad G = 56.0958$ $\quad (P_T$ in $lb/in^2)$

$\gamma = 1.40$ $\quad G = 57.105$ $\quad (P_T$ in $lb/in^2)$

In the foregoing it has been assumed that $\frac{P_{T_5}}{P_{T_4}}$ is known - for isentropic flow $\frac{P_{T_5}}{P_{T_4}} = 1$ but where the diffusion efficiency is not 100% it may be determined as follows, assuming an adiabatic efficiency η .

$$\therefore \frac{P_5}{P_4} = \left[(1 - \eta) + \eta \left(\frac{T_5}{T_4} \right) \right]^{\frac{\gamma}{\gamma-1}}$$

$$= \left[(1 - \eta) + \eta \left(\frac{1 + \frac{\gamma-1}{2} M_4^2}{1 + \frac{\gamma-1}{2} M_5^2} \right) \right]^{\frac{\gamma}{\gamma-1}}$$

as $T_{T_4} = T_{T_5}$ for no heat added or lost. Also if $M_5 \longrightarrow 0$

$$\therefore \frac{P_5}{P_4} = \left[(1 - \eta) + \eta \left(1 + \frac{\gamma-1}{2} M_4^2 \right) \right]^{\frac{\gamma}{\gamma-1}}$$

$$= \left[1 + \frac{\gamma-1}{2} (\sqrt{\eta}\ M_4)^2 \right]^{\frac{\gamma}{\gamma-1}}$$

and as $M_5 \longrightarrow 0 \quad P_5 \longrightarrow P_{T_5}$

$$\therefore \frac{P_{T_5}}{P_4} = \left[1 + \frac{\gamma-1}{2} (\sqrt{\eta}\ M_4)^2 \right]^{\frac{\gamma}{\gamma-1}}$$

$$\therefore \frac{P_{T_5}}{P_{T_4}} = \left[\frac{1 + \frac{\gamma-1}{2} M_4^2}{1 + \frac{\gamma-1}{2} (\sqrt{\eta}\ M_4)^2} \right]^{\frac{\gamma}{1-\gamma}} \qquad (15)$$

which can be determined for values of M_4 and $\sqrt{\eta}\ M_4$ from flow-tables.

An alternative analysis only applicable to isentropic flow can be developed as follows.

From equation (12) substituting

$$\frac{T_4}{T_5} = \left(\frac{P_4}{P_5}\right)^{\frac{\gamma-1}{\gamma}}$$

$$\frac{A_4}{A_5} = \frac{P_5}{P_4}\ \frac{M_5}{M_4}\sqrt{\frac{1}{\left(\frac{P_5}{P_4}\right)^{\frac{\gamma-1}{\gamma}}}} \qquad (16)$$

and

$$\frac{P_5}{P_4} = \left(\frac{1 + \frac{\gamma-1}{2} M_4^2}{1 + \frac{\gamma-1}{2} M_5^2}\right)^{\frac{\gamma}{\gamma-1}} \qquad \text{if} \quad P_{T_4} = P_{T_5}$$

hence

$$M_5 = \frac{1 + \frac{2}{(\gamma-1) M_4^2}\left(1 - \left(\frac{P_5}{P_4}\right)^{\frac{\gamma-1}{\gamma}}\right)}{\left(\frac{P_5}{P_4}\right)^{\frac{\gamma-1}{\gamma}}}$$

$$= \frac{1 - y}{\left(\frac{P_5}{P_4}\right)^{\frac{\gamma-1}{\gamma}}}$$

where

$$y = \frac{2}{(\gamma-1)\ M_4^2} \cdot \left[\left(\frac{P_5}{P_4}\right)^{\frac{\gamma-1}{\gamma}} - 1\right] \qquad (17)$$

hence substituting in (16)

$$\frac{A_4}{A_5} = \left(\frac{P_5}{P_4}\right)^{\frac{1}{\gamma}} (1 - y)^{\frac{1}{2}} \qquad (18)$$

thus for M_4 and $\frac{A_4}{A_5}$, $\frac{P_5}{P_4}$ is obtained this being the form of the theoretical diffuser results presented in Reference 9 (see Fig.16 of that report.)

1.4 Injector pump characteristic

From section 1.1 $\frac{P_{T_4}}{P_{T_a}}$ is obtained in terms of β and also M_a and M_4 for given values of $\frac{T_{T_j}}{T_{T_a}}$, $\frac{P_{T_j}}{P_{T_a}}$ and α.

From section 1.3 $\frac{P_{T_4}}{P_o}$ is obtained in terms of M_4 hence the total pressure rise can be obtained in terms of β for

$$\frac{\Delta P_T}{P_o} = \frac{P_o - P_{T_a}}{P_o} = 1 - \frac{P_{T_a}}{P_o}$$

$$= 1 - \frac{P_{T_4}}{P_o} \Big/ \frac{P_{T_4}}{P_a} \qquad (19)$$

each term of which is known for values of M_4 (i.e. β) for the given values of $\frac{P_{T_j}}{P_{T_a}}$ $\frac{T_{T_j}}{T_{T_a}}$ and α.

2 Hawthorne and Cohens' analysis

In an earlier analysis by Hawthorne and Cohen[5] the static pressures P_j and P_a were assumed to be the same - that is the jet was assumed to be completely expanded.

This assumption automatically fixes the ratio $\frac{P_{T_j}}{P_{T_a}}$ for given jet and induced air Mach numbers, giving a particular solution of the foregoing general analysis.

Hawthornes and Cohens report give charts for the computation of pressure changes based on non-dimensional parameters B and C and M_a.

For the arrangements of Fig.1, the parameters B and C are given by

$$C = \frac{1}{1+\alpha} \sqrt{(1+\beta)\left(1+\beta\,\frac{T_{T_j}}{T_{T_a}}\right)}$$

$$B = \frac{1}{1 + \alpha}\left(1 + \beta \frac{v_j}{v_a}\right) = \frac{1}{1 + \alpha}\left(1 + \frac{\beta^2}{\alpha} \frac{T_{T_j}}{T_{T_a}}\right)$$

where

$$\frac{v_j}{v_a} = \frac{M_j}{M_a}\sqrt{\frac{T_j}{T_a}} = \frac{\beta}{\alpha} \frac{T_j}{T_a}$$

and

$$\beta = \alpha \frac{M_j}{M_a}\sqrt{\frac{T_a}{T_j}}$$

the flow throughout the mixing length is assumed frictionless and mixing is assumed complete.

The end diffuser characteristics were the same as those taken for the General Analysis.

3 Rolls Royce analysis

Rolls Royce Ltd[8] have presented an analysis in the form of a generalized mixing chamber characteristic (see Fig.26) based on a flow parameter and, a pressure parameter which are equal when there are no pressure or friction losses.

These parameters include terms that allow for the pressure rise in the diffuser exhausting the flow to atmosphere. In the present notation these parameters are

Flow Parameter

$$\left(\frac{\beta}{\alpha} - 1\right)\left(\frac{\beta}{\alpha} \frac{T_{T_j}}{T_{T_a}} - 1\right) + \frac{1}{2\alpha}\left[1 - \left(\frac{A_4}{A_5}\right)^2\right](1 + \beta)\left(1 + \beta \frac{T_{T_j}}{T_{T_a}}\right)$$

Pressure Drop Parameter

$$\left\{1 + \frac{P_o - P_{T_a}}{P_{T_a} - P_a}\right\} \quad \left\{1 + \tfrac{1}{2}\left[\frac{1}{\alpha} + \alpha\right]\right\}$$

Initially it was not clear on what assumptions the analysis was based or what was the character of these parameters so the analysis was repeated; for completeness it is included as follows. After some investigation it became evident that the parameters were based on incompressible flow i.e. the temperature equivalent of velocity was neglected and that, at the inlet to the mixing chamber, the driving jet and induced air static pressure were assumed the same.

MIXING SECTION

Consider first the mixing section.

From conservation of mass

$$m_a + m_j = m_4$$

whence

$$\frac{\rho_4 v_4}{\rho_a v_a} = \frac{1 + \beta}{1 + \alpha} \tag{20}$$

From conservation of energy

$$m_a C_{P_a} T_{T_a} + m_j C_{P_j} T_{T_j} = m_4 C_{P_4} T_{T_4}$$

assuming specific heats are the same

$$\frac{T_{T_4}}{T_{T_a}} = \frac{1 + \beta \frac{T_{T_j}}{T_{T_a}}}{1 + \beta} \tag{21}$$

From conservation of momentum

$$A_4 (P_4 + \rho_4 v_4^2) = A_a (P_a + \rho_a v_a^2) + A_j (P_j + \rho_j v_j^2)$$

$$\therefore \quad P_4 + \rho_4 v_4^2 = \frac{A_a}{A_4} P_a + \frac{A_j}{A_4} P_j + \frac{A_a}{A_4} \rho_a v_a^2 + \frac{A_j}{A_4} \rho v_j^2$$

Assuming $P_a = P_j$

$$P_4 + \rho_4 v_4^2 = P_a + \rho_a v_a^2 B \tag{22}$$

where

$$B = \left[\frac{A_a}{A_4} + \frac{A_j}{A_4} \frac{\rho_j v_j^2}{\rho_a v_a^2} \right]$$

$$= \frac{1}{1 + \alpha} \left[1 + \beta \frac{v_j}{v_a} \right]$$

$$= \frac{1}{1 + \alpha} \left[1 + \frac{\beta^2}{\alpha} \frac{T_{T_j}}{T_{T_a}} \right] \tag{23}$$

It is to be noted that this parameter B is the same as Hawthornes and Cohens for assuming incompressible flow

$$\beta = \frac{\rho_J \, v_J \, A_J}{\rho_a \, v_a \, A_a}$$

$$\therefore \quad \frac{v_J}{v_a} = \frac{\beta}{\alpha} \quad \frac{\rho_a}{\rho_J}$$

with incompressible flow, the temperature equivalent of velocity neglected.

$$\therefore \quad \frac{\rho_a}{\rho_J} = \frac{T_{T_J}}{T_{T_a}} \tag{24}$$

thus

$$\frac{v_j}{v_a} = \frac{\beta}{\alpha} \quad \frac{T_{T_j}}{T_{T_a}} \tag{25}$$

Hence from eqn.(22)

$$\frac{P_4 - P_a}{P_{T_a} - P_a} = \frac{\rho_a \, v_a^{\,2} \, B - \rho_4 \, v_4^{\,2}}{\frac{1}{2} \rho_a \, v_a^{\,2}}$$

$$= 2 \left(B - \frac{\rho_4 \, v_4^{\,2}}{\rho_a \, v_a^{\,2}} \right)$$

From (23)

$$= 2 \left[B - \frac{T_{T_4}}{T_{T_a}} \left(\frac{\rho_4 \, v_4}{\rho_a \, v_a} \right)^2 \right]$$

from (20)

$$= 2 \left[B - \frac{T_{T_4}}{T_{T_a}} \left(\frac{1 + \beta}{1 + \alpha} \right)^2 \right]$$

from (21)

$$= 2 \left[B - \frac{1}{(1 + \alpha)^2} \left(1 + \beta \, \frac{T_{T_j}}{T_{T_a}} \right) (1 + \beta) \right]$$

from (23)

$$= 2\left[\frac{1}{1+\alpha}\left(1+\frac{\beta^2}{\alpha}\frac{T_{T_j}}{T_{T_a}}\right)-\frac{1}{(1+\alpha)^2}\left(1+\beta\frac{T_{T_j}}{T_{T_a}}\right)(1+\beta)\right]$$

$$= \frac{2\alpha}{(1+\alpha)^2}\left[1+\frac{\beta^2}{\alpha^2}\frac{T_{T_j}}{T_{T_a}}-\frac{\beta}{\alpha}-\frac{\beta}{\alpha}\frac{T_{T_j}}{T_{T_a}}\right]$$

$$= \frac{2\alpha}{(1+\alpha)^2}\left\{\frac{\beta}{\alpha}-1\right\}\left\{\frac{\beta}{\alpha}\frac{T_{T_j}}{T_{T_a}}-1\right\} \qquad (26)$$

DIFFUSER SECTION

As flow is incompressible from continuity

$$A_4 v_4 = A_5 v_5$$

$$\therefore \quad 1-\left(\frac{v_5}{v_4}\right)^2 = 1-\left(\frac{A_4}{A_5}\right)^2$$

but

$$1-\left(\frac{v_5}{v_4}\right)^2 = \frac{\frac{1}{2}\rho\,(v_4^2 - v_5^2)}{\frac{1}{2}\rho\, v_4^2}$$

Assuming $P_{T_5} = P_{T_4}$ i.e. diffusion is esentropic

$$= \frac{P_5 - P_4}{P_{T_4} - P_4}$$

but $P_5 = P_o$ atmospheric pressure.

$$\therefore \frac{P_o - P_4}{P_{T_a} - P_a} = \frac{P_{T_4} - P_4}{P_{T_a} - P_a} \left(1 - \left(\frac{A_4}{A_5}\right)^2\right)$$

$$= \frac{\rho_4 v_4^2}{\rho_a v_a^2} \left(1 - \left[\frac{A_4}{A_5}\right]^2\right)$$

$$= \frac{T_{T_4}}{T_{T_a}} \left(\frac{1+\beta}{1+\alpha}\right)^2 \left\{1 - \left(\frac{A_4}{A_5}\right)^2\right\}$$

$$= \frac{\left(1 + \beta \frac{T_{T_j}}{T_{T_a}}\right)(1+\beta)}{(1+\alpha)^2} \left\{1 - \left(\frac{A_4}{A_5}\right)^2\right\}$$

$$= \frac{2\alpha}{(1+\alpha)^2} \left[\frac{1}{2\alpha} \left\{1 + \beta \frac{T_{T_j}}{T_{T_a}}\right\} \left\{1+\beta\right\} \left\{1 - \frac{A_4^2}{A_5^2}\right\}\right] \quad (27)$$

COMBINED MIXING SECTION AND EXIT DIFFUSER

Static pressure rise due to

mixing section $\Delta P_m = P_4 - P_a$

Static pressure rise due to

exit diffuser $\Delta P_o = P_o - P_4$

$\therefore$ Combined static pressure rise $= \Delta P_m + \Delta P_o$

$$\therefore \frac{\text{Combined static pressure rise}}{\text{Inlet dynamic head}} = \frac{P_o - P_a}{P_{T_a} - P_a}$$

$$= 1 + \frac{P_o - P_{T_a}}{P_{T_a} - P_a}$$

but $$\frac{\text{Combined static pressure rise}}{\text{Inlet dynamic head}} = \frac{P_4 - P_a}{P_{T_a} - P_a} + \frac{P_o - P_4}{P_{T_a} - P_a}$$

hence

$$\left\{1 + \frac{P_o - P_{T_a}}{P_{T_a} - P_a}\right\} = \frac{P_4 - P_a}{P_{T_a} - P_a} + \frac{P_o - P_4}{P_{T_a} - P_a} \qquad (28)$$

substitute eqns.(26) and (27)

$$\left\{1 + \frac{P_o - P_{T_a}}{P_{T_a} - P_a}\right\} = \frac{2\alpha}{(1+\alpha)^2}\left[\left\{\frac{\beta}{\alpha} - 1\right\}\left\{\frac{\beta}{\alpha}\frac{T_{T_j}}{T_{T_a}} - 1\right\} + \frac{1}{2\alpha}\left\{1 + \beta\frac{T_{T_j}}{T_{T_a}}\right\}\left\{1 + \beta\right\}\right.$$

$$\left. \times \left\{1 - \left(\frac{A_4}{A_5}\right)^2\right\}\right]$$

but

$$\frac{(1+\alpha)^2}{2\alpha} = 1 + \tfrac{1}{2}\left\{\frac{1}{\alpha} + \alpha\right\}$$

hence

$$\left\{1 + \frac{P_o - P_{T_a}}{P_{T_a} - P_a}\right\}\left\{1 + \tfrac{1}{2}\left(\frac{1}{\alpha} + \alpha\right)\right\}$$

$$= \left(\frac{\beta}{\alpha} - 1\right)\left(\frac{\beta}{\alpha}\frac{T_{T_j}}{T_{T_a}} - 1\right) + \frac{1}{2\alpha}\left\{1 - \left(\frac{A_4}{A_5}\right)^2\right\}\left\{1 + \beta\frac{T_{T_j}}{T_{T_a}}\right\}\left\{1 + \beta\right\}$$

which is the form of the pressure and flow parameters presented by Rolls Royce.

If the effect of the exit diffuser is not considered these parameters may be written in the form

$$\left\{1 + \frac{P_4 - P_{T_a}}{P_{T_a} - P_a}\right\}\left\{1 + \tfrac{1}{2}\left(\frac{1}{\alpha} + \alpha\right)\right\}$$

$$= \left\{\frac{\beta}{\alpha} - 1\right\}\left\{\frac{\beta}{\alpha}\frac{T_{T_j}}{T_{T_a}} - 1\right\}$$

whence

$$\frac{P_4}{P_{T_a}} = \frac{\left\{\frac{\beta}{\alpha} - 1\right\}\left\{\frac{\beta}{\alpha}\frac{T_{T_j}}{T_a} - 1\right\}\left(1 - \frac{P_a}{P_{T_a}}\right)}{\left\{1 + \tfrac{1}{2}\left(\frac{1}{\alpha} + \alpha\right)\right\}} + \frac{P_a}{P_{T_a}} \qquad (29)$$

This gives then for any values of α . M_a , M_J and $\frac{T_{T_J}}{T_{T_a}}$ the value of $\frac{P_{T_4}}{P_{T_a}}$ as

$$\beta = \alpha \frac{M_J}{M_a} \sqrt{\frac{T_{T_a}}{T_{T_J}}}$$

on the basis of incompressible flow

i.e.

$$\frac{\beta}{\alpha} = \frac{M_J}{M_a} \sqrt{\frac{T_{T_a}}{T_{T_J}}}$$

To obtain M_4, the Mach number at the end of the mixing section, from eqn.(20)

$$\frac{\rho_4 \, v_4}{\rho_a \, v_a} = \frac{1 + \beta}{1 + \alpha}$$

substitute

$$\frac{T_{T_a}}{T_{T_4}} = \frac{\rho_4}{\rho_a} \qquad \text{and} \qquad a = \sqrt{\gamma R T_T}$$

$$\frac{M_4}{M_a} \frac{T_{T_a}}{T_{T_4}} \sqrt{\frac{T_{T_4}}{T_{T_a}}} = \frac{1 + \beta}{1 + \alpha}$$

where

$$M_4 = M_a \left(\frac{1 + \beta}{1 + \alpha} \right) \sqrt{\frac{T_{T_4}}{T_{T_a}}}$$

but from eqn.(21)

$$\frac{T_{T_4}}{T_{T_a}} = \frac{1 + \beta \frac{T_{T_J}}{T_{T_a}}}{1 + \beta}$$

$$\therefore \quad M_4 = M_a \left(\frac{1 + \beta}{1 + \alpha} \right) \sqrt{\frac{1 + \beta \frac{T_{T_J}}{T_{T_a}}}{1 + \beta}} \qquad (30)$$

APPENDIX C

Suction Pump Characteristics

1 Suction pump characteristics at normal engine maximum R.P.M.

Assumptions

(a) Final nozzle and turbine inlet guide vanes choked.

(b) The compressor work input is a function of R.P.M. alone.

(c) Compressor polytropic efficiency $\eta_c = 80\%$.

(d) Turbine polytropic efficiency $\eta_t = 90\%$.

(e) Maximum temperature $T_{T_{III}}$ = Case (1) 1150°K Case (2) 1250°K.

(f) Compression ratio $\left(\frac{P_{T_{II}}}{P_{T_I}}\right)$ 5, 10, etc.

From the assumed compression ratio $\frac{P_{T_{II}}}{P_{T_I}}$ and the inlet conditions P_{T_I} and T_{T_I}, the compressor temperature rise θ_c is determined from

$$\theta_c = T_{T_I}\left[\left(\frac{P_{T_{II}}}{P_{T_I}}\right)^{\frac{\gamma-1}{\eta_c \gamma}} - 1\right]$$

As the turbine work equals the compressor work done

$$m_{III}\, k_t\, \theta_t = m_{air}\, k_c\, \theta_c \quad , (m_{III} = m_{air} + f)$$

hence the turbine temperature drop θ_t is given by

$$\theta_t = \frac{\theta_c}{\frac{k_t}{k_c}\left(1 + \frac{f}{m_{air}}\right)} \qquad \text{assuming } \frac{k_t}{k_c} = 1.135$$

$$= \frac{\theta_c}{1.135 \times 1.015} \qquad \frac{f}{m_{air}} = 0.015$$

Hence

$$T_{T_{IV}} = T_{T_{III}} - \theta_t \quad \text{where} \quad T_{T_{III}} = 1150°K \text{ (or } 1250°K).$$

Hence

$$\frac{P_{T_{IV}}}{P_{T_I}} = \frac{P_{T_{IV}}}{P_{T_{III}}} \cdot \frac{P_{T_{III}}}{P_{T_{II}}} \cdot \frac{P_{T_{II}}}{P_{T_I}}$$

$$= \left(\frac{P_{T_{IV}}}{T_{T_{III}}}\right)^{\frac{\gamma}{\eta_t(\gamma-1)}} \frac{P_{T_{III}}}{P_{T_{II}}} \cdot \frac{P_{T_{II}}}{P_{T_I}}$$

where $\frac{P_{T_{II}}}{P_{T_I}}$ is known from assumptions

$\frac{P_{T_{III}}}{P_{T_{II}}} = 0.96$ say, to allow for pressure drop in combustion chamber.

Hence assuming a series of values of the ratio $\frac{P_{T_I}}{P_o}$ (i.e. of ram pressure ratios less than one) thence $\frac{P_{T_{IV}}}{P_o}$ can be determined.

If a normal jet pipe is fitted the mass flow/unit area of jet pipe can be determined from figure 28 (reference 18) provided $\frac{P_{T_{IV}}}{P_o}$ exceeds the choking value (approximately 1.85) and hence $\frac{m_j}{A_j}$ can be plotted against $\frac{P_{T_I}}{P_o}$.

If an end diffuser is fitted instead of the normal jet pipe the guide vane nozzles and inlet to the diffuser (equivalent to the jet pipe nozzle) will remain choked for much lower values of $\frac{P_{T_{IV}}}{P_o}$. In section 1.3 of Appendix B, it has been shown how the ratio $\frac{P_{T_{IV}}}{P_o}$ varies with $\frac{m_{IV}\sqrt{T_{T_{IV}}}}{A_{IV}\ P_{T_{IV}}}$ and the choking value of $\frac{m_{IV}\sqrt{T_{T_{IV}}}}{A_{IV}\ P_{T_{IV}}}$ can be determined, thus it is also possible to plot $\frac{P_{T_I}}{P_o}$ to $\frac{m_{IV}}{A_{IV}}$ for an engine used as a suction pump but fitted with an end diffuser instead of the normal jet pipe.

2 Suction pump characteristics at part load

2.1 Determination of engine component characteristics

As the engine component characteristics were not available, these were estimated from the manufacturers Performance Data Sheets as follows. The engine taken (as before) was a R.R. Nene II.

The assumed constant polytropic efficiencies were

Compressor	80%
Turbine	90%
Jet Pipe	90%
Turbine Nozzle	90%

2 11 Determination of jet pipe characteristics

Static test-bed conditions were used (i.e. ram pressure ratio = 1.0) the performance data sheets give the mass flow (m_j) the jet pipe temperature (T_{T_J}) the gross thrust (F_G) and the S.F.C. are obtained from R.P.M.(N)^2 and inlet conditions.

From thrust relationship

$$F_G = \frac{m_j v_j}{g} + A_J (P_J - P_o)$$

if nozzle is not choked then $P_J = P_o$, hence

$$F_G = \frac{m_j v_j}{g}$$

i.e.

$$v_j = \frac{m_j F_G}{g}$$

hence

$$\frac{v_j^2}{2gJ}$$

is found corresponding to N, P_{T_I} and T_{T_I}.

The fuel flow (f) is obtained from

$$f = \frac{\text{S.F.C.} \times F_G}{3600}$$

and $m_{air} = m_j - f$ hence $\frac{f}{m_{air}}$ is determined and the total enthalpy (H_{T_J}) is found from enthaply tables for values of $\frac{f}{m_{air}}$. Hence $H_j = H_{T_J} - \frac{v_j^2}{2gJ}$ and T_J can be found from tables corresponding to H_j.

Hence $\frac{T_{T_J}}{T_J}$ is found and the total pressure of the jet may be obtained from

$$\frac{P_{T_J}}{P_J} = \left(\frac{T_{T_J}}{T_J}\right)^{\frac{\gamma}{\gamma-1}}$$

The estimated part load characteristics of the jet pipe of a 5000 lb thrust engine are shown in Fig.22 for $T_o = 288^oK$ and $P_o = 14.7$ lb/in^2.

It is also of interest to determine the conditions at the inlet to the jet pipe, i.e. following the turbine. Here $T_{T_{IV}} = T_{T_J}$ and $P_J = P_o$

and if the jet pipe efficiency is $\eta_{J.P.} = 90\%$, then

$$\frac{P_{T_{IV}}}{P_o} = \frac{P_{T_{IV}}}{P_j} = \left(\frac{T_{T_{IV}}}{T_j}\right)^{\frac{\gamma}{\eta_{J.P.}(\gamma-1)}} = \left(\frac{T_{T_j}}{T_j}\right)^{\frac{\gamma}{\eta_{J.P.}(\gamma-1)}}$$

and $\frac{P_{T_{IV}}}{P_o}$ can be plotted against $\frac{m_{IV}\sqrt{T_{T_{IV}}}}{A_{IV}\ P_{T_{IV}}}$ as in figure 17.

If the thrust relation is not given v_j can be obtained from

$$v_j = \sqrt{2gJ\ k_p\ (T_{T_j} - T_j)}$$

From continuity

$$m_j = A_j\ \rho_j\ v_j = A_j \frac{P_j}{RT_j} v_j$$

hence

$$\frac{m_j\sqrt{T_{T_j}}}{P_{T_j}\ A_j} = \frac{\sqrt{2gJ\ k_p}}{R} \cdot f\left(\frac{P_{T_j}}{P_j}\right)$$

where

$$f\left(\frac{P_{T_j}}{P_j}\right) = \frac{1}{\left(\frac{P_{T_j}}{P_j}\right)^{\frac{1}{\gamma}}} \sqrt{1 - \frac{1}{\left(\frac{P_{T_j}}{P_j}\right)^{\frac{\gamma-1}{\gamma}}}}$$

hence $\frac{P_{T_j}}{P_j}$ can be plotted for values of $\frac{m_j\sqrt{T_{T_j}}}{P_{T_j}\ A_j}$ and substituting the choking value of $\frac{P_{T_j}}{P_j}$ a constant value for $\frac{m_j\sqrt{T_{T_j}}}{P_{T_j}\ A_j}$ is obtained.

Beeton[18] has given in figure 28 a more accurate method of determining the choking characteristics of a jet pipe based on the enthalpy of the gases.

2.12 Determination of compressor characteristic

The basis for the determination of the compressor characteristic was the selection of the compressor temperature rise such that the corresponding pressure rise should be equal to the pressure drop through the combustion chamber, turbine and jet pipe, i.e.

$$\frac{P_{T_{II}}}{P_{T_I}} = \frac{P_{T_{II}}}{P_{T_{III}}} \cdot \frac{P_{T_{III}}}{P_{T_{IV}}} \cdot \frac{P_{T_{IV}}}{P_{T_I}}$$

but

$$\frac{P_{T_{II}}}{P_{T_I}} = \left(1 + \frac{\theta_c}{T_{T_I}}\right)^{\frac{\eta_c \gamma}{\gamma-1}}$$

$$\frac{P_{T_{II}}}{P_{T_{III}}} = \text{a constant say } \frac{1}{0.96}$$

$$\frac{P_{T_{III}}}{P_{T_{IV}}} = \left(1 - \frac{\theta_t}{T_{T_{IV}}}\right)^{\frac{\gamma}{\eta_t(\gamma-1)}}$$

$$\frac{P_{T_{IV}}}{P_{T_I}} = \frac{P_{T_{IV}}}{P_o} \quad \text{as} \quad P_{T_I} = P_o$$

under test bed conditions and $\frac{P_{T_{IV}}}{P_o}$ is obtained from paragraph 2.11. Hence

$$\theta_c = T_{T_I}\left[\left(\frac{\frac{P_{T_{IV}}}{P_o}}{0.96}\right)^{\frac{\gamma-1}{\eta_c\gamma}}\left(1 - \frac{\theta_c}{T_{T_{IV}}\,1.135\left(1 + \frac{f}{m_{air}}\right)}\right)^{\frac{1}{\eta_t\eta_c}} - 1\right]$$

in which for a given R.P.M. and T_{T_I}, $\frac{P_{T_{IV}}}{P_o}$, $T_{T_{IV}}$, $\frac{f}{m_{air}}$ are known, hence θ_c is found for the R.P.M. and also the corresponding value of θ_t and in general, θ_c is a function of R.P.M. alone, hence this determination should apply for all conditions of operation.

2.13 Determination of turbine, and combined turbine-jet pipe characteristics

At any given R.P.M. $T_{T_{III}}$ is determined

$$T_{T_{III}} = T_{T_{IV}} + \theta_t = T_{T_j} + \theta_t \quad \left[T_{T_{IV}} = T_{T_j}\right]$$

and hence it is possible to plot

$$\frac{\theta_t}{T_{T_{III}}} \text{ against } \frac{P_{T_{III}}}{P_{T_{IV}}} \text{ and } \frac{P_{T_{III}}}{P_o} \text{ (see figure 16)}$$

as

$$\frac{P_{T_{III}}}{P_{T_{IV}}} = \left(1 + \frac{\theta_t}{T_{T_{IV}}}\right)^{\frac{\gamma}{\eta_t(\gamma-1)}} \text{ in para. 2.12}$$

and $\frac{P_{T_{IV}}}{P_o}$ is obtained from para. 2.11. As the area of the nozzle in the turbine guide vane ring was not given it was determined from the choking value of the dimensionless flow parameter $\frac{m_{III}\sqrt{T_{T_{III}}}}{A_{III}\ P_{T_{III}}}$ (alternatively figure 28 could have been used).

Hence A_{III} was determined for each R.P.M. and as it was evident from the manufacturers Data sheets that the nozzle was choked at each R.P.M. the mean value gave a reasonable estimate for A_{III}.

2.14 Determination of turbine-jet pipe-diffuser characteristic

As the annulus area was not known it was more convenient for the purpose of calculation to assume that the diffuser started from the final nozzle of the jet pipe, i.e. the area A_{IV} at the inlet to the diffuser = A_j the area of the jet nozzle.

From para. 1.3 of Appendix B it has been shown how the diffuser mass flow parameter $\frac{m_{IV}\sqrt{T_{T_{IV}}}}{A_{IV}\ P_{T_{IV}}}$ can be determined in terms of $\frac{P_{T_{IV}}}{P_o}$.

As in section 2.13 it is desired to plot $\frac{\theta_t}{T_{T_{III}}}$ against $\frac{P_{T_{III}}}{P_{T_{IV}}}$ and $\frac{P_{T_{III}}}{P_o}$ and in fact the first curve will be the same as the turbine characteristic is unaltered.

To obtain $\frac{P_{T_{III}}}{P_o} = \frac{P_{T_{III}}}{P_{T_{IV}}} \cdot \frac{P_{T_{IV}}}{P_o}$ the value of $\frac{P_{T_{IV}}}{P_o}$ corresponding to a given value of $\frac{P_{T_{III}}}{P_{T_{IV}}}$ i.e. $\frac{\theta_t}{T_{T_{III}}}$ must be obtained. But $\frac{P_{T_{IV}}}{P_o}$ is given in terms of $\frac{m_{IV}\sqrt{T_{T_{IV}}}}{A_{IV}\ P_{T_{IV}}}$ but

$$\frac{m_{IV}\sqrt{T_{T_{IV}}}}{A_{IV}\ P_{T_{IV}}} = \frac{m_{III}\sqrt{T_{T_{III}}}}{A_{III}\ P_{T_{III}}}\ \frac{A_{III}}{A_{IV}}\ \frac{P_{T_{III}}}{P_{T_{IV}}}\sqrt{\frac{T_{T_{IV}}}{T_{T_{III}}}}$$

$$= \frac{m_{III}\sqrt{T_{T_{III}}}}{A_{III}\ P_{T_{III}}}\ \frac{A_{III}}{A_{IV}}\ \frac{P_{T_{III}}}{P_{T_{IV}}}\sqrt{1 - \frac{\theta_t}{T_{T_{III}}}}$$

As the turbine nozzles are choked $\frac{m_{III}\sqrt{T_{T_{III}}}}{A_{III}\ P_{T_{III}}}$ is constant. Hence for a given value of $\frac{\theta_t}{T_{T_{III}}}$, $\frac{m_{IV}\sqrt{T_{T_{IV}}}}{A_{IV}\ P_{T_{IV}}}$ is determined and hence $\frac{P_{T_{IV}}}{P_o}$.

Hence $\frac{\theta_t}{T_{T_{III}}}$ may be plotted against $\frac{P_{T_{III}}}{P_o}$ (see figure 16). N.B. A_{III} is determined in para. 2.13 and A_{IV} is given in Data sheets.

2.2 Determination of pump characteristics

From the assumed inlet conditions (T_{T_I} and P_{T_I}) and the engine R.P.M. (N), θ_c is determined from para.2.12, (i.e. figure 15) and hence

$$\frac{P_{T_{II}}}{P_{T_I}} = \left(1 + \frac{\theta_c}{T_{T_I}}\right)^{\frac{\eta_c \gamma}{\gamma-1}}$$

thus the value of $\frac{P_{T_{III}}}{P_o}$ is obtained as P_{T_I} and P_o are known, (i.e. $\frac{P_{T_I}}{P_o}$) and $\frac{P_{T_{III}}}{P_{T_{II}}} = 0.96$ say. As in para.1 θ_t can be obtained and using the above value of $\frac{P_{T_{III}}}{P_o}$ a value of $\frac{\theta_t}{T_{T_{III}}}$ can be obtained from the curve of para.2.13 if a normal jet pipe is used or para.2.14 if an end diffuser is used.

Thus $T_{T_{III}}$ may be determined and also $T_{T_{IV}}$ also the ratio $\frac{P_{T_{IV}}}{P_o}$ may be determined for the known value of $\frac{\theta_t}{T_{T_{III}}}$.

With this value of $\frac{P_{T_{IV}}}{P_o}$ the value of $\frac{m_{IV}\sqrt{T_{T_{IV}}}}{A_{IV}\ P_{T_{IV}}}$ may be determined from the appropriate curve of para.2.12 or para.2.14. And thus m_{IV} can be obtained corresponding to $\frac{P_{T_{III}}}{P_o}$, i.e. $\frac{P_{T_I}}{P_o}$, each value of $\frac{P_{T_I}}{P_o}$ corresponding to a value $\frac{\Delta P_T}{P_o} \times 14.7$. And thus the pump characteristic $\frac{\Delta P_T}{P_o} \times 14.7$ to mass flow (m) is obtained for the assumed inlet conditions and R.P.M. (N).

APPENDIX D

Theoretical Determination of Induction and Suction Parallel Pumping Characteristics

1 Flow around engine

The total drag between the end stations of the engine section will consist of three parts:-

(a) Drag of Engine Nacelle.

(b) Drag of Struts supporting the engine.

(c) Drag due to tunnel wall friction.

The drag of a Meteor nacelle is given in reference 19 as

$$D_{nacelle} = 0.05 \tfrac{1}{2} \rho V^2 d^2$$

where d is the diameter in feet (d approximately equals 4 ft). It is stated that the result is only from low speed tests (as are considered here) and it is in reasonably good agreement with wind tunnel tests on similar nacelles.

No extra allowance need be made for "additive" intake drag as the drag is not being compared with the engine thrust, but purely to obtain the pressure difference required to maintain flow between the two stations.

The drag of the struts may be taken as

$$D_{struts} = C_D \cdot \tfrac{1}{2} \rho V^2 \ell L$$

where $C_D = 0.086$

ℓ = width of strut

L = length of strut, i.e.

$$D_{struts} = 0.086 \tfrac{1}{2} \rho V^2 A_f$$

where A_F = frontal projected area of struts.

The drag due to tunnel wall friction can be obtained in the same manner as for the mixing chamber in the injector pump case. Hence considering the total drag over a small length dL of the channel annulus if a circular tunnel with a single coaxial engine is assumed. Then

$$D_{nacelle} = C_{D_{nacelle}} \tfrac{1}{2} \rho V^2 d^2$$

$$= \tfrac{1}{2} \gamma P M^2 \frac{4 C_{D_{nac}}}{\pi} \left(\frac{d}{D}\right)^2 A_3$$

$$D_{struts} = C_{D_{struts}} \tfrac{1}{2} \rho V^2 A_f$$

$$= \tfrac{1}{2} \gamma P M^2 \cdot C_{D_{strut}} \left(\frac{A_f}{A_3}\right) A_3$$

$$\Delta D_{\text{wall friction}} = C_f \tfrac{1}{2} \rho V^2 \pi D \, dL$$

$$= \tfrac{1}{2} \gamma P M^2 \frac{4 C_F \, dL}{D} A_3 \, .$$

Hence

$$\Delta D_{\text{annulus}} = \Delta D_{\text{nacelle}} + \Delta D_{\text{struts}} + \Delta D_{\text{wall friction}}$$

$$\therefore \Delta D_{\text{annulus}} = \tfrac{1}{2}\gamma P M^2 \left[\frac{4 C_{D_{nac}}}{\pi} \left(\frac{d}{D}\right)^2 + C_{D_{strut}} \left(\frac{A_f}{A_3}\right) + \frac{4 C_f dL}{D} \right] A_3$$

$$\therefore D_{\text{annulus}} = A_3 \left[\frac{4 C_{D_{nac}}}{\pi} \left(\frac{d}{D}\right)^2 + C_{D_{strut}} \left(\frac{A_f}{A_3}\right) + 4 C_f \frac{L}{D} \right]$$

$$\times \int_0^L \tfrac{1}{2} \gamma P M^2 \, dL$$

$$= A_3 K \left[\gamma P_2 M_2^2 + \gamma P_a M_a^2 \right]$$

to a first approximation if the drag coefficients are assumed independent of P and M where

$$K = \left[\frac{C_{D_{nac}}}{\pi} \left(\frac{d}{D}\right)^2 + \frac{C_{D_{strut}}}{4} \left(\frac{A_f}{A_3}\right) + C_f \frac{L}{D} \right] .$$

From conservation of momentum

$$A_a P_2 (1 + \gamma M_2^2) - A_a P_a (1 + \gamma M_a^2) = D_a$$

$$\therefore P_2 + \gamma P_2 M_2^2 - P_a - \gamma P_a M_a^2 = \frac{A_3}{A_a} K \left[\gamma P_2 M_2^2 + \gamma P_a M_a^2 \right]$$

$$P_2 \left[1 + \gamma M_2^2 - (1+\alpha) K \gamma M_2^2 \right] = P_a \left[1 + \gamma M_a^2 + (1+\alpha) K \gamma M_a^2 \right]$$

$$\therefore \frac{P_2}{P_a} = \frac{\left[1 + \left\{ \gamma + (1+\alpha) K \gamma \right\} M_a^2 \right]}{\left[1 + \left\{ \gamma - (1+\alpha) K \gamma \right\} M_2^2 \right]} .$$

From conservation of mass

$$\rho_2 V_2 = \rho_a V_a$$

as the area is constant, hence

$$\frac{P_2 M_2}{\sqrt{T_2}} = \frac{P_a M_a}{\sqrt{T_a}}$$

but

$$\sqrt{T_2} = \sqrt{T_{T_2}} \left(1 + \frac{\gamma-1}{2} M_2^2\right)^{-\frac{1}{2}}$$

and

$$\sqrt{T_a} = \sqrt{T_{T_a}} \left(1 + \frac{\gamma-1}{2} M_a^2\right)^{-\frac{1}{2}}$$

with no heat addition or loss

$$\sqrt{T_{T_2}} = \sqrt{T_{T_a}}$$

$$P_2 M_2 \left(1 + \frac{\gamma-1}{2} M_2^2\right)^{\frac{1}{2}} = P_a M_a \left(1 + \frac{\gamma-1}{2} M_a^2\right)^{\frac{1}{2}}$$

$$\therefore \frac{P_2}{P_a} = \frac{M_a \left(1 + \frac{\gamma-1}{2} M_a^2\right)^{\frac{1}{2}}}{M_2 \left(1 + \frac{\gamma-1}{2} M_2^2\right)^{\frac{1}{2}}} .$$

Hence

$$\frac{1 + \left\{\gamma + (1-\alpha) K\gamma\right\} M_a^2}{1 + \left\{\gamma - (1+\alpha) K\gamma\right\} M_2^2} = \frac{M_a \left(1 + \frac{\gamma-1}{2} M_a^2\right)^{\frac{1}{2}}}{M_2 \left(1 + \frac{\gamma-1}{2} M_2^2\right)^{\frac{1}{2}}}$$

i.e.

$$\frac{1 + \xi_a M_a^2}{M_a \left(1 + \frac{\gamma-1}{2} M_a^2\right)^{\frac{1}{2}}} = \frac{\left(1 + \xi_2 M_2^2\right)}{M_2 \left(1 + \frac{\gamma-1}{2} M_2^2\right)^{\frac{1}{2}}}$$

where $\xi_a = \gamma + (1-\alpha) K\gamma$

$\xi_2 = \gamma - (1+\alpha) K\gamma$.

Hence ξ_a and ξ_2 can be determined for a given configuration and for given values of M_2 the corresponding value of M_a may be determined (see figure 20).

Knowing M_2 and M_a, $\frac{P_2}{P_{T_2}}$, $\frac{P_a}{P_{T_a}}$ and $\frac{P_2}{P_a}$ hence

$$\frac{P_{T_a}}{P_{T_2}} = \frac{\frac{P_2}{P_{T_2}}}{\frac{P_a}{P_{T_a}}} \cdot \frac{1}{\frac{P_2}{P_a}}$$

is found (see figure 20).

Thus knowing P_{T_2} from tunnel characteristics P_{T_a} can be determined for the value of M_2 assumed, i.e. M_a assumed.

2 Suction pump characteristics

From para.1 for assumed values of M_a and P_{T_2} the corresponding values of P_{T_a} and M_a can be found, hence P_a.

The equivalent ram pressure ratio for the engine $\frac{P_{T_I}}{P_o} = \frac{P_{T_2}}{P_a}$

assuming $P_{T_2} = P_{T_I}$ also $T_{T_2} = T_{T_I}$.

Hence for a given R.P.M.(N) T_{T_j} and m_j can be determined from the Manufacturers Data Sheets and also P_{T_j} from figure 28 assuming choking conditions. Thus the value of $\beta = \frac{m_j}{m_a}$ corresponding to an assumed value of m_a can be obtained.

3 Induction pump characteristics

For the given value of m_a the corresponding values of β, $\frac{P_{T_j}}{P_{T_a}}$, $\frac{T_{T_j}}{T_{T_a}}$ and α are known, hence from the induction pump characteristic charts (figs.11-13) $\frac{\Delta P_T}{P_o} \times 14.7$ can be obtained. The total pressure recovery ΔP_T must be decreased by a factor of 0.10 lb/in^2 to allow for friction loss in the mixing chamber. (Alternatively ΔP_T may be obtained directly as in Appendix B.) Hence P_{T_a}' $(= P_o - \Delta P)$ is determined and can be plotted against m_a also P_{T_a} can be plotted against m_a and, hence the value of m_a found for which $P_{T_a}' \equiv P_{T_a}$.

From the corresponding value of β, m_2 may be determined and hence the combined pump flow characteristic is obtained for P_{T_a}, T_{T_a} and the engine R.P.M. (see figure 21).

APPENDIX E

Some Examples of Basic Tunnel Designs

The following examples are intended to indicate how possible wind tunnel configurations can be quickly determined by the use of the generalized pump characteristic curves of the various methods of drive and the wind tunnel characteristics.

Once the basic configuration has been established by these methods a detailed check of the design can be made by developing the actual pump characteristic directly from the appropriate analysis and also the actual tunnel characteristics.

Hence the tunnel performance under engine part load conditions is also determined. An outline example of this procedure is also given.

Example 1

For a proposed induction type supersonic wind tunnel, with a working section of 1 sq ft, Mach numbers between 1.2 and 1.8 are desired. The tunnel is to be of conventional configuration with atmospheric intake. If the injector drive is by Rolls-Royce Nene II engines, how many engines and what injector configuration will be required?

(a) Engine performance

As the design basis is to establish the minimum number of engines under which the desired tunnel performance can be achieved only maximum engine performance need be considered.

From Rolls-Royce Data Sheets for a Nene II at the maximum R.P.M. = 12,200 and $T_o = 288^\circ K$

$$m_j = 85.3 \text{ lb/sec}$$

$$T_{T_J} = 956^\circ K$$

$$A_j = 1.7 \text{ ft}^2$$

From figure 28 for a choking nozzle at $T_{T_j} = 683^\circ C$, then

$$\frac{A_j P_{T_j}}{m_j} = 79.2$$

i.e.

$$P_{T_j} = 27.57 \text{ lb/in}^2 .$$

(b) Working section characteristics

From figure 23 a working section total temperature of about 125°C would be needed to satisfactorily eliminate humidity effects in this Mach number range, but such high temperatures would be unsuitable from general operational considerations.

If it is possible to obtain partially dried air some recirculation may be possible to suppress the remaining effects of humidity. For the present example a working section total temperature of 60°C is assumed for the sake of comparison with the pumping characteristics of other tunnel types.

Using this value the mass flow for 1 sq ft section can be computed as follows

M w/s	M_a (lb/sec)	ΔP_T
1.2	45.6	4.1
1.4	42.0	4.55
1.6	37.4	5.35
1.8	32.6	6.30

The pressure loss through the tunnel is taken from curve 1, figure 8

(c) Matching table

In all cases $\frac{T_{T_j}}{T_{T_a}} = 2.9 \approx 3.0$

$M_{w/s}$	β/for one engine	β/for two engines	P_{T_a}	$\frac{P_{T_j}}{P_{T_a}}$
1.2	1.87	3.74	10.6	2.60
1.4	2.03	4.06	10.15	2.72
1.6	2.285	4.57	9.35	2.95
1.8	2.62	5.24	8.4	3.29

(d) Injector characteristics

From an inspection of the curves of figure 13 of $\frac{\Delta P_T}{P_o} \times 14.7$ to β for $\frac{P_{T_j}}{P_{T_a}} = 3$ which is an upper value and $\frac{T_{T_j}}{T_{T_a}} = 3$ it is apparent that only a jet to induction area ratio (α) of 0.5 will give the order of pressure rise required.

Assume $\frac{A_5}{A_4}$ and taking first β corresponding to one engine then from Figure 11-13

β	$\Delta P_T \left(\frac{P_{T_j}}{P_{T_a}} = 3.0\right)$	$\Delta P_T \left(\frac{P_{T_j}}{P_{T_a}} = 2.5\right)$	$\Delta P_T \left(\frac{P_{T_j}}{P_{T_a}} = 2.0\right)$
1.87	5.64	4.83	3.77
2.03	5.70	4.88	3.81
2.285	5.77	4.96	3.87
2.62	5.87	5.02	3.93

From this table ΔP has been plotted against $\frac{P_{T_j}}{P_{T_a}}$ for the constant values of β hence the values of P_T could be obtained for the values of $\frac{P_{T_j}}{P_{T_a}}$ in section (c), i.e. corresponding to each β hence

$M_{w/s}$	β/one engine	ΔP_T (injector characteristic)	ΔP_T (tunnel characteristic)
1.2	1.87	5.00	4.1
1.4	2.03	5.27	4.55
1.6	2.285	5.70	5.35
1.8	2.62	6.30	6.30

Hence a working section of 1 sq ft at Mach numbers of 1.2 to 1.8 can be obtained with a single Nene II engine with an injector area ratio $\alpha = 0.5$ assuming no losses in the mixing chamber.

Example II

What size working section can be obtained in a high speed tunnel which has an injector drive by three Rolls-Royce Nene II engines?

Temperature ratio $\frac{T_{T_j}}{T_{T_a}} = 3.0$ and area ratio $\alpha = 0.10$ or 0.15.

(a) Engine characteristics

As in previous example.

(b) Working section characteristics

From curve 5 of figure 8 taking $M_{w/s} = 1.0$ as maximum condition, then

$$\Delta P_T = 1.6 \text{ lb/in}^2$$

and

$$m_a = A_{w/s}\, \rho_s \frac{\rho_{w/s}}{\rho_o}\, a_o \frac{V_{w/s}}{a_o} \sqrt{\frac{T_{T_{w/s}}}{T_{T_o}}}$$

$$= A_{w/s} \times 47.1$$

and

$$\frac{P_{T_j}}{P_{T_a}} = 2.1 \,.$$

(c) Injector characteristics

From figures 11-13 for $\Delta P = 1.6$, $\alpha = 0.10$ and

$$\frac{P_{T_j}}{P_{T_a}} = 3.0 \qquad \beta = 0.235$$

$$\frac{P_{T_j}}{P_{T_a}} = 2.5 \qquad \beta = 0.310$$

$$\frac{P_{T_j}}{P_{T_a}} = 2.0 \qquad \beta = 1.060$$

Plotting $\frac{P_{T_j}}{P_{T_a}}$ to β hence for $\frac{P_{T_J}}{P_{T_a}} = 2.1$, $\beta = 0.74$, and

$$A_{w/s} = \frac{M_a}{47.1} = \frac{M_j}{\beta \times 47.1}$$

$$= 2.45 \text{ ft}^2$$

for $\Delta P = 1.6$ and $\alpha = 0.15$ and $\frac{A_5}{A_4} = 4$

$\frac{P_{T_j}}{P_{T_a}}$		β	
	3.0	=	0.300
	2.5	=	0.300
	2.0	=	0.41

Again plotting, and $\beta = 0.385$ for

$$\frac{P_{T_J}}{P_{T_a}} = 2.1$$

$$\therefore A_{w/s} = \frac{85.3}{0.385 \times 47.1} = 4.7 \text{ ft}^2.$$

Hence for three engines and

$\alpha = 0.10$	$A_{w/s} = 2.45 \times 3$	=	7.35 ft^2
0.15	$A_{w/s} = 4.71 \times 3$	=	14.2 ft^2

without losses in the mixing chamber.

Example 3

Determine the engine settings at various working section Mach numbers for a high speed subsonic induction tunnel with a working section area of 4 ft^2 with humidity control by recirculation and a Nene II engine drive. Aero ratio $\alpha = 0.15$.

The jet characteristics below choking at various R.P.M. were determined as in Appendix C for the engine used, curves similar to figure 27 being obtained.

From the tunnel characteristics P_{T_a} and M_a can be determined corresponding to the working section Mach number and taking given values of these two parameters the corresponding values of P_{T_a} for different engine settings can be computed as in Appendix B allowance being made for friction loss in the mixing chamber as its geometry is known. Hence the engine R.P.M. can be determined at which the value of P_{T_a} required by the tunnel characteristic is the same as the pump characteristic. Such a design is illustrated in figure 29.

Example 4

What size working section can be obtained at $M = 1.2$ assuming induction pumping with $\alpha = 0.50$ $T_{T_{w/s}} = 60^{o}C$ and a single Nene II drive at maximum R.P.M.?

(a) Engine characteristics

As for Example 1.

(b) Working section characteristics

From curve 1 of figure 8 at $M = 1.2$

$$\frac{\Delta P_T}{P_o} \times 14.7 = 3.5 \text{ lb/in}^2$$

with

$$T_{T_{w/s}} = 60^{o}C \quad \text{and} \quad M_{w/s} = 1.2$$

$$m_a = 45.6 \text{ lb/sec per sq ft.}$$

(c) Injector characteristics

From curves for $\alpha = 0.50$ and $\frac{A_5}{A_4} = 4$ in figures 11-13, the values of β corresponding to $\frac{\Delta P_T}{P_o} \times 14.7 = 3.6 \text{ lb/in}^2$ are (N.B. $\frac{\Delta P_T}{P_o} \times 14.7$ is increased by 0.1 to allow for friction loss in mixing chamber) are,

$\frac{P_{T_j}}{P_{T_a}}$ =	2.0	2.5	3.0
β	1.47	0.883	1.018

From (a) $P_{T_j} = 27.57 \text{ lb/in}^2$.

From (b) $P_{T_a} = 11.2 \text{ lb/in}^2$, $\therefore \frac{P_{T_j}}{P_{T_a}} = 2.46$, and by interpolation the corresponding value of β is 0.89.

Hence

$$m_{w/s} = \frac{m_j}{\beta} = \frac{85.3}{0.89}$$

$$= 95.7 \text{ lb/sec.}$$

i.e.

$$A_{w/s} = \frac{m_{w/s}}{45.6} = 2.1 \text{ ft}^2$$

say 2 ft^2.

Wt.2078.CP107.K3. Printed in Great Britain.

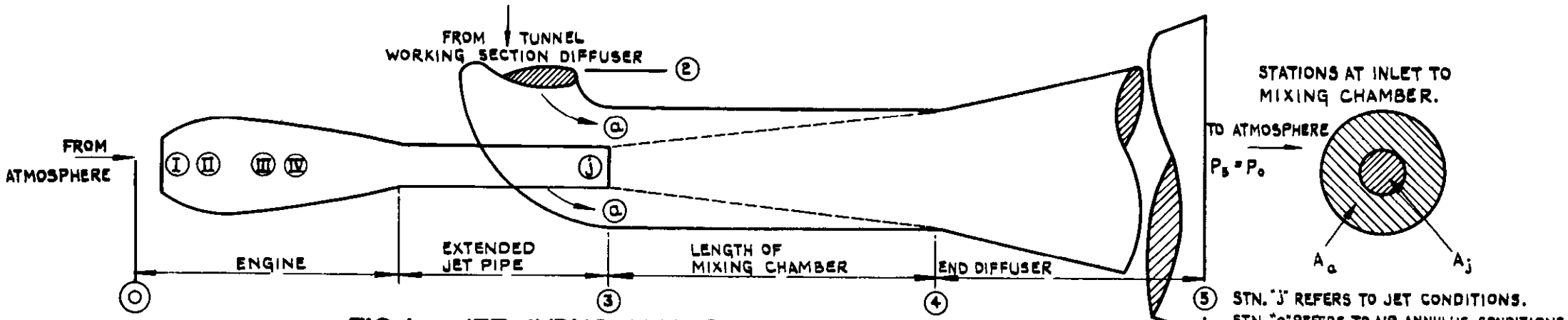

FIG. 1 JET INDUCTION PUMP

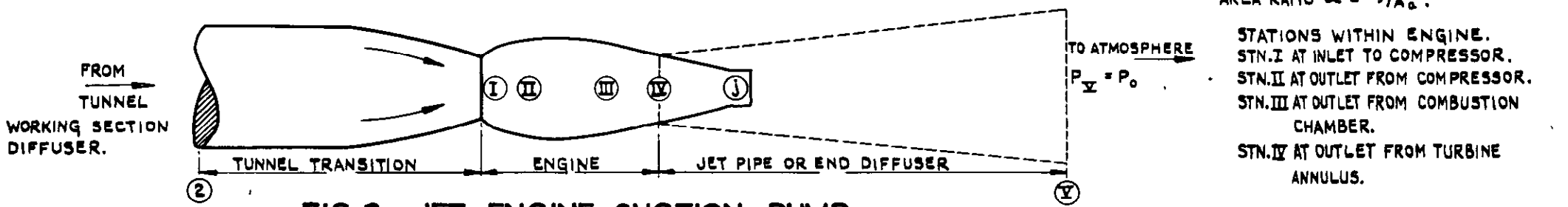

FIG. 2 JET ENGINE SUCTION PUMP

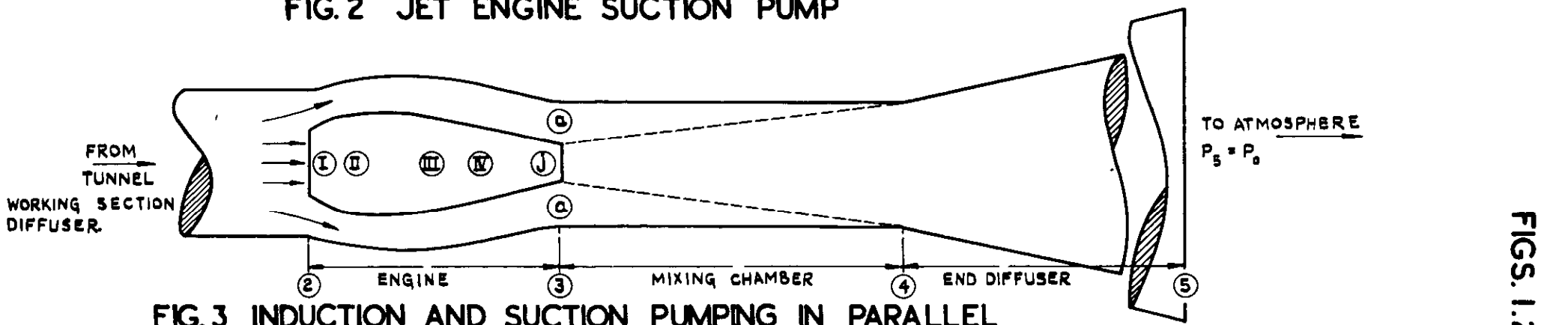

FIG. 3 INDUCTION AND SUCTION PUMPING IN PARALLEL

FIG. 1. 2. & 3 SCHEMATIC LAYOUT OF JET ENGINE PUMPING SYSTEMS

FIGS. 1.2&3.

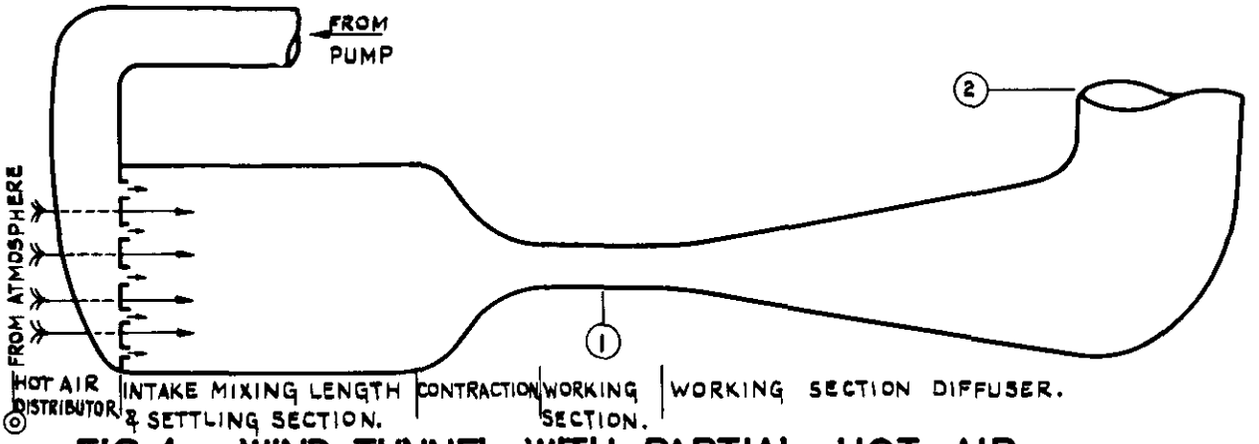

FIG.4 WIND TUNNEL WITH PARTIAL HOT AIR RECIRCULATION FOR HUMIDITY CONTROL

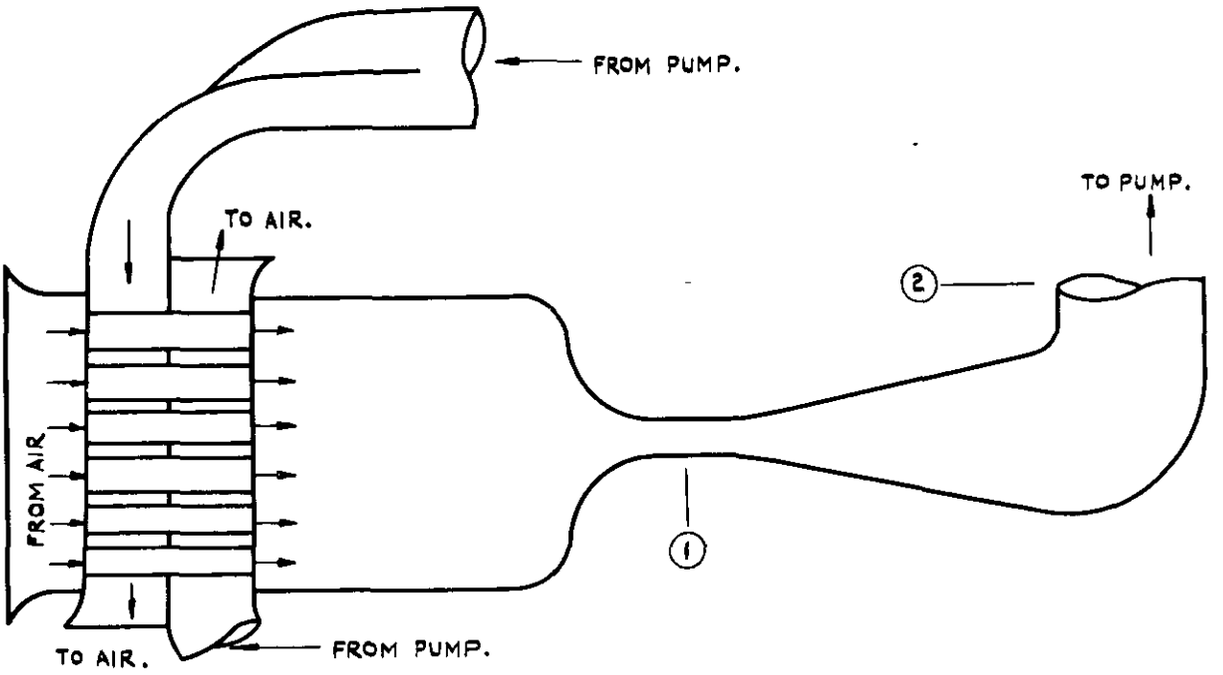

FIG. 5 WIND TUNNEL WITH HEAT EXCHANGER AT INLET

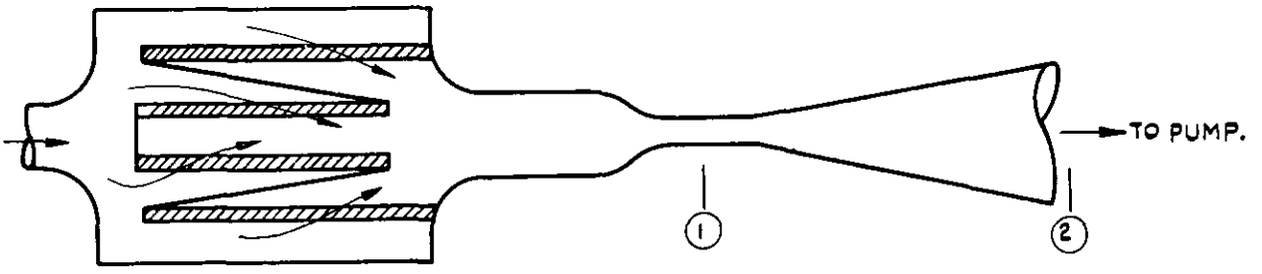

FIG. 6 WIND TUNNEL WITH SILICA GEL DRYER

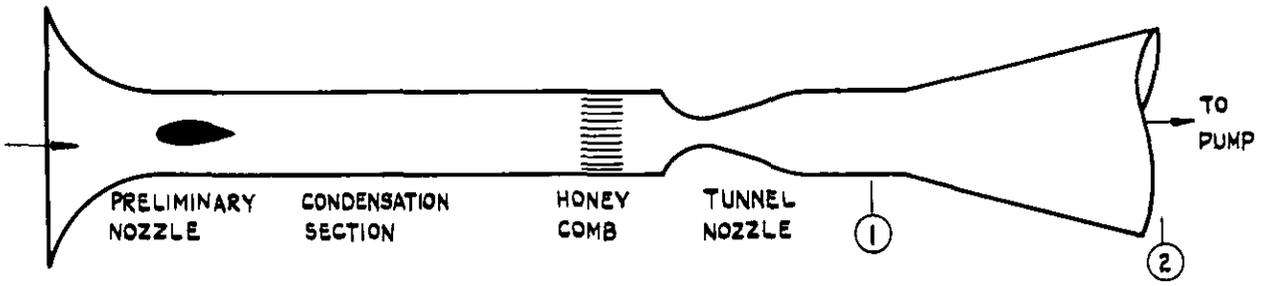

FIG. 7 SUPERSONIC TUNNEL WITH AUXILARY CONDENSATION NOZZLE

FIGS.4.5.6 & 7 HUMIDITY CONTROL ARRANGEMENT FOR WIND TUNNELS WITH JET ENGINE PUMPING SYSTEMS.

FIG.8.

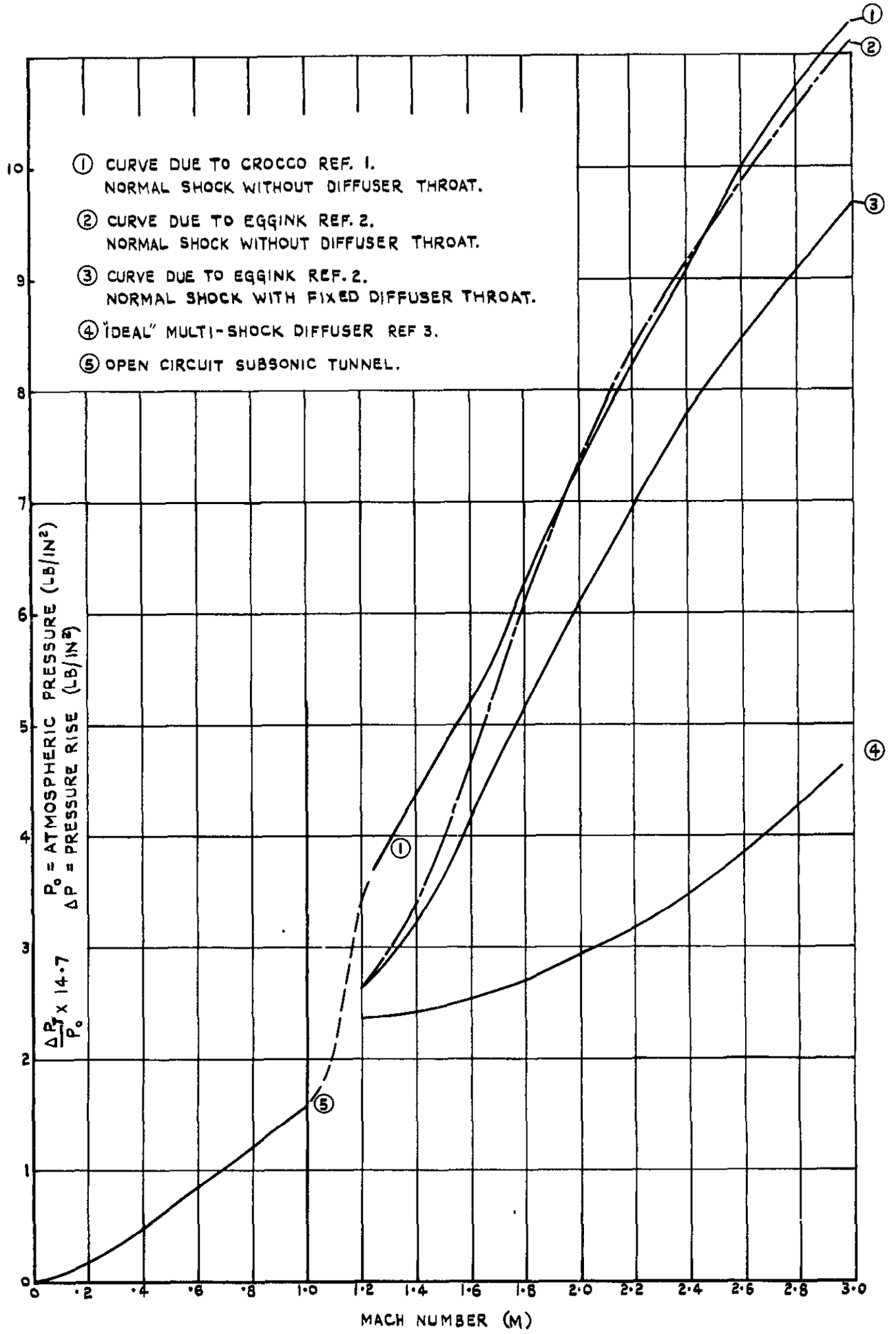

FIG.8. PRESSURE LOSS TO WORKING SECTION MACH NUMBER CHARACTERISTICS OF VARIOUS CLOSED JET WIND TUNNELS.

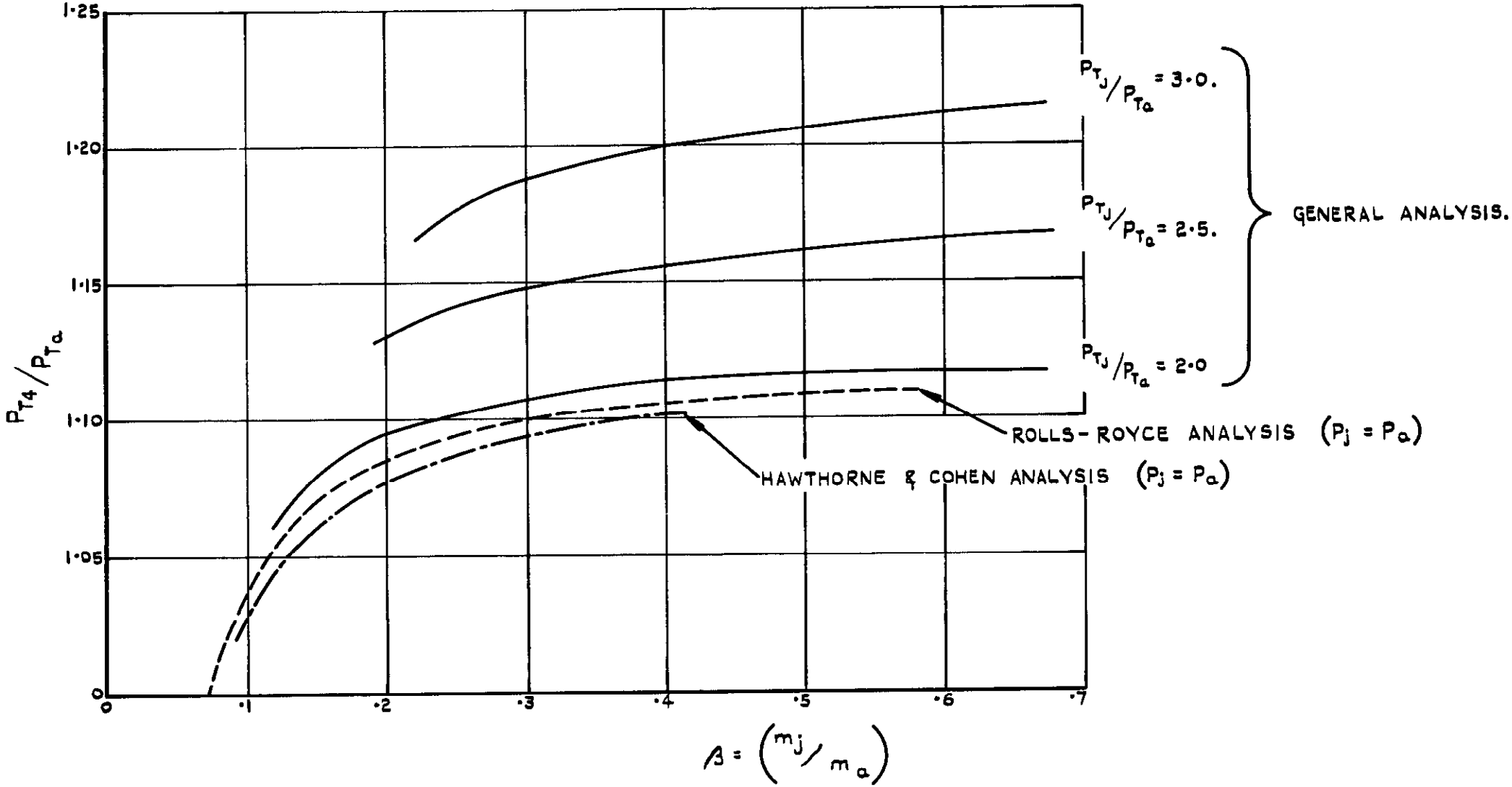

FIG. 9.

FIG. 9. COMPARISON OF ESTIMATED PRESSURE RECOVERY RATIOS TO MASS FLOW RATIO FROM VARIOUS INDUCTION SYSTEM ANALYSES.

(α = 0·10 T_{TJ}/T_{Ta} = 3·0 IN ALL CASES.)

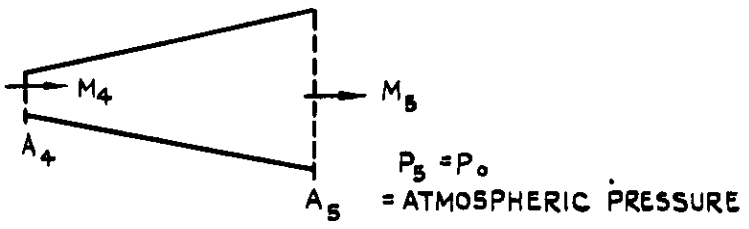

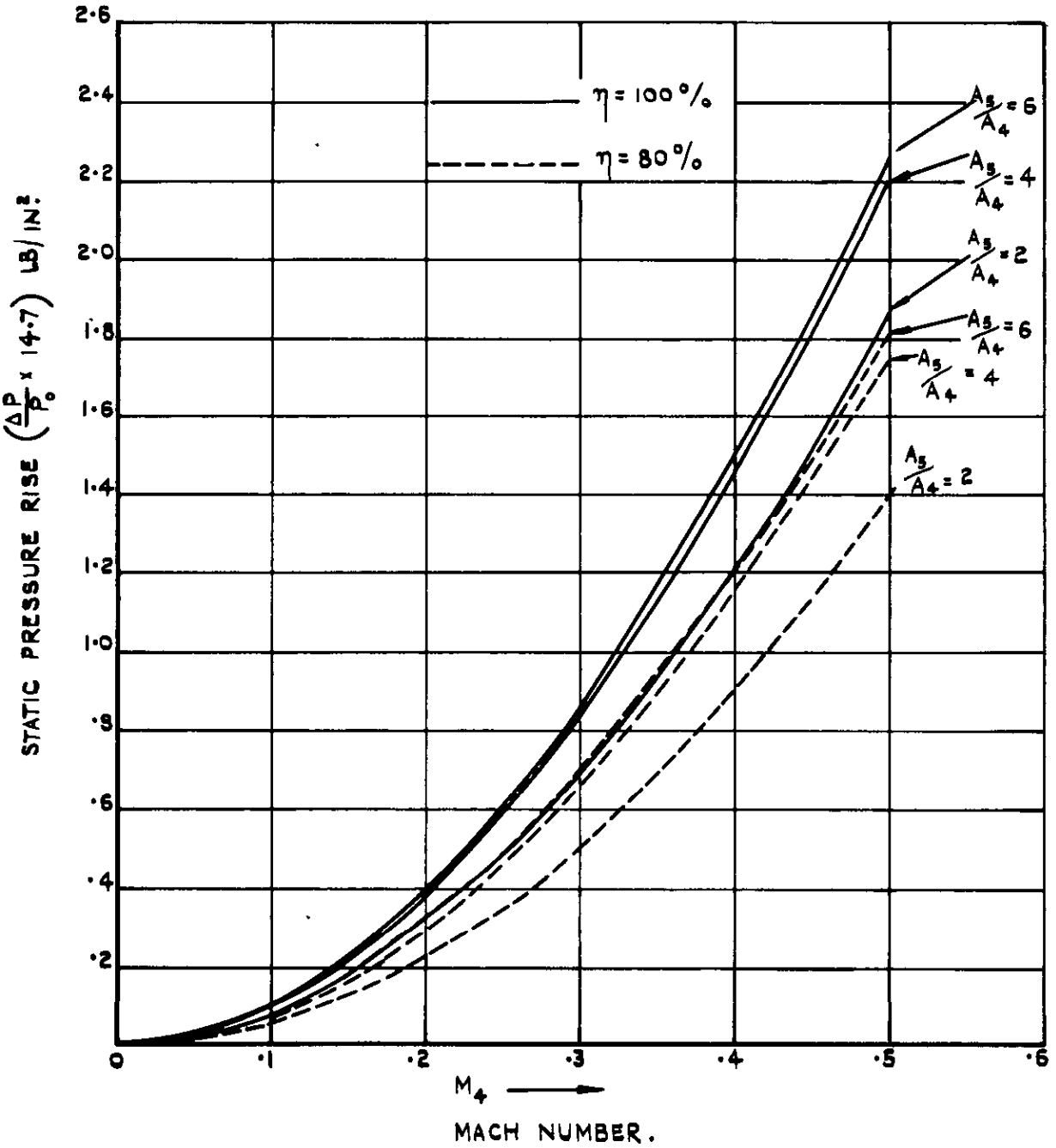

FIG.10. END DIFFUSER CHARACTERISTICS.

FIG.11.

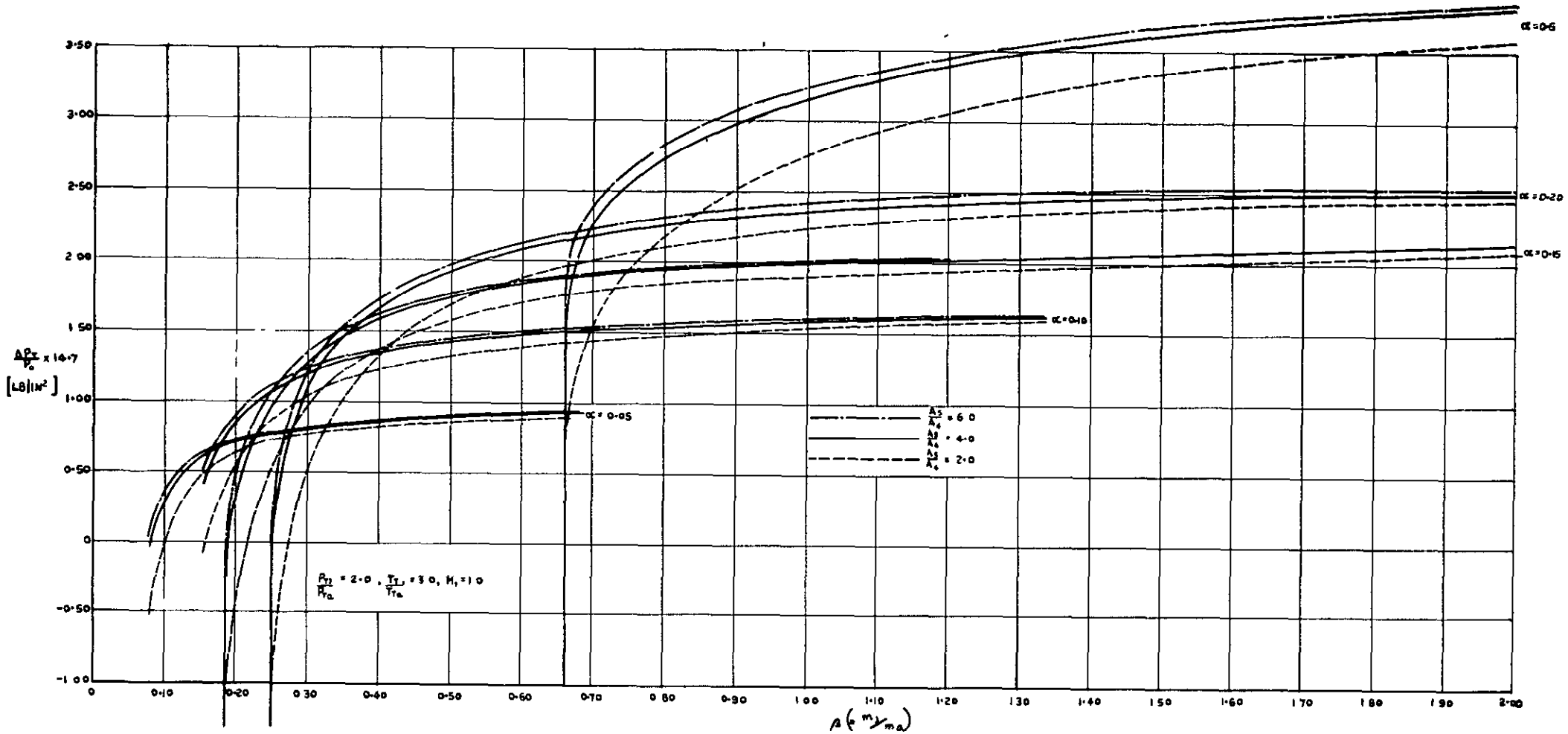

FIG.11 PRESSURE RISE TO MASS FLOW RATIO FOR INDUCTION PUMPS.

P_{Tj}/P_{Ta} = 2·0 T_{Tj}/T_{Ta} = 3·0 α = ·05, 10, ·15, ·20, & ·50

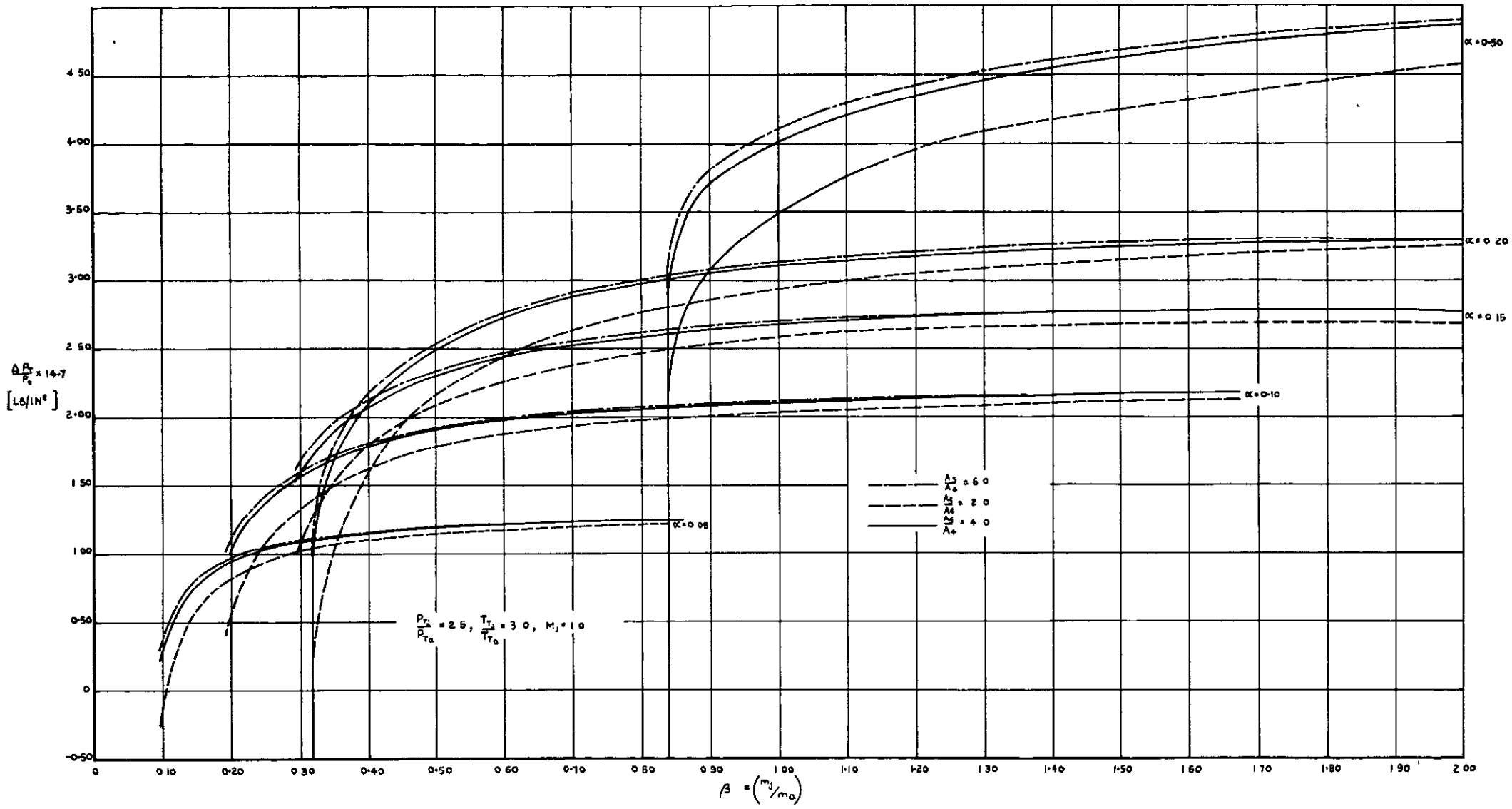

FIG.12. PRESSURE RISE TO MASS FLOW RATIO FOR INDUCTION PUMPS.
$P/P = 2{\cdot}0$, $T/T = 3{\cdot}0$, $\alpha = {\cdot}05, {\cdot}10, {\cdot}15, {\cdot}20, \& {\cdot}50$.

FIG.12

FIG13

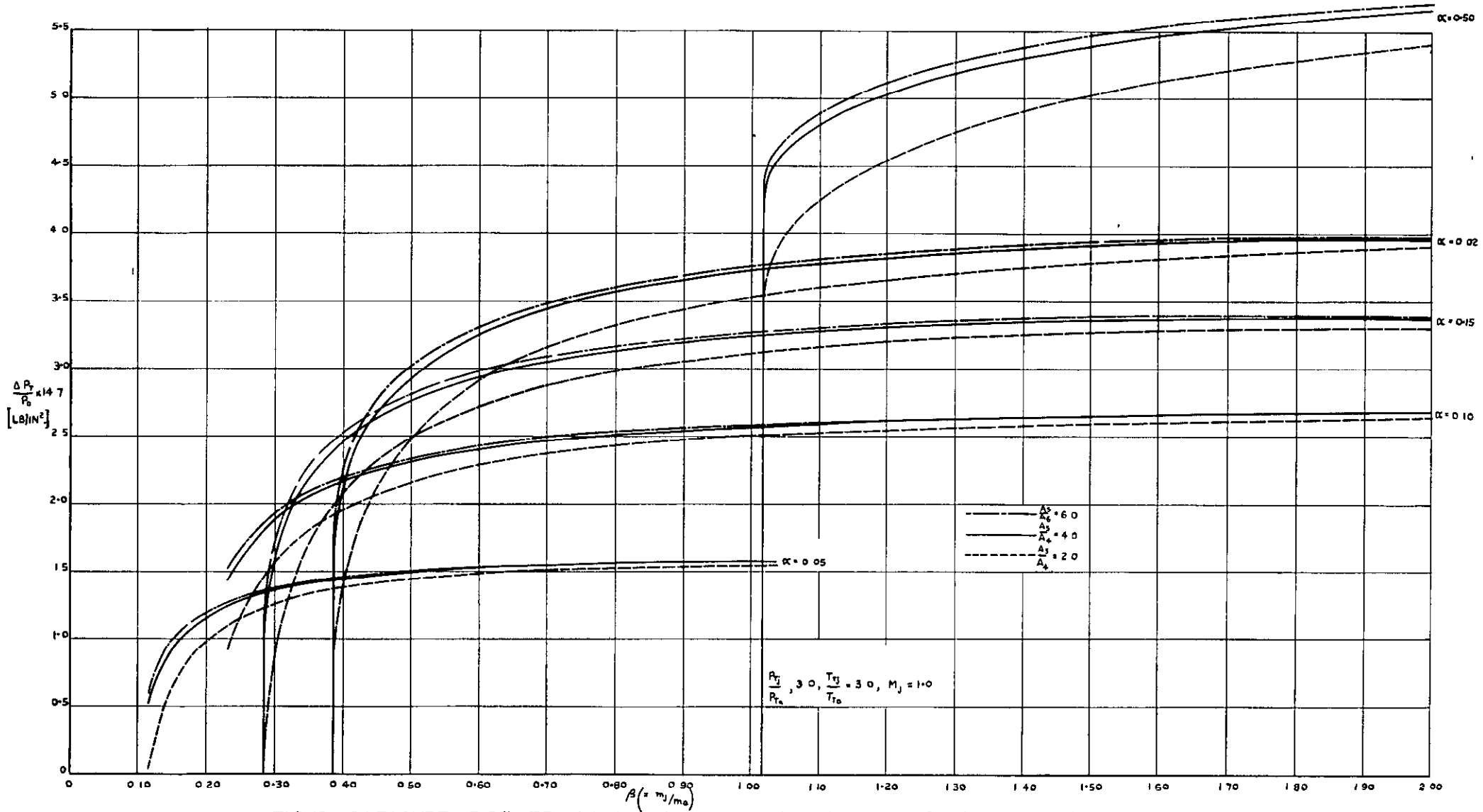

FIG 13 PRESSURE RISE TO MASS FLOW RATIO FOR INDUCTION PUMPS
P_{TJ}/T_{Ta} = 3·0 T_{TJ}/T_{Ta} = 3·0 α = ·05, 10, 15, 20 & 50.

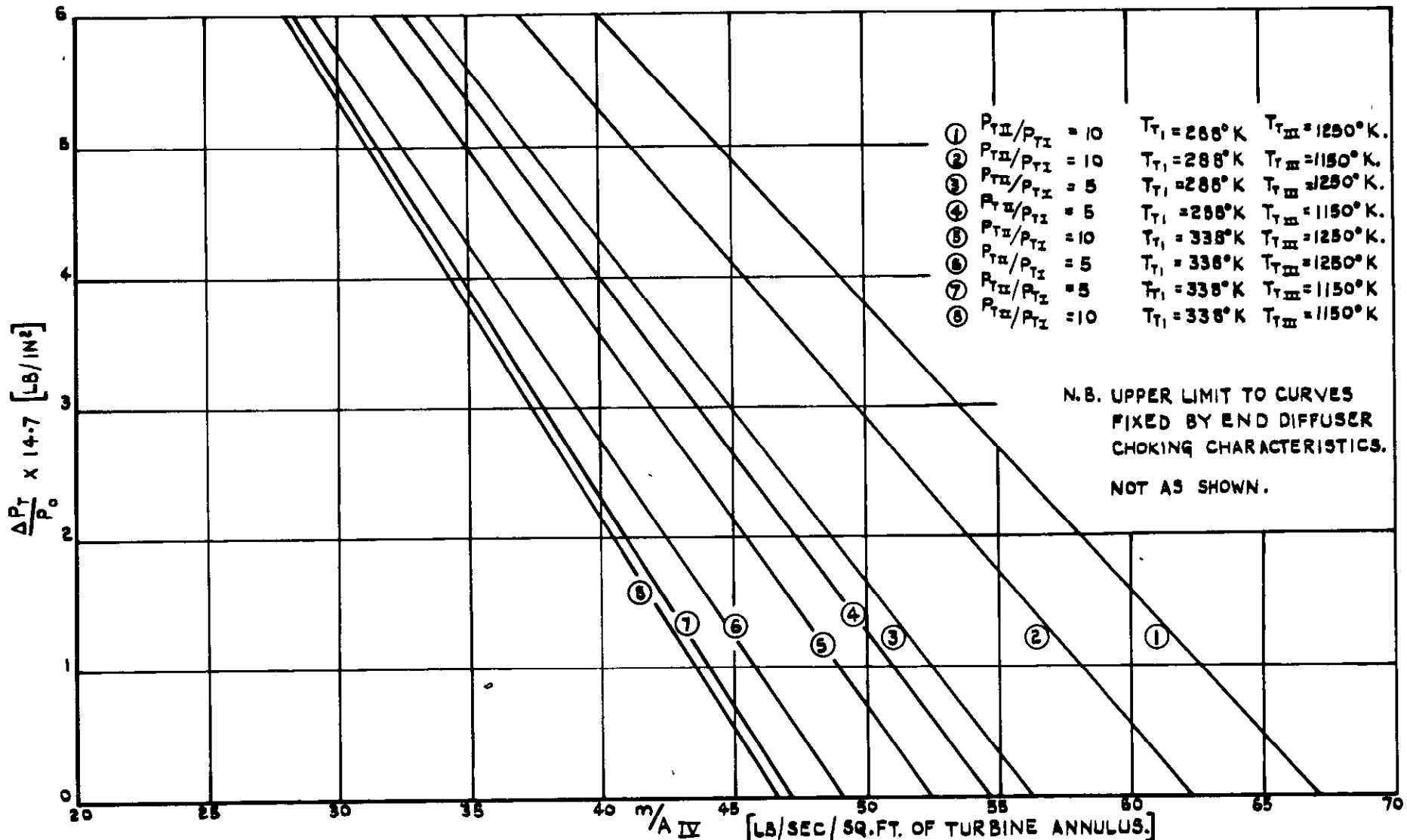

FIG.14. SUCTION PUMP CHARACTERISTICS FOR JET ENGINES WITH COMPRESSOR RATIOS 5 AND 10 AT FULL R.P.M. WITH END DIFFUSER.

FIG.14.

FIG 15

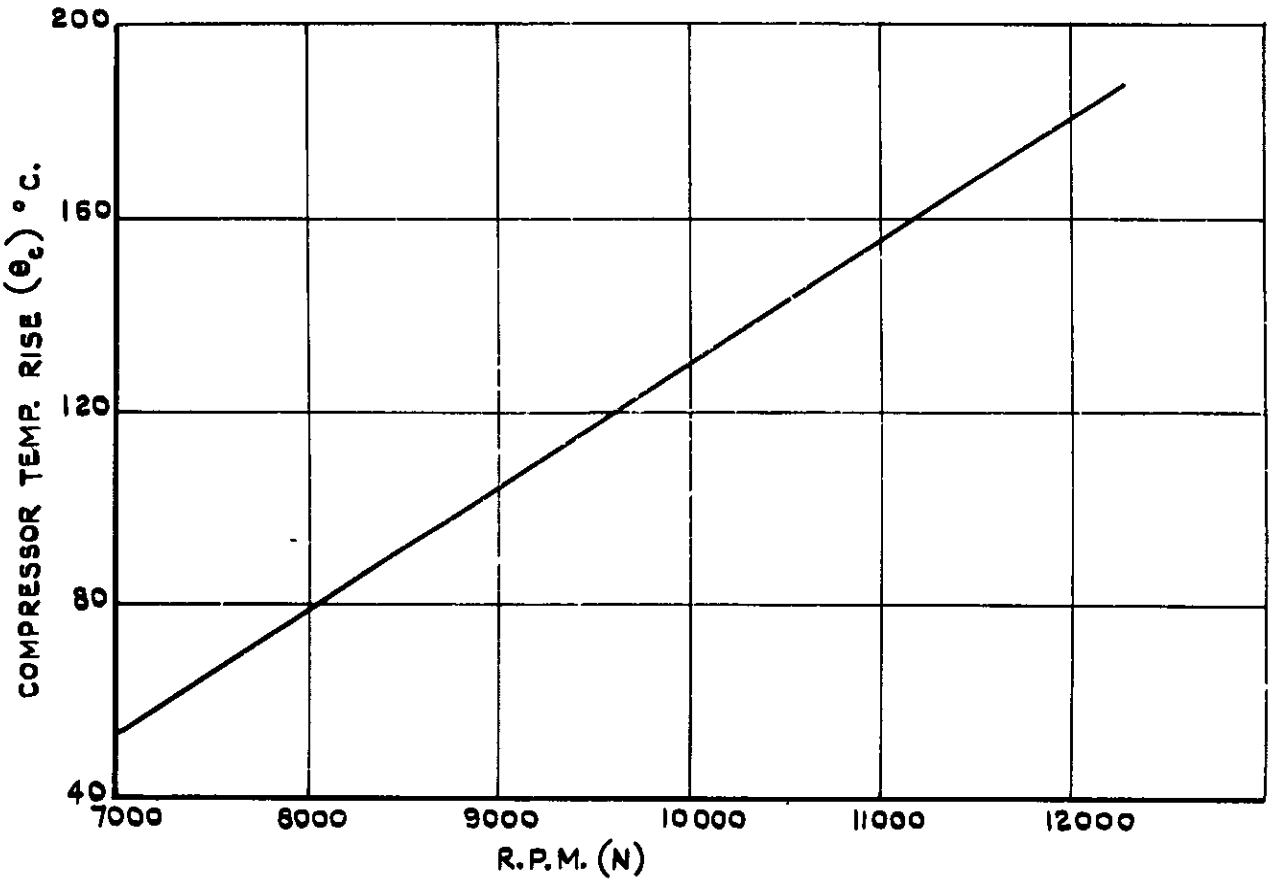

FIG. 15 ESTIMATED COMPRESSOR TEMPERATURE RISE TO R.P.M. CHARACTERISTIC FOR A TYPICAL 5000LB. THRUST JET ENGINE.

FIG. 16.

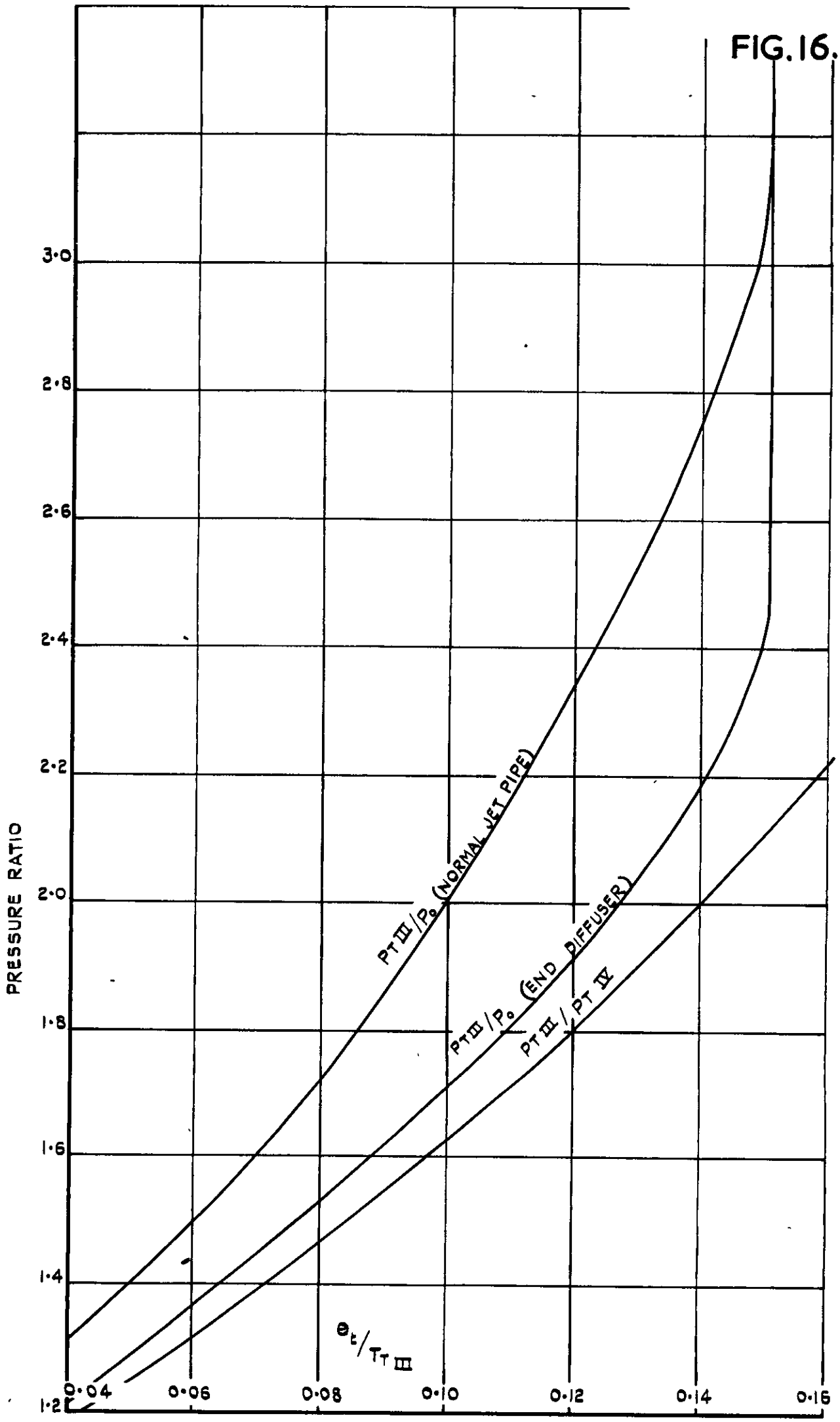

FIG. 16. ESTIMATED TURBINE TEMPERATURE RATIO TO PRESSURE RATIO CHARACTERISTICS OF A TYPICAL 5000 LB. THRUST JET ENGINE.

FIG.17.

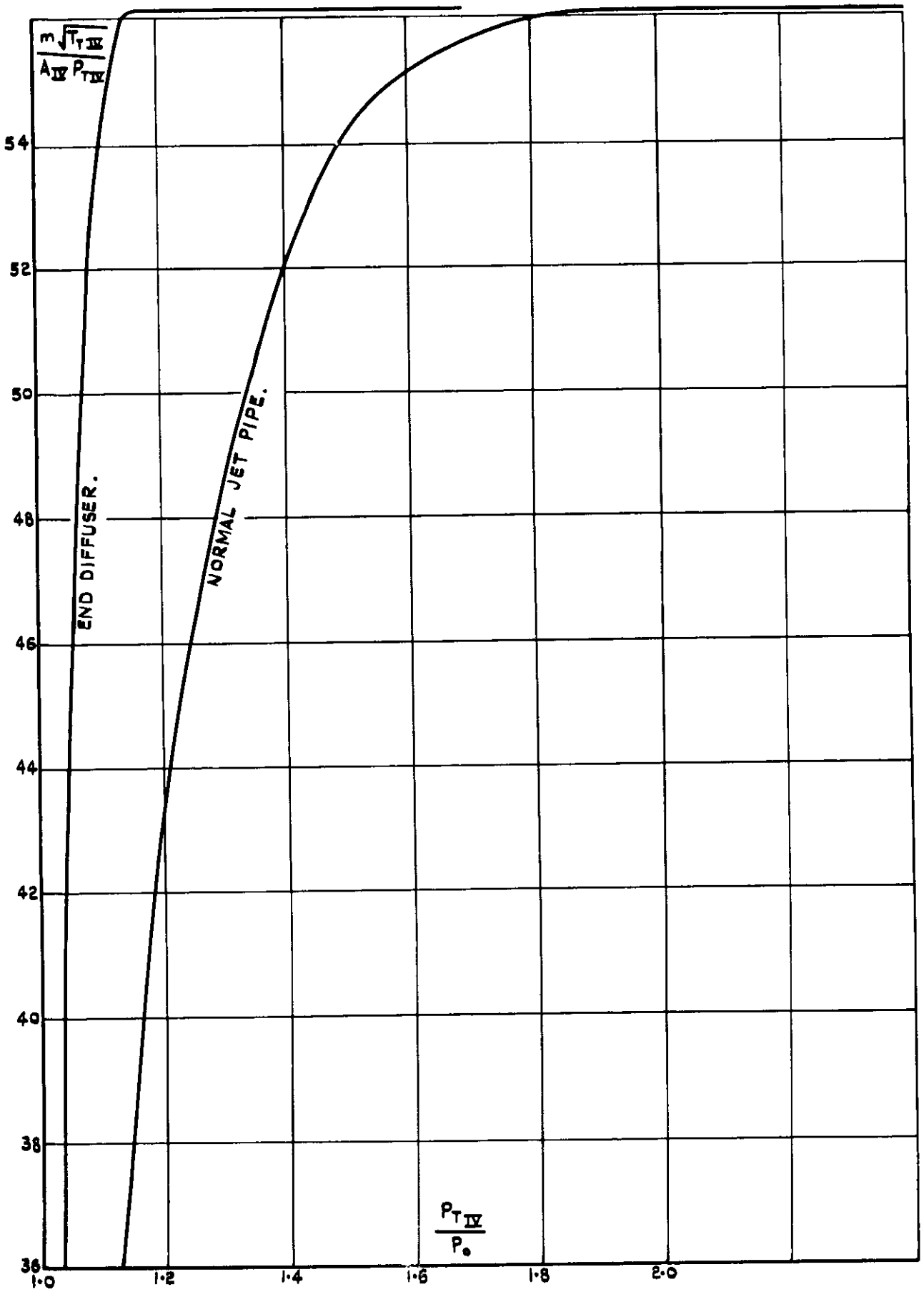

FIG.17 ESTIMATED MASS FLOW TO EXHAUST PRESSURE RATIO CHARACTERISTICS OF A TYPICAL 5000LB. THRUST JET ENGINE.

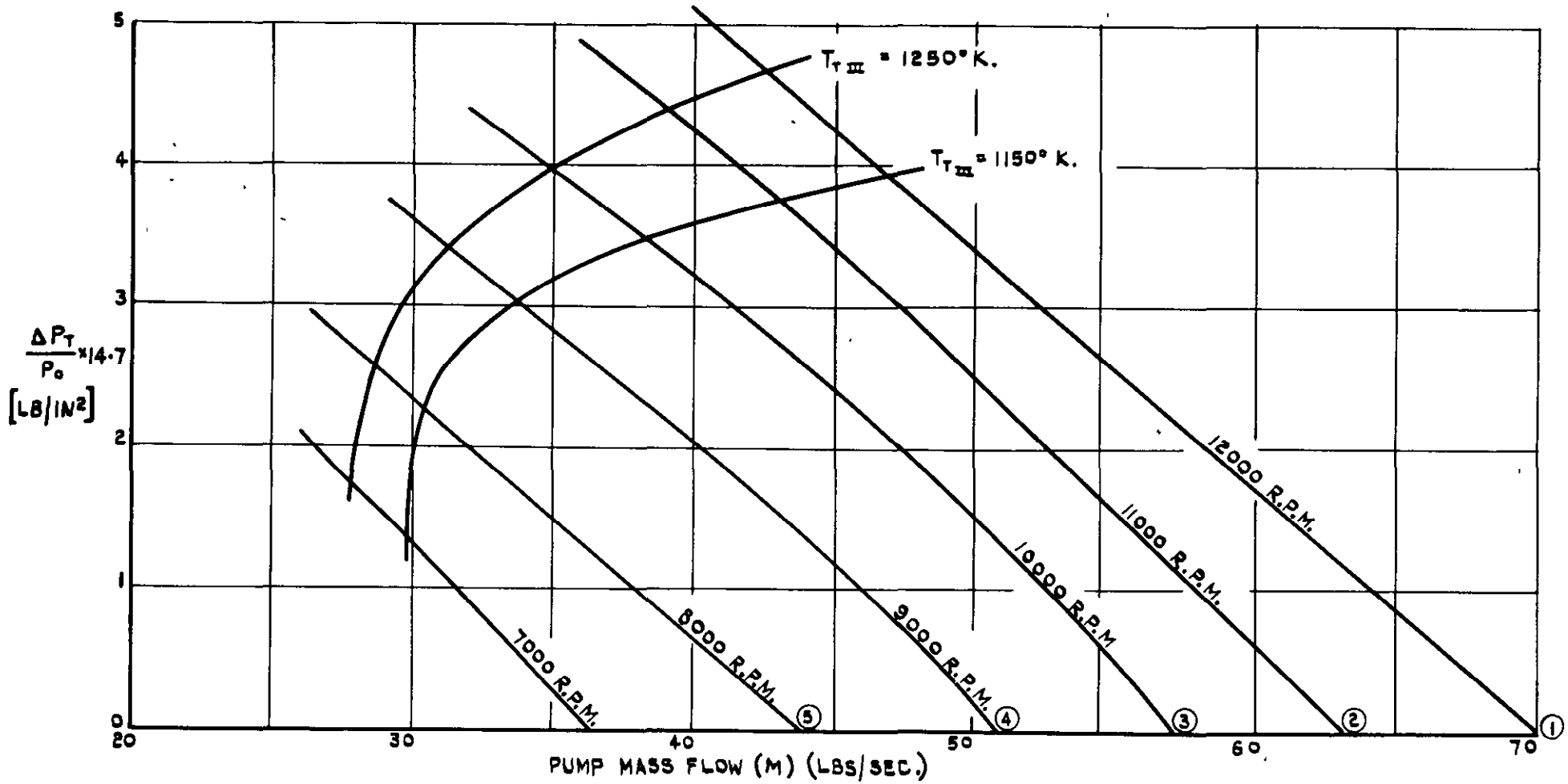

FIG. 18 ESTIMATED SUCTION PUMP CHARACTERISTICS OF A TYPICAL 5000LB. THRUST JET ENGINE AT VARIOUS R.P.M. WITH NORMAL JET PIPE EXHAUST.

FIG.18

FIG.19.

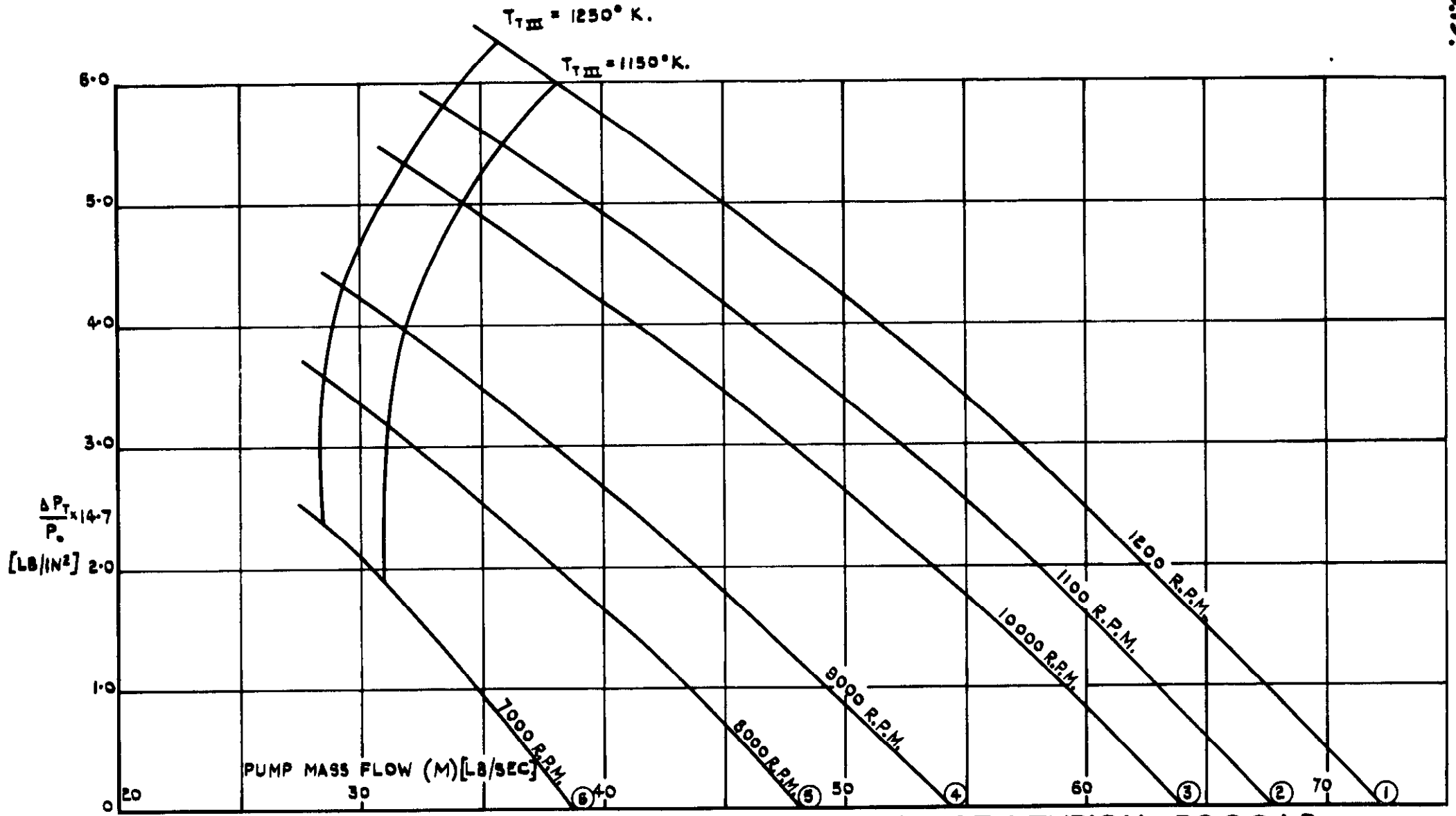

FIG.19. ESTIMATED SUCTION PUMP CHARACTERISTICS OF A TYPICAL 5000 LB. THRUST JET ENGINE AT VARIOUS R.P.M. WITH END DIFFUSER.

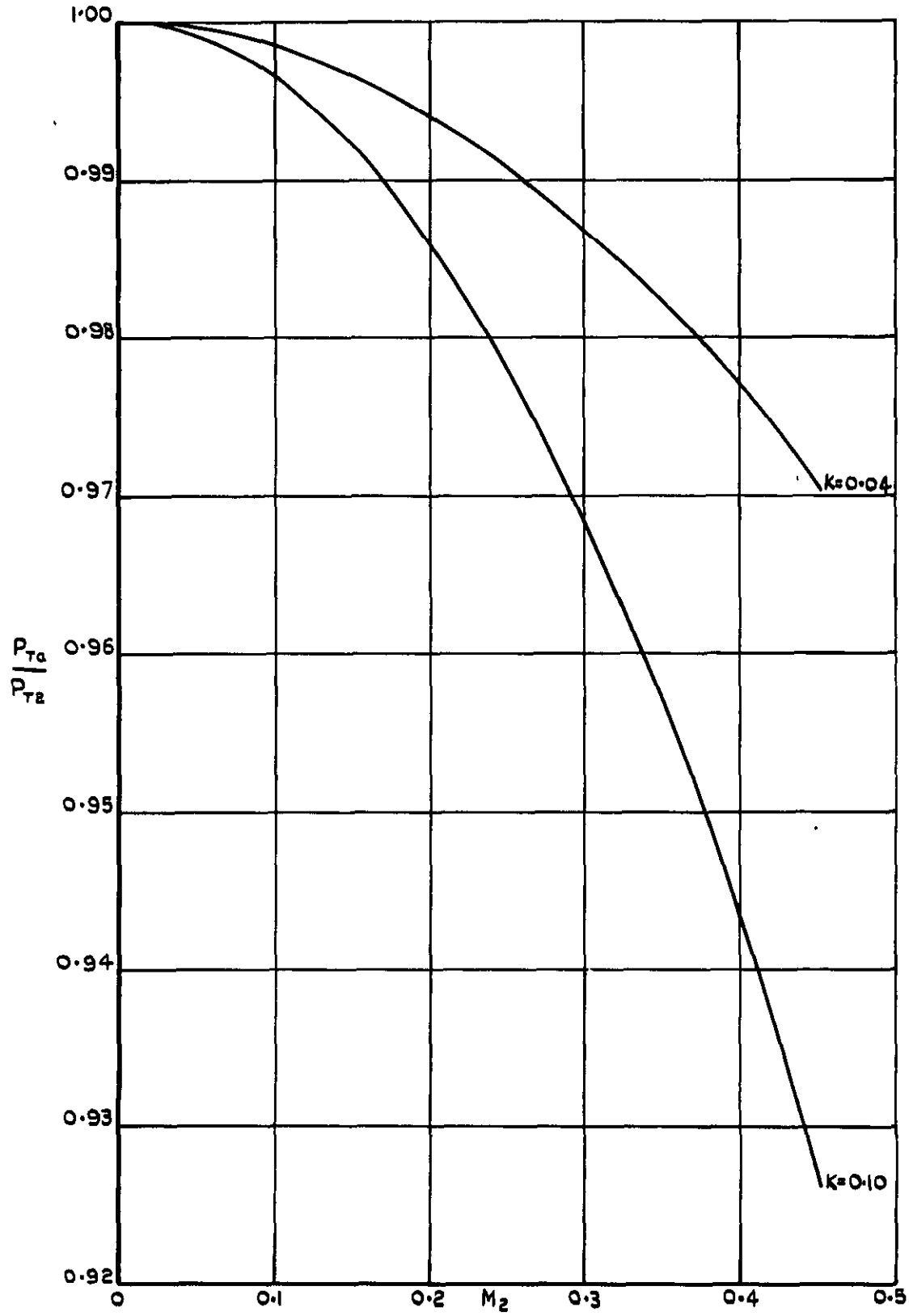

FIG. 20(a) TOTAL PRESSURE RATIO AROUND AN ENGINE NACELLE IN A TUNNEL.

FOR $K = 0{\cdot}04$
$K = 0{\cdot}10$

WHERE $K = \left[\frac{C_{D\ NACELLE}}{\pi} \left(\frac{d}{D}\right)^2 + \frac{C_{D\ STRUT}}{4} \frac{A_{STRUT}}{A_3} + C_f \frac{L}{D} \right]$

FIG. 20(b).

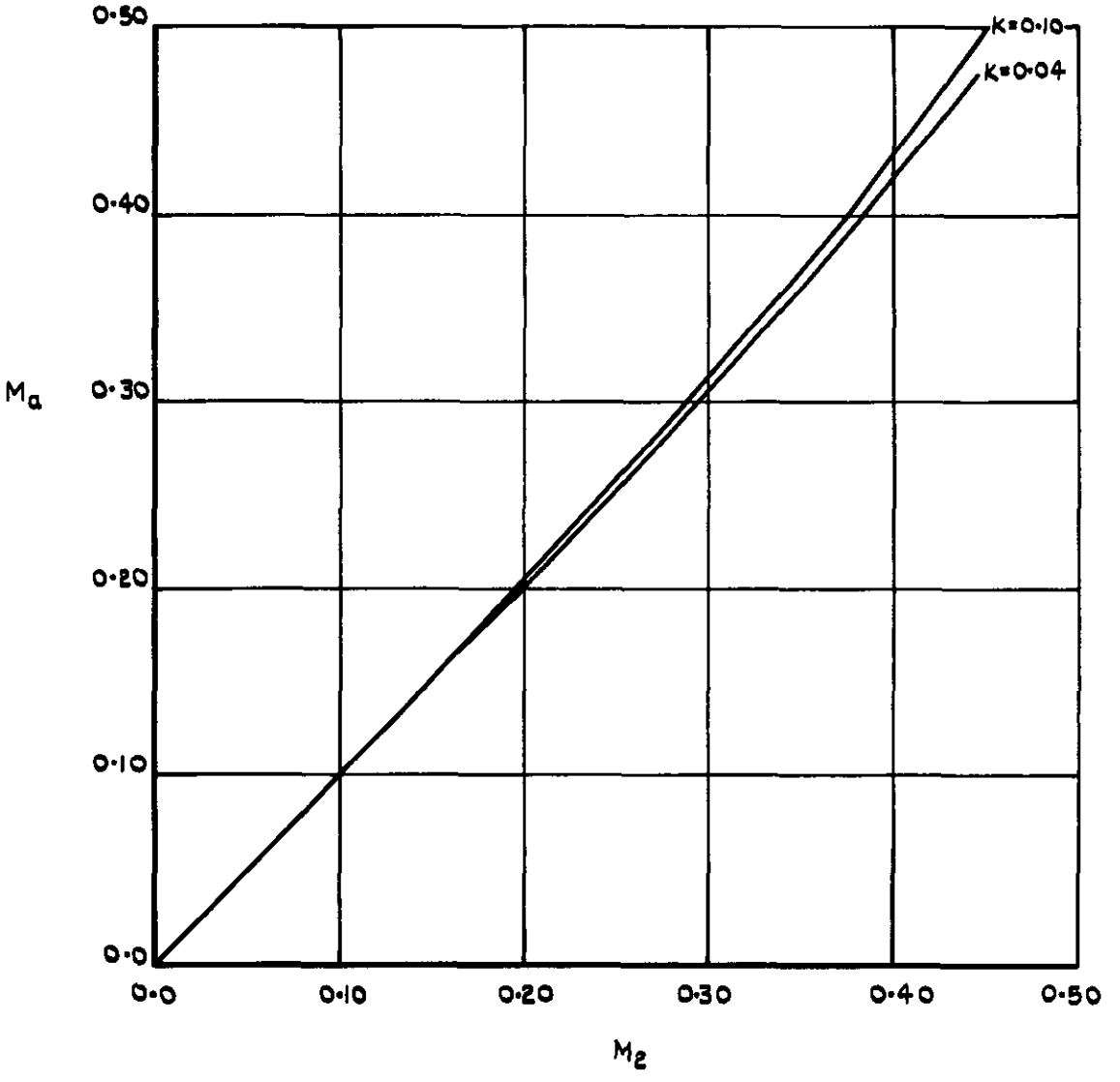

FIG. 20(b). MACH NUMBER CHANGE AROUND AN ENGINE NACELLE IN A TUNNEL.

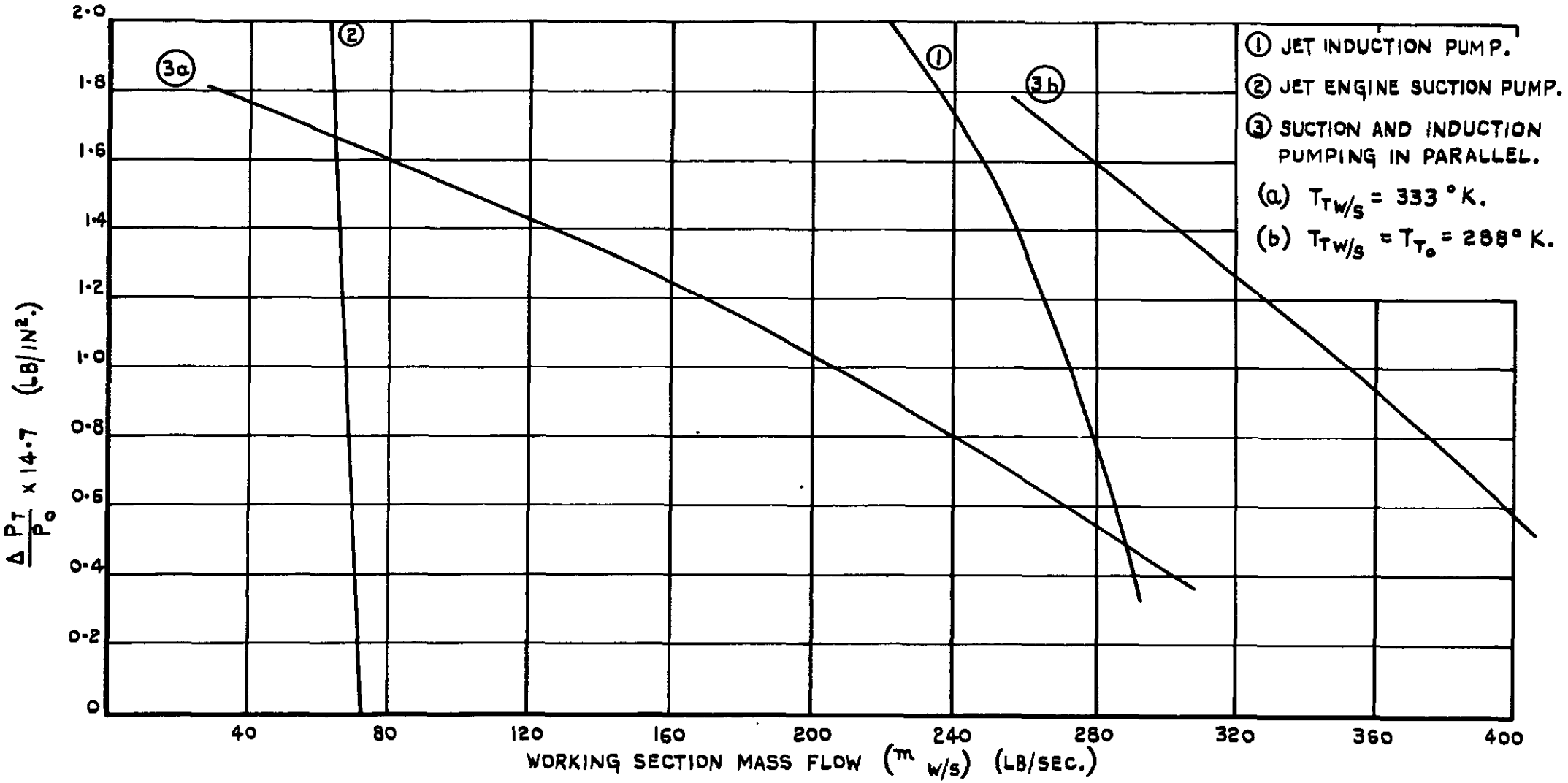

FIG. 21. A COMPARISON OF THE PUMP CHARACTERISTICS OF THREE METHODS OF JET ENGINE DRIVE FOR A HIGH SPEED SUBSONIC TUNNEL AT ENGINE MAXIMUM R.P.M.

FIG. 21.

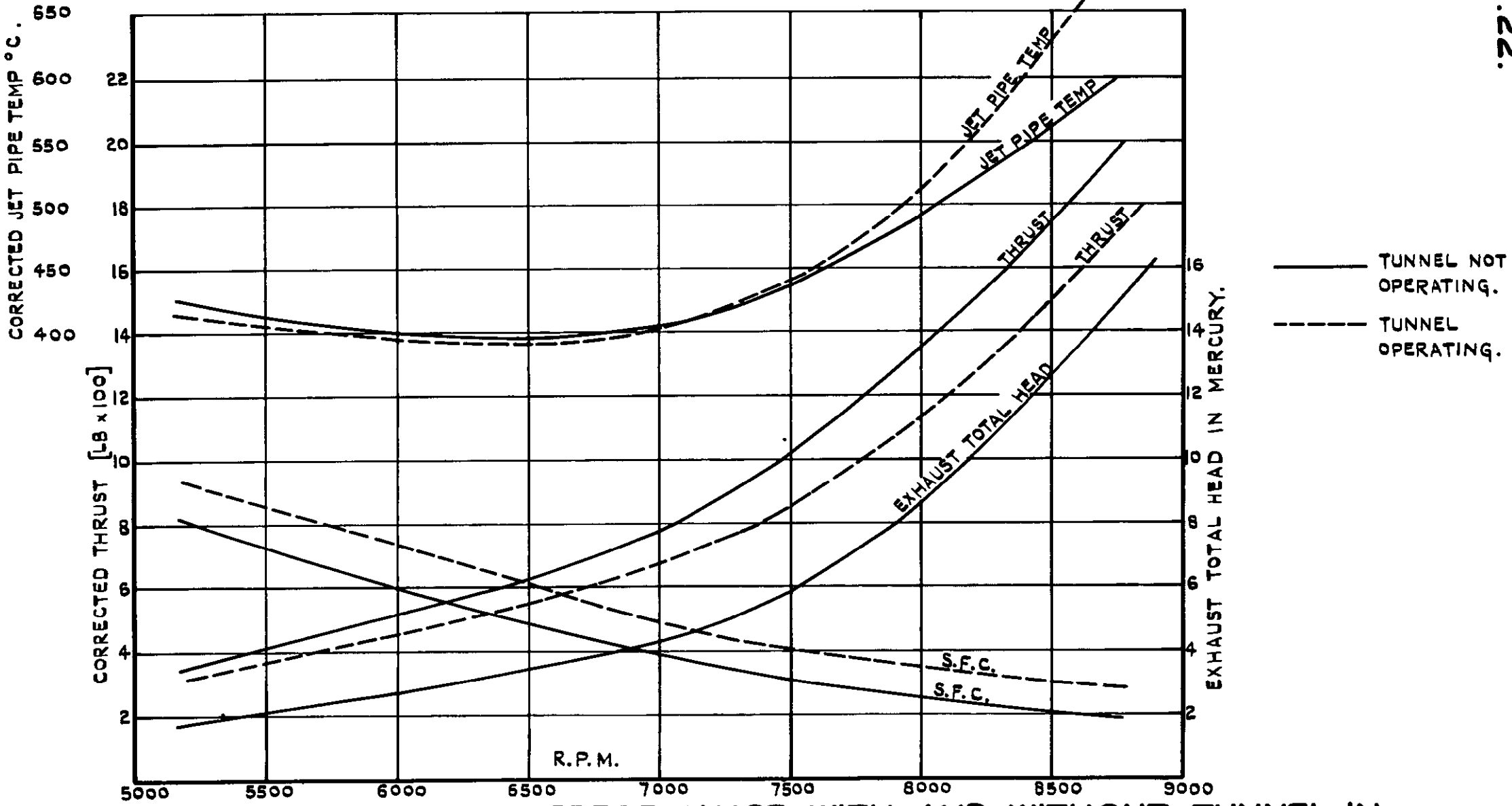

FIG. 22. JUMO, 004 ENGINE PERFORMANCE WITH AND WITHOUT TUNNEL IN OPERATION FOR PARALLEL SUCTION AND INDUCTION PUMPING. (REFERENCE 14.)

FIG. 22.

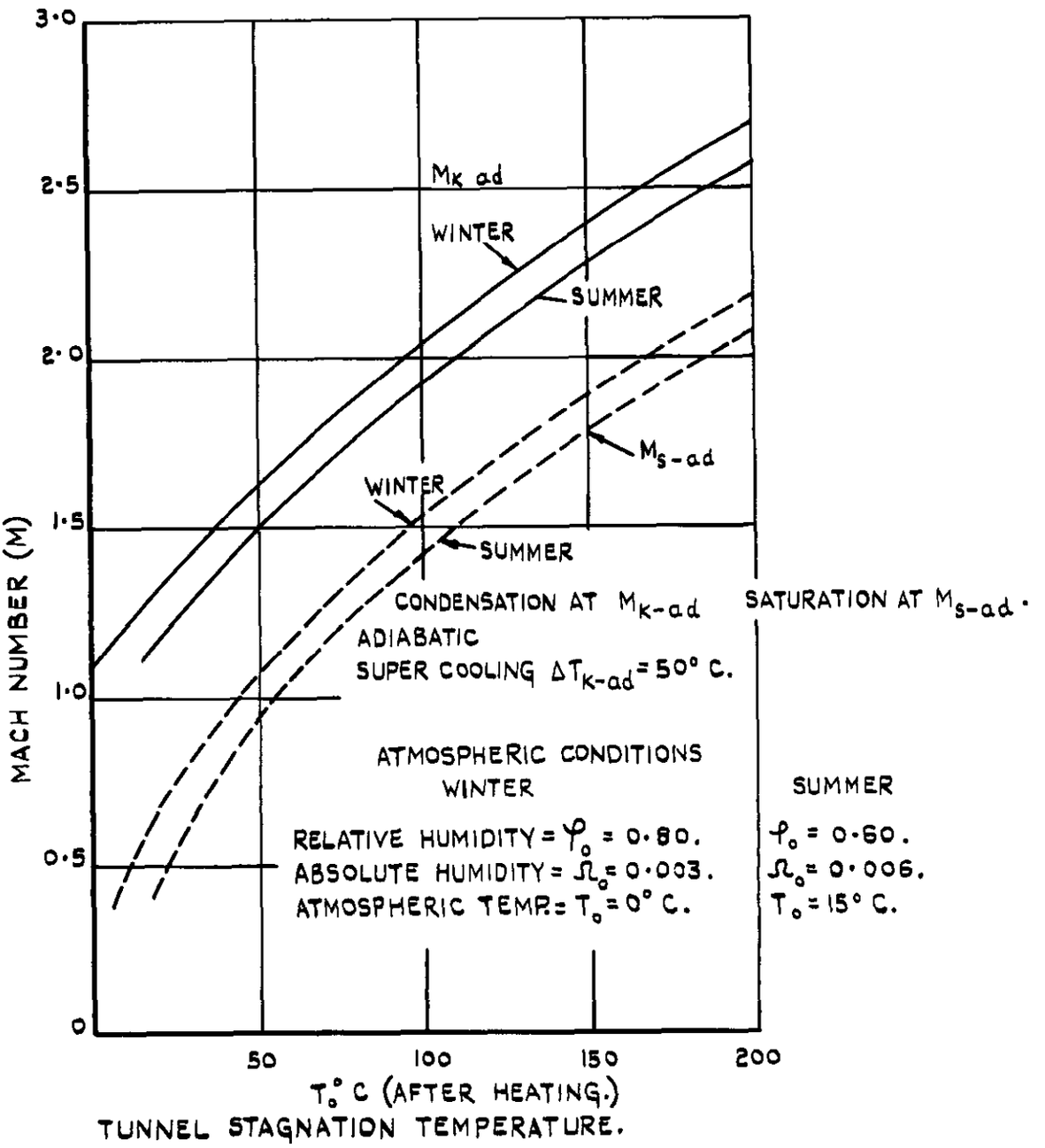

FIG.23. EFFECT OF STAGNATION TEMPERATURE ON MACH NUMBER AT WHICH CONDENSATION OCCURS FOR TYPICAL ATMOSPHERIC CONDITIONS.

(REFERENCE 16.)

FIG. 24.

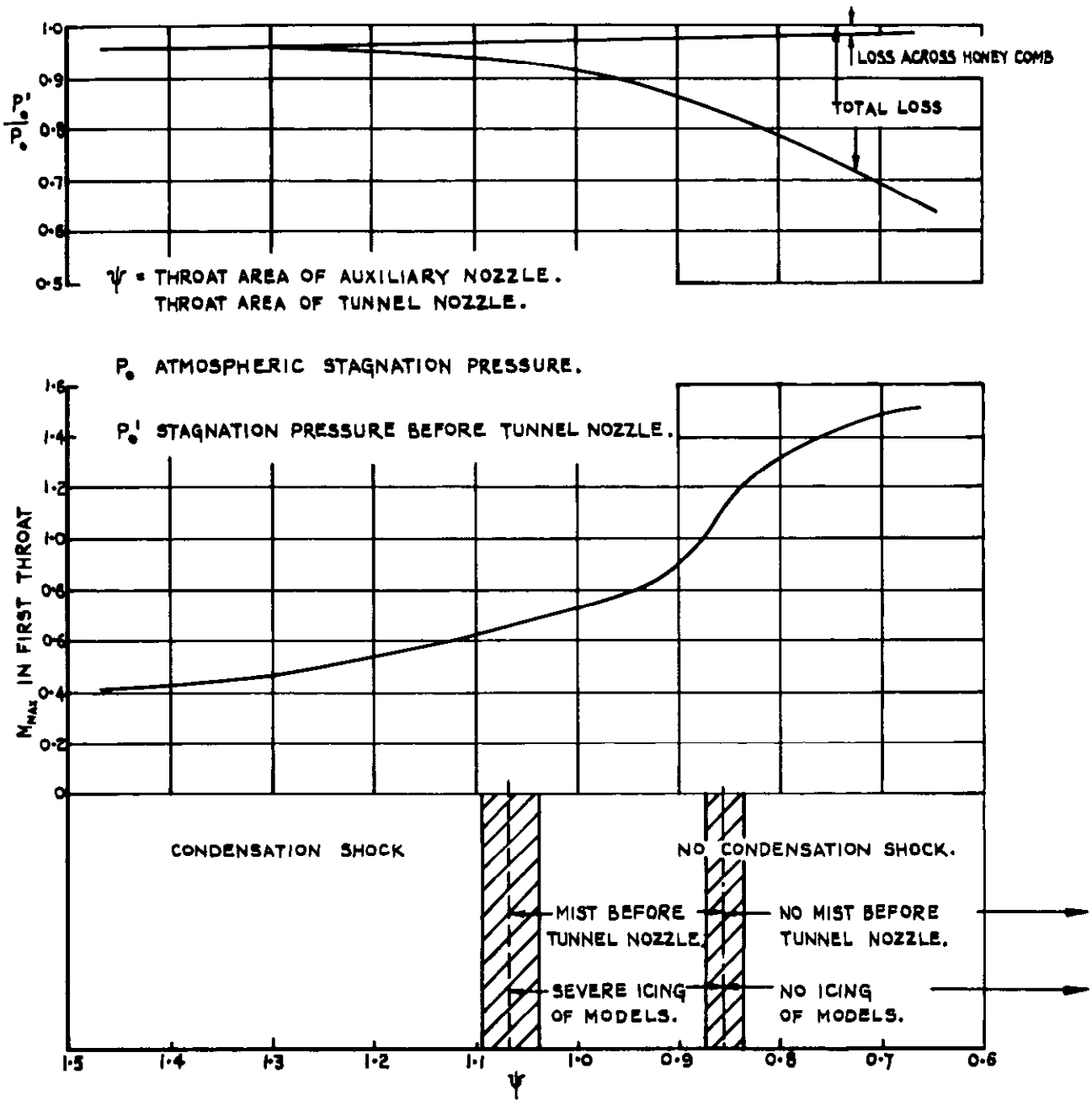

FIG. 24. PRESSURE LOSSES AND VELOCITIES IN PRE EXPANSION NOZZLE FOR HUMIDITY CONTROL.
(REFERENCE 17.)

FIG 25

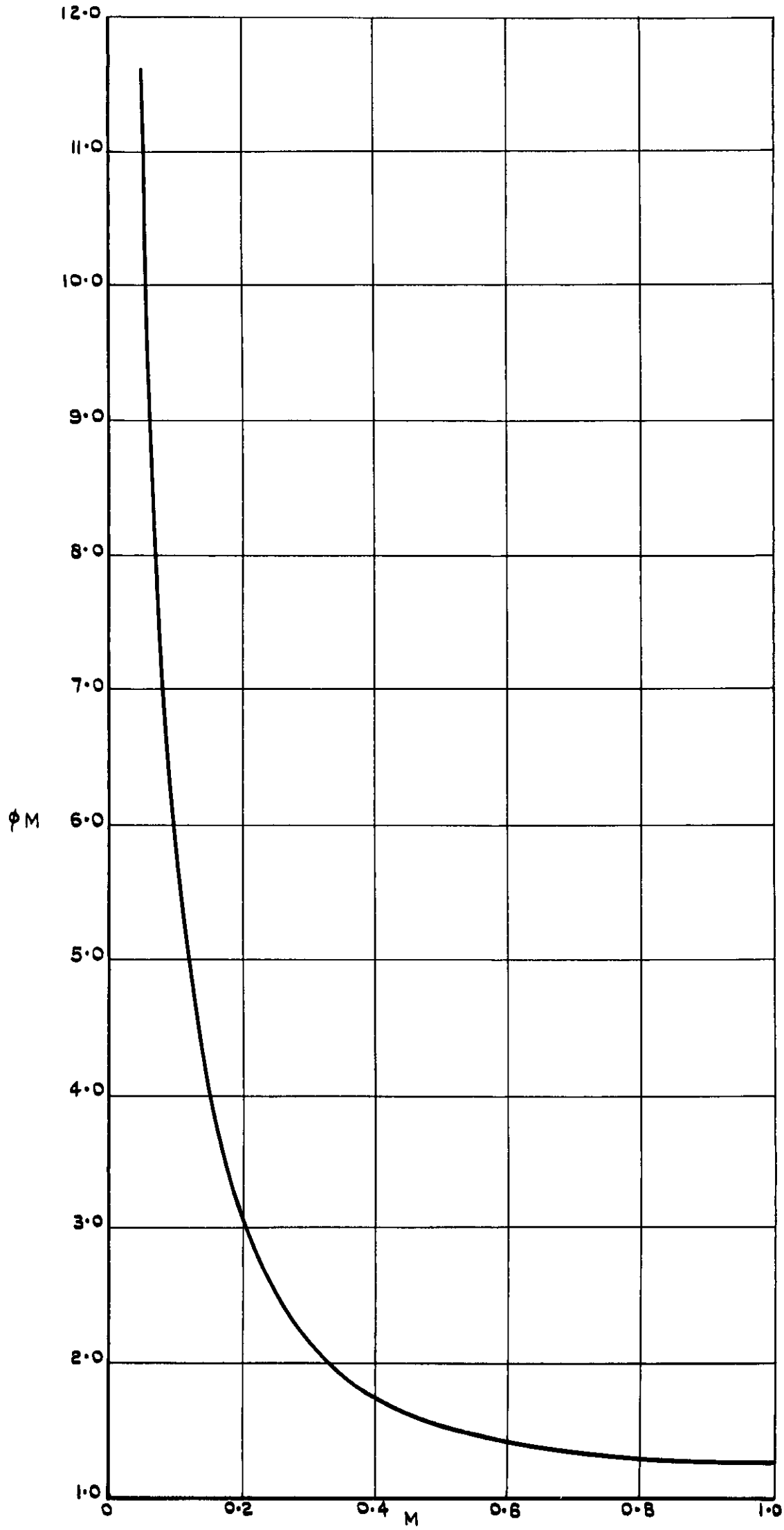

FIG. 25. FUNCTION ϕ_2 (M) TO M

FIG. 26.

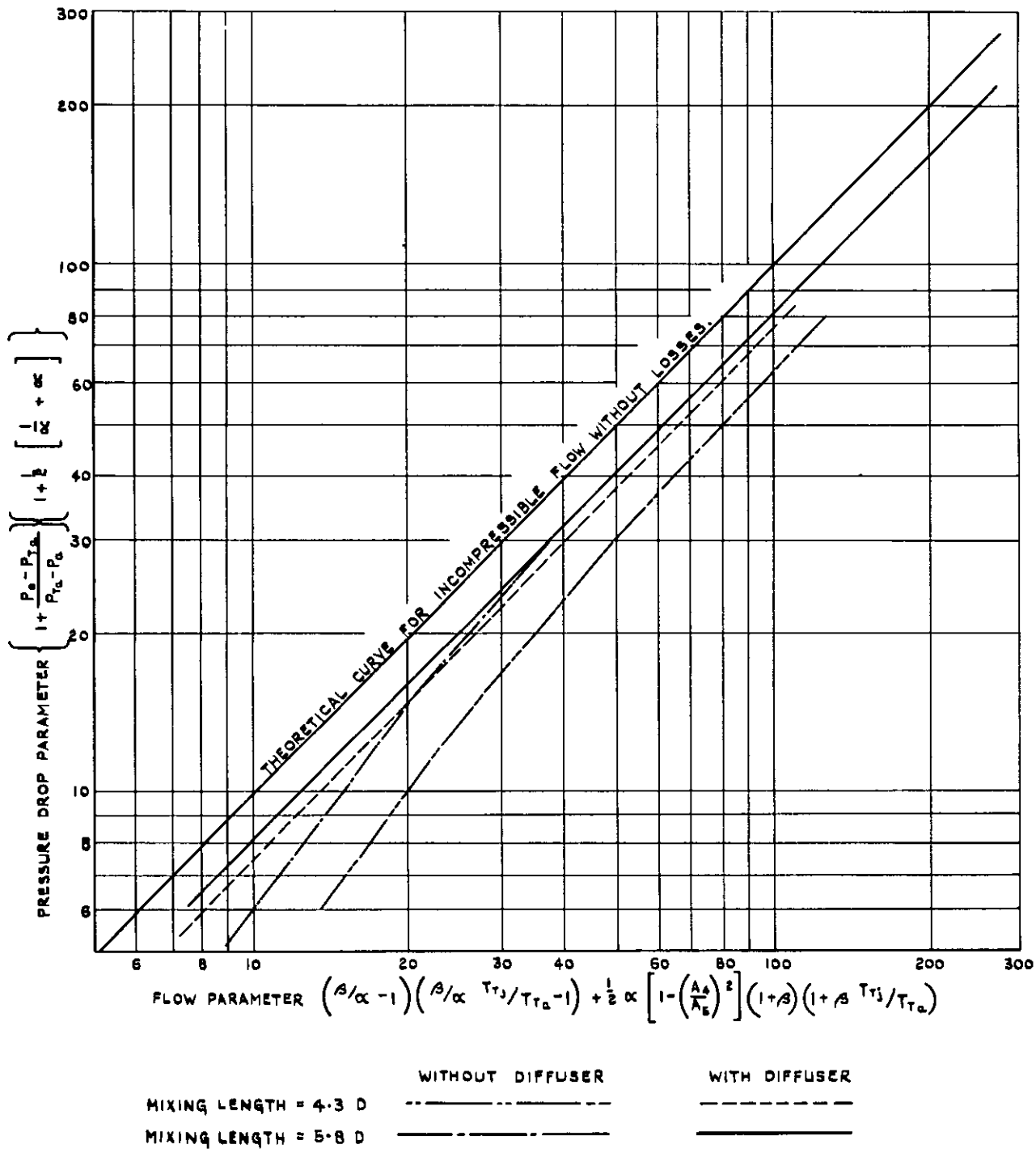

FIG. 26 INDUCTION PUMP CHARACTERISTICS FROM ROLLS ROYCE TESTS ON 1/10 SCALE MODEL TUNNEL.

(REFERENCE 6.)

FIG.27.

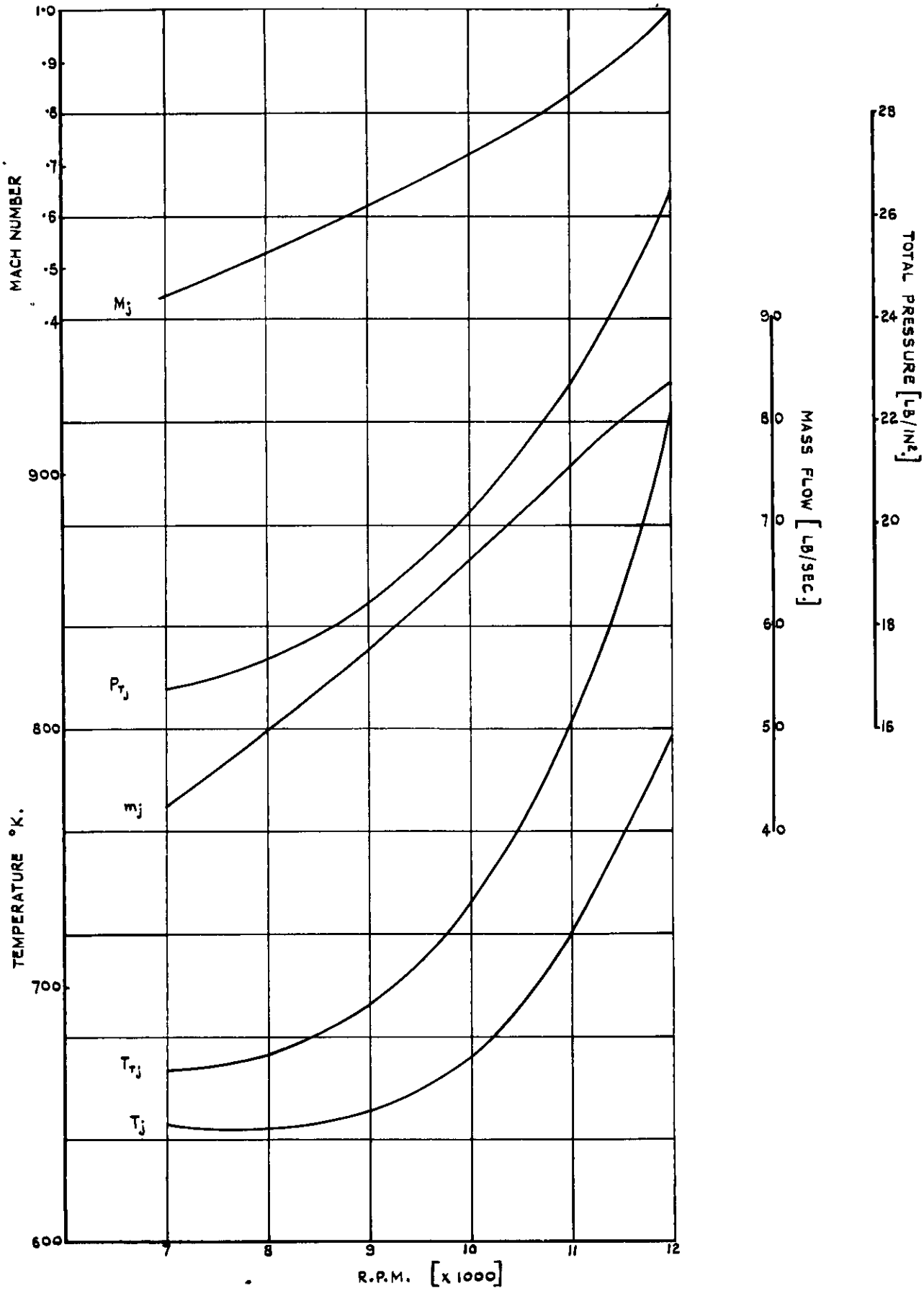

FIG. 27. ESTIMATED 5000 LB. THRUST JET ENGINE TEST BED CHARACTERISTICS OF JET FLOW.

FIG.28.

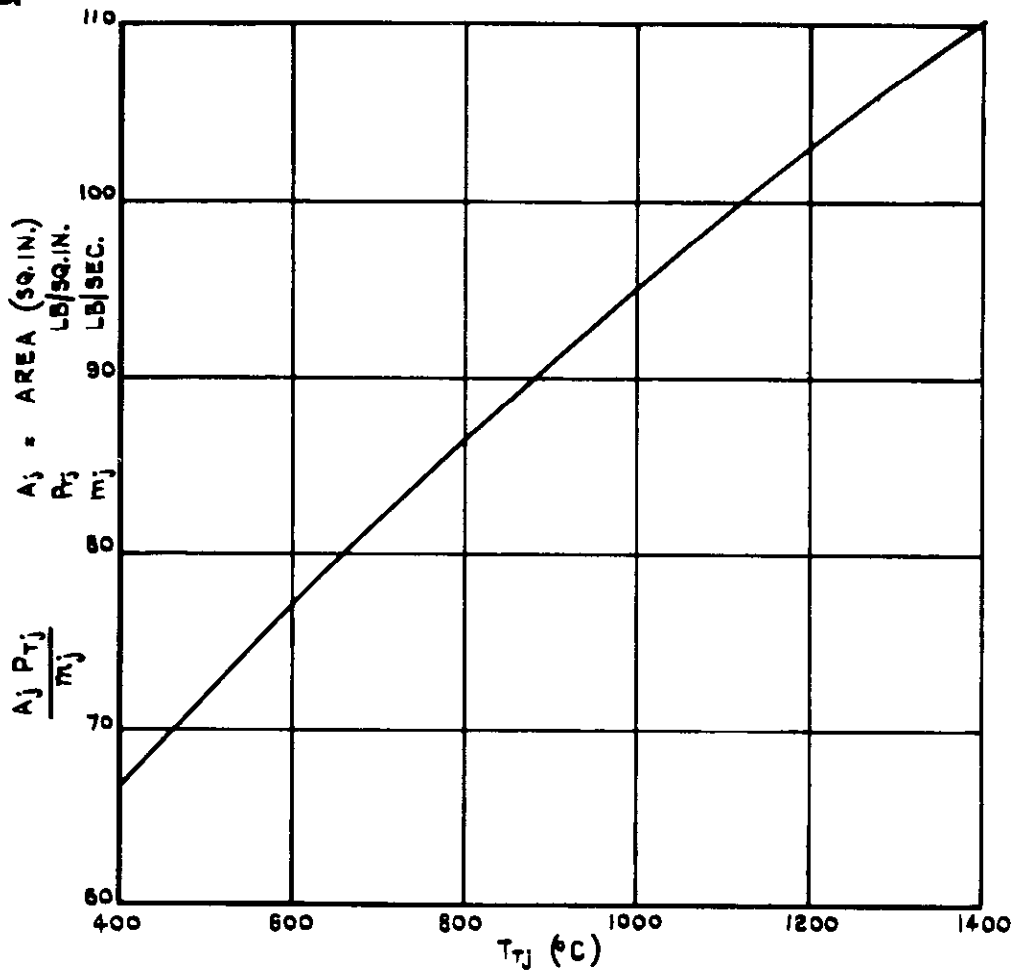

FIG.28. CHOKING CHARACTERISTICS OF THE FINAL NOZZLE OF A JET ENGINE.
(REFERENCE 18)

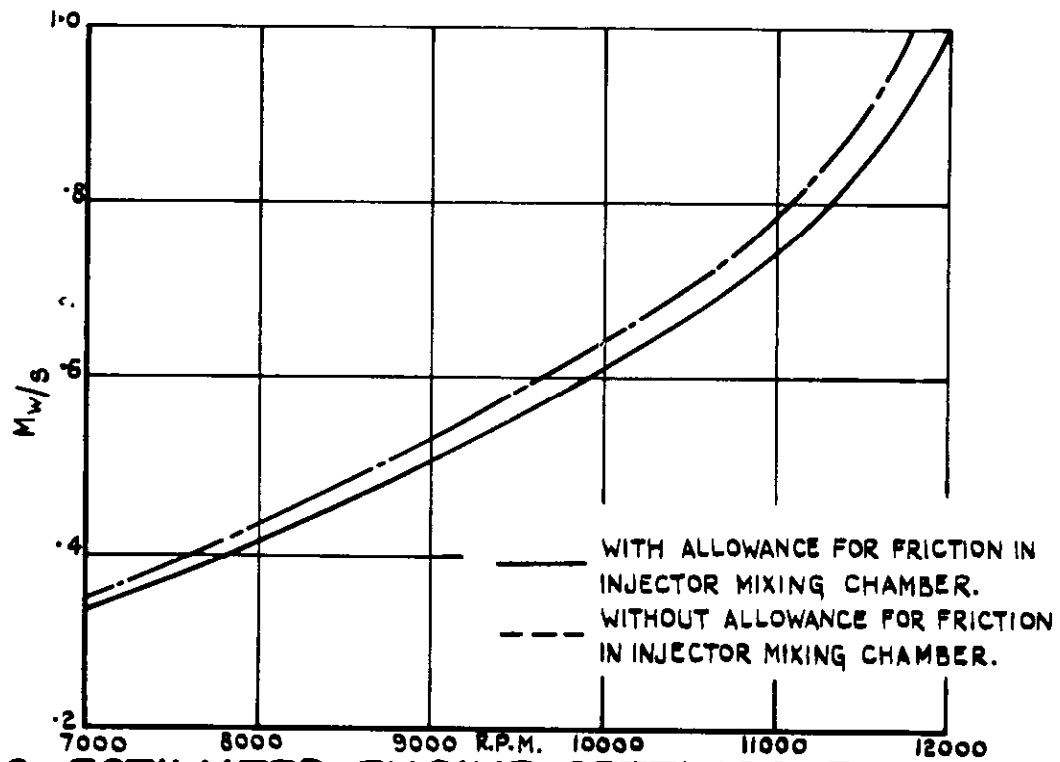

FIG.29. ESTIMATED ENGINE SETTINGS FOR WORKING SECTION MACH NUMBERS (TUNNEL EMPTY) TUNNEL SIZE 4 FT^2. DRIVE SINGLE NENE II INJECTOR PUMP. $\alpha = 0.15$.

C.P. No. 107
(13,539)
A.R.C. Technical Report

PUBLISHED BY HER MAJESTY'S STATIONERY OFFICE

To be purchased from
York House, Kingsway, LONDON, W C 2. 423 Oxford Street, LONDON, W.1
P.O. BOX 569, LONDON, S E 1
13a Castle Street, EDINBURGH, 2 | 1 St. Andrew's Crescent, CARDIFF
39 King Street, MANCHESTER, 2 | Tower Lane, BRISTOL, 1
2 Edmund Street, BIRMINGHAM, 3 | 80 Chichester Street, BELFAST
or from any Bookseller

1953

Price 16s. 0d. net

PRINTED IN GREAT BRITAIN

S.O. Code No. 23-9007-7